UNIVERSITY OF ALBERTA

TEMPORAL AND SPATIAL PATTERN FILTER DESIGN FOR EPILEPTIC SEIZURES IN THE EEG

BY

NORA SUSAN O'NEILL

©

A thesis submitted to the Faculty of Graduate Studies and Research
in partial fulfillment of the requirements for the degree of

MASTER OF SCIENCE

DEPARTMENT OF ELECTRICAL AND COMPUTER ENGINEERING

Edmonton, Alberta

FALL 1998

National Library of Canada
Acquisitions and Bibliographic Services
395 Wellington Street
Ottawa ON K1A 0N4
Canada

Bibliothèque nationale du Canada
Acquisitions et services bibliographiques
395, rue Wellington
Ottawa ON K1A 0N4
Canada

Your file Votre référence

Our file Notre référence

The author has granted a non-exclusive licence allowing the National Library of Canada to reproduce, loan, distribute or sell copies of this thesis in microform, paper or electronic formats.

The author retains ownership of the copyright in this thesis. Neither the thesis nor substantial extracts from it may be printed or otherwise reproduced without the author's permission.

L'auteur a accordé une licence non exclusive permettant à la Bibliothèque nationale du Canada de reproduire, prêter, distribuer ou vendre des copies de cette thèse sous la forme de microfiche/film, de reproduction sur papier ou sur format électronique.

L'auteur conserve la propriété du droit d'auteur qui protège cette thèse. Ni la thèse ni des extraits substantiels de celle-ci ne doivent être imprimés ou autrement reproduits sans son autorisation.

0-612-34398-7

Canada

The Lord said:

". . . if you accept my words
and store up my commands within you,

turning your ear to wisdom
and applying your heart to understanding,

and if you call out for insight
and cry aloud for understanding,

and if you look for it as for silver
and search for it as for hidden treasure,

then you will understand the fear of the Lord
and find the knowledge of God.

For the Lord gives wisdom,
and from his mouth comes knowledge and understanding."

Proverbs 2:1-6 (NIV)

UNIVERSITY OF ALBERTA

FACULTY OF GRADUATE STUDIES AND RESEARCH

The undersigned certify that they have read, and recommended to the Faculty of Graduate Studies and Research for acceptance, a thesis entitled TEMPORAL AND SPATIAL PATTERN FILTER DESIGN FOR EPILEPTIC SEIZURES IN THE EEG submitted by NORA SUSAN O'NEILL in partial fulfillment of the requirements for the degree of MASTER OF SCIENCE.

Dr. Z. J. Koles

Dr. M. Javidan

Dr. H. Marquez

DATE: August 26, 1998

ABSTRACT

Visual identification of the epileptic seizure onset and location in the surface EEG is often difficult. To improve the efficacy of the surface EEG, data dependent digital filtering techniques can be utilised. Traditional bandpass filters eliminate baseline shifts and other artifacts while temporal and spatial pattern filters reduce the pre-ictal background and exclude extraneous ictal activity. The data dependant temporal and spatial pattern filters are derived from the singular value decomposition of composite autocovariance and covariance matrices formed from abnormal and normal segments of the EEG. The temporal and spatial patterns which account for maximal variance in the abnormal segment are used in the filters. The filtering was applied to one simulated and two clinical EEGs with combinations of surface, subdural, and intracranial EEG recordings. The surface tracings initially failed to lateralize the seizure onset, whereas after filtering the seizure onset was clearly identifiable and the responsible source easily localised.

ACKNOWLEDGMENTS

All praise and glory be to the God and Father of our Lord Jesus Christ, for without His guidance, faithfulness, forgiveness, mercy and grace this dream would not be a reality.

I would like to thank Dr. Zoltan. J. Koles for his perseverance, encouragement and support throughout these years of graduate study. I appreciate his ability to allow me the time to work things out on my own and to let me run with an idea while be involved enough to provide guidance when necessary. I truly value the confidence and working relationship which grew as the challenges were faced.

I would also like to extend my gratitude to Dr. Mano Javidan. The many hours of reviewing EEGs and discussions were an education in themselves. This interaction and the exposure to the weekly Epilepsy Conferences were unmeasurable in their value. I sincerely appreciate all the extra work that the EEG technicians put in preparing the clinical data for my analysis. As well, I acknowledge and am grateful for the clinical data that Dr. Javidan and Dr. S. S. Spencer provided from the Yale School of Medicine as it was of significant importance in this research.

I strongly believe that it was the opportunity afforded by the interdisciplinary interactions and the working relationships established between the University of Alberta departments of Biomedical Engineering, Electrical Engineering and the University of Alberta Hospital Staff that fueled my motivation daily and continues to drive me to learn, to understand and to search for answers.

Personally, through this graduate experience I have grown in faith and character as well as professionally. It has challenged me like no other experience and I leave this program more satisfied and fulfilled than I have any other professional experience. For this I am most thankful. No man or women is an island and therefore I share this accomplishment with my family and friends. My mother for her continued faith and love, my brother and sister-in-law for their unwavering belief and support, Shadow and KC for their lessons of faithfulness and devotion and my father for his support as well as for Snowflake. Throughout these years numerous friends have come and gone, and some have stayed. I thank each of them for the time they shared with me as they fit into my crazy schedule. Especially I wish to first thank Tina Burns and Dr. P. Smy for without their first words of encouragement and belief this might not have been. As well, I appreciated the prayers and support from the family at Heimtal; especially Brenda, Art and Mary, and Beth and Art. I have to mention my friends from the barn, Art, Iris and Lynn, who were most gracious in their time and horses and I thank them for those moments I could escape to the peace of the country. Also it is with prayers and best wishes from the Book club in BC, especially those from Pat and Donna, that I returned home to renew my studies with hope. Finally but no means the least, I am beholden to those friends who listened and encouraged me daily, Michelle, Liz and Lynn; thank you for the treasure of your friendship.

Yahooh - we did it! Thank you all. May God enrich all your lives as he has enriched mine with these blessings.

TABLE OF CONTENTS

1. INTRODUCTION 1

Problem Statement 1

Problem Overview 2

Area of Application 6

Previous Research 7

Research Objective 9

Document Overview 11

2. MEDICAL BACKGROUND 12

Bioelectric Potentials from the Brain 13

EEG Descriptive Traits 18

EEG Classifications 20

Epileptic Seizures 22

The Recording Electrodes 24

3. MATHEMATICAL BACKGROUND 29

Approximation of Source Potentials 29

EEG Data Matrix 31

Spatio-Temporal Decomposition 32

Basis Vectors 34

Singular Value Decomposition 35

Linear Transformations 37

Covariance Matrix 39

Whitening Transformation 41

Composite Covariance Matrix 43

Simultaneous Diagonalization 44

4. METHOD **49**

Method Overview 49

Data Dependent Filter Design Procedure 50

Naming Conventions 51

Equation Summary 52

Temporal Bandpass Filtering 54

Temporal Pattern Filtering 55

Step 1. Temporal Basis Vectors: 56

Step 2. TPF Temporal Waveforms: 59

Step 3. Partitioning of Matrices: 61

Step 4. Filter Design and Application: 62

Spatial Pattern Filtering 65

Step 1. Spatial Basis Vectors: 66

Step 2. Temporal Waveforms: 68

Step 3. Partitioning of Matrices: 69

Step 4. Filter Design and Application: 69

5. RESULTS **71**

Filter Parameters 72

Simulated Data 74

Data Matrix Construction 79

Temporal Filtering 79

Spatial Filtering 84

Filter Design Comparison 89

Clinical Data 93

Clinical Validation Results 93

Clinical Trial Results.....112

6. CONCLUSION.....123

Future Work.....126

REFERENCES.....128

LIST OF TABLES

Table 2.1 Electrode Angles 26

Table 4.1 Filter Design Naming Conventions 52

Table 4.2 Comparative Summary of Filter Design Equations 53

Table 5.1 Filter Design Parameters 72

Table 5.2 Spatial Patterns; Simulated Data 76

Table 5.3 Common Spatial Patterns, Simulated Data 86

Table 5.4 Alignment Error Comparisons, Simulated EEG 92

Table 5.5 Comparison of Abnormal Spatial Patterns; Patient 1 107

LIST OF FIGURES

Figure 2.1 Parts of the Brain 14

Figure 2.2 Cortical Layers 15

Figure 2.3 Cortical Dipole Field Potential 16

Figure 2.4 Cortical Tissue with Electrodes 24

Figure 2.5 Electrode Positions- The Extended International 10/20 System 25

Figure 2.6 Tip and Spin 26

Figure 5.1 Source Waveforms; Simulated Data 74

Figure 5.2 Spatial Maps; Simulated Data 77

Figure 5.3 Raw EEG; Simulated Data 78

Figure 5.4 TPF Temporal Waveforms; Simulated Data 80

Figure 5.5 TPF Temporal Waveforms corresponding to the Temporal Patterns which account for the four largest variances in the abnormal segment; Simulated Data. 81

Figure 5.6 Temporal Filter Frequency Response; Simulated Data 82

Figure 5.7 Temporal Bandpass Filtered EEG; Simulated Data 83

Figure 5.8 Temporally Filtered EEG; Simulated Data 84

Figure 5.9 SPF Temporal Waveforms; Simulated Data 85

Figure 5.10 Mapping of Derived Spatial Patterns; Simulated Data 87

Figure 5.11 Temporally and Spatially Filtered EEG; Simulated Data 89

Figure 5.12 Frequency Response for 7 Temporal Pattern Filters; Simulated Data 90

Figure 5.13 MRI Tracing of Electrode Locations; Patient 1 94

Figure 5.14 Raw EEG; Patient 1 95

Figure 5.15 Temporal Bandpass Filtered EEG; Patient 1 97

Figure 5.16 TPF Temporal Waveforms for Temporal Pattern Filter Designed Using a Depth Electrode; Patient 1 99

Figure 5.17 TPF Temporal Waveforms for a Temporal Pattern Filter Designed Using a Surface Electrode; Patient 1 99

Figure 5.18 Frequency Response for Depth and Surface Designed Temporal Filters; Patient 1 100

Figure 5.19 Temporally Filtered EEG Using A Depth Designed Temporal Pattern Filter; Patient 1 102

Figure 5.20 Temporally Filtered EEG Using A Surface Designed Temporal Pattern Filter; Patient 1 102

Figure 5.21 SPF Temporal Waveforms of Surface Electrode Recordings Using A Depth Designed Temporal Filter; Patient 1 103

Figure 5.22 SPF Temporal Waveforms of Surface Electrode Recordings Using A Surface Designed Temporal Filter; Patient 1 104

Figure 5.23 Scaled Temporally and Spatially Filtered Surface Electrode Recordings Using A Depth Designed Temporal Filter; Patient 1 105

Figure 5.24 Scaled Temporally and Spatially Filtered Surface Electrode Recordings Using A Surface Designed Temporal Filter; Patient 1 105

Figure 5.25 SPF Temporal Waveforms for a Filter Designed without a Temporal Pattern Filter; Patient 1 106

Figure 5.26 Mapping of Abnormal Spatial Patterns for Depth and Surface Designed Temporal Filters and a Filter without a Temporal Pattern Filter; Patient 1 109

Figure 5.27 Comparison of Filtered Electrode Recordings Resulting from Depth and Surface Designed Temporal Filters; Patient 1 110

Figure 5.28a Raw EEG; Patient 2 113

Figure 5.28b Raw EEG; Patient 2 114

Figure 5.29a Temporally Bandpass Filtered EEG, Patient 2 115

Figure 5.29b Temporally Bandpass Filtered EEG, Patient 2 115

Figure 5.30a TPF Temporal Waveforms; Patient 2 116

Figure 5.30b TPF Temporal Waveforms; Patient 2 116

Figure 5.31 Frequency Response for Temporal Pattern Filter; Patient 2 117

Figure 5.32a Temporally Filtered EEG; Patient 2 118

Figure 5.32b Temporally Filtered EEG; Patient 2 118

Figure 5.33a SPF Temporal Waveforms; Patient 2 119

Figure 5.33b SPF Temporal Waveforms; Patient 2 120

Figure 5.34 Mapping of the Spatial Patterns which Account for the 2 Largest Variances in the Abnormal EEG, Patient 2 120

Figure 5.35a Temporally and Spatially Filtered EEG, Patient 2 121

Figure 5.35b Temporally and Spatially Filtered EEG, Patient 2 122

1. INTRODUCTION

Problem Statement

An intriguing problem and challenge in digital signal processing is the separation of specific signals from a conglomerate of background signals, artifacts and noise. The research which this thesis describes, addresses this problem as it pertains to the clinical application of invasive and non-invasive recording of the electrical activity of the brain, the electroencephalogram (EEG). The goal is to enhance the characteristic signal of an epileptic seizure within the EEG by eliminating those signal components which do not contribute to this abnormal activity.

The method through which this goal is achieved incorporates three filters; a temporal bandpass, a temporal pattern and a spatial pattern filter. It is the combination of the three filters which consistently achieves the desired results. Both the temporal pattern and the spatial pattern filters are designed following the same four steps of a data dependent design procedure. First, through the use of equations for potentials based on the current dipole model, singular value decomposition and spatio-temporal decomposition, a set of optimal basis vectors are determined. These basis vectors, referred to as temporal or spatial patterns, span a measurement space which embodies the data points of two EEG segments. Second, using a linear transformation which optimally aligns the basis vectors, the corresponding temporal waveforms are calculated. Third, the

abnormal and normal basis vectors and corresponding temporal waveforms are identified and separated. The last step utilizes a selected set of the abnormal basis vectors to derive the filter. The filter is then applied to an extended segment of the EEG resulting in filtered EEG with the abnormal activity enhanced. Finally, the spatio-temporal decomposition of a temporally and spatially filtered EEG effectively isolates the abnormal activity. This decomposition provides estimates of the abnormal source waveforms and spatial patterns. The abnormal source waveforms display the seizure onset and the abnormal spatial patterns lead to the location in the brain of the responsible sources.

Problem Overview

The term EEG generally refers to a set of tracings which display measurements taken at the multiple electrode sites spread internally in the brain or externally over the surface of the head. The EEG presents tracings of the simultaneous measurements taken from the electrode sites stacked vertically. Thus the horizontal perspective presents the signals as they develop over time. The vertical perspective presents the brain activity as it changes through time. Each tracing is a recording of the activity from the perspective of a different electrode location. Neurologists typically use EEGs in combination with neurological examinations, neuropsychological profiles, Nuclear Magnetic Resonance Imaging (MRI) and Single Photon Emission Computed Tomography (SPECT) procedures, along with patient history and clinical symptoms to analyze the activity in the brain. The EEGs are recorded during the

diagnosis and treatment of patients who are suspected of having a wide range of neurological problems, including epileptic seizures. It is the objective of the electroencephalographer to relate the potentials measured on the scalp to the underlying physiological processes.

In a clinical setting, expert analysts identify distinctive rhythms as normal and abnormal brain processes based on their temporal and spatial characteristics as presented in the EEG. Segments of the EEG display the amplitude, polarity, and frequency content temporally and spatially as distinctive rhythms. In addition to these attributes, it is the temporal development and the spatial progression of the rhythms over an extended EEG which provides valuable information to the experienced analyst. When the two dimensions of the EEG, temporal and spatial, are viewed simultaneously, it is the noticeable changes in each electrode tracing and differences between the electrode tracings which provide information regarding the underlying processes. This information provides an encoded view of abnormal and normal behavior present and possibly suggests the location of the responsible sources.

One of the most difficult EEGs to confidently analyze is one where the distinctive abnormal pattern is swamped by the strength of other potentials present at the electrode sites. In this case, the distinctive rhythm may not stand out against the other activity, thereby not providing visibility of the underlying abnormal process. Since the brain tissue is considered a conductive medium, each

electrode is able to sense every source even those with very small amplitudes. The challenge is to remove the interference and to expose distinctive patterns of the underlying abnormal process. This research endeavors to decompose the EEG into temporal and spatial components and these components are analyzed separately to determine seizure onset and source location.

To this end, the brain activity may be viewed as the intermingling of electric fields generated by multiple internal sources. Potentials measured at an electrode site result from the collective activity of many nerve cells. When the potentials in a group of neurons change synchronously they create distinctive rhythmical patterns. In some situations, the collective strength of a single pattern may be large enough to dominate potentials generated by other groups of neurons. In this case, the single pattern may be seen clearly in the EEG tracings at the closest electrode site and most probably at adjacent electrode sites. This dominant pattern can be identified as being associated with an abnormal or normal process. The coexistence of the abnormal and normal processes leads to the total brain activity being decomposed into subsets of abnormal and normal processes.

Since, the potential variations recorded at the electrode sites are composite signals, the model for the genesis of the EEG can be based on the superposition principle [Hjorth et al. 1988]. This principle states that the recorded signal can be represented as the linear sum of the signals generated by each of the sources whether

abnormal or normal. The following equation represents this principle for the potential at the i^{th} electrode site:

$$V_i = \sum_{j=1}^{p} M_{i,j} S_j \qquad (1.1)$$

Each row of the N channel EEG, as shown in equation 1.1, can be considered the linear combination of source waveforms. The elements of the row vector, $[M_{i,1}\ M_{i,2}\ \ldots\ M_{i,p}]$, are the weighting coefficients corresponding to each of the p source waveforms, S_1 through S_p. Since all of the p sources are common to all the rows of the EEG, the complete EEG can be decomposed into matrices **M** and **S**. The matrix **M** contains the stacked row vectors of weighting coefficients and the matrix **S** contains the row vectors of source waveforms. When viewed as a set of column vectors, the matrix **M** details the spatial characteristics, which specifies the distribution strengths at each electrode site, corresponding to the temporal characteristics, the source waveforms. The matrix **M** is referred to as the spatial pattern matrix and each column as a spatial pattern. The source waveforms display temporal patterns of normal and abnormal activity. The specific intent of this research is to isolate and identify the temporal and spatial characteristics attributed to abnormal processes.

For this purpose, the EEG can be viewed as a matrix of data samples with characteristics, relationships and dependencies which relate the temporal and spatial characteristics. Digital signal processing techniques such as singular value decomposition, spatio-temporal decomposition, and linear transformations can be applied

to derive temporal pattern and spatial pattern filters. The application of these filters, in combination with a traditional temporal bandpass filter, can be used to isolate the abnormal activity within an EEG. In fact, the data matrix can be decomposed into subsets of abnormal and normal spatial patterns, $\mathbf{M}_a$ and $\mathbf{M}_n$, and corresponding temporal waveforms, $\mathbf{S}_a$ and $\mathbf{S}_n$ [Koles 1991]. Thus, the spatio-temporal decomposition equation for the data matrix, $\mathbf{V}$, can be written as

$$\mathbf{V} = \mathbf{M}\,\mathbf{S} = \begin{bmatrix}\mathbf{M}_a \mathbf{M}_n\end{bmatrix}\begin{bmatrix}\mathbf{S}_a \\ \mathbf{S}_n\end{bmatrix} \tag{1.2}$$

Filtering the EEG should expose the temporal waveforms of the abnormal processes, $\mathbf{S}_a$, which exhibits the seizure onset and the spatial patterns, $\mathbf{M}_a$, from which the location of the sources of the abnormal processes can be determined [Koles 1991].

Area of Application

The medical condition towards which this research is focused is epilepsy. Individuals with epilepsy have distinctive types of EEG abnormalities which occur between and during clinically detectable seizures. The general term for the persistent abnormal activity particular to epilepsy is epileptiform activity [Tyner et al. 1983]. As described in more detail in the next chapter, the epileptiform activity typically has a rhythmical pattern which persists for various lengths of time, ranging from seconds to portions of minutes.

As previously mentioned, the EEG displays the collective summation of normal background activity, artifacts and abnormal activity. The term artifact refers to any electrical activity other than that generated by the patient's brain which is present in the tracing of the potentials at the electrode sites [Tyner et al. 1983]. All these signals combined in varying strengths hamper the identification of seizure onset and the source location. Therefore, the goal is to first separate the epileptiform activity from normal background signals, other abnormal signals and artifactual activity and second to quantify the temporal and spatial characteristics of the epileptiform activity.

Previous Research

Many filter design techniques have been employed to extract the abnormal activity from the EEG. Over the years, filters have changed from analog filters to digital filters. However, the result was still some combination of low-pass, high-pass and bandpass filters. These filters were designed using conventional filter design procedures, where the frequency response was known and the filter was designed to achieve that response. An example of this is the use of digital filtering to remove the electromyographic (EMG) artifact [Gotman et al. 1981].

Filters tuned to specific signals emerged from the quest to determine where and when a specific waveform appeared in an EEG. Matched inverse filters incorporating the autocorrelation of the EEG were used [Lopes Da Silva et al. 1977, Pfurtscheller et al. 1977,

Barlow 1979] to prepare the EEG prior to the use of event detection algorithms. In these filters, the frequency response of a filter template was based on a desired impulse response. Typically, the EEG was filtered using a filter selected from a stored set of standard waveforms representing standard epileptiform activities. Thereby the abnormal activity in the filtered EEG approximated a standard epileptiform activity.

A form of filtering, as applied to epilepsy, has been used [Gotman et al. 1976, Gotman 1982] to detect seizure onset through the decomposition of the EEG into wave segments. The pattern of these wave segments, in combination with the appearance of appropriate circumstances which typically precede an epileptic seizure, signify the likelihood of the onset of a seizure. These detection algorithms are used to trigger EEG recording machines.

Commonly, EEG research projects are based on the superposition principle [Hjorth et al. 1988]. Some also make use of autoregressive modeling used alone [Franaszczuk, 1994] or combined with inverse filtering [Pfurtscheller, 1977]. Autoregressive modeling assumes that an electrode potential can be predicted from the sum of previous potentials plus noise.

The similarity between all of the methods employed by the research projects mentioned above, is that they determine the filter based on standardized characteristics of the epileptic seizure. This addresses the challenge to design a process or filter which could be used for all seizures. The problem that arises is that this filter design tends to be broader in bandwidth and not specific enough to

eliminate the majority of extraneous activity. More recently, Kobayashi et al. [1996] utilized the source location to design a data dependent filter to extract obscure activity during an epileptic seizure from the EEG. Koles et al. [1995] developed a data dependent spatial filtering procedure which determined the spatial patterns of an EEG. These spatial patterns were then used to determine the source location. The research presented in this thesis builds on the concept of a data dependent filter. The design procedure developed was applied to evolve both temporal and spatial pattern filters specific to a patient's EEG. The application of these filters result in the isolation of the abnormal activity present in the EEG.

Research Objective

This research employs a traditional digital temporal bandpass filter, a newly developed data dependent temporal pattern filter followed with a previously developed [Koles, 1991] data dependent spatial filter. The bandpass filter is used to eliminate the base line shifts and any higher frequencies such as the EMG artifact or the 60 Hz power line noise.

The temporal data dependent filter design procedure decomposes a single electrode recording into a set of temporal pattern filtered (TPF) temporal waveforms. An epileptologist selects those waveforms which exhibit the particular epileptiform activity specific to each EEG. The selection is guided by the percentage of variance which the corresponding temporal basis vectors account for in the normal and abnormal activity. The

temporal pattern filter results from the recombination of temporal basis vectors which correspond to the selected TPF temporal waveforms. The filter is a template for the precise temporal characteristic of the abnormal process within a particular EEG. In the time domain, the temporal pattern filter defines the rhythmical potential variations characteristic of the abnormal process as seen horizontally in the EEG tracings. In the frequency domain, the temporal pattern filter is transformed into a set of frequency components with corresponding magnitudes which characterize the abnormal temporal process, defining the filter's frequency response.

The spatial pattern filter design procedure, applied to the temporally filtered EEG, determines the optimal common spatial patterns and the corresponding spatial pattern filtered (SPF) temporal waveforms. The spatial patterns which specify the relative amplitudes of the corresponding temporal waveforms at each electrode site can be used to determine the source location within the brain [Koles et al. 1995].

The ultimate objective of this research area is to filter the EEG separating the epileptiform activity into a single abnormal SPF temporal waveform and abnormal spatial pattern. The source location can then be derived from this spatial pattern. Therefore, isolating the abnormal temporal and spatial patterns is analogous to finding the key which decodes the EEG into the address for the group of neurons responsible for the epileptic behavior.

Document Overview

This document continues with a chapter reviewing the medical background of epilepsy, specifically the epileptic seizure, the genesis of potentials in the head, EEG terminology and types of electrodes. The third chapter presents the mathematical background from which the data dependent filter design procedure is developed. The fourth chapter describes the method used in this research. The method specifies, in detail, the application of the temporal bandpass filter and the four step filter design procedure for the design and application of the temporal pattern and the spatial pattern filters. The fifth chapter presents the results and the discussion of the filtering method as applied to three EEGs. These EEGs include a simulated EEG, a clinical EEG recorded from electrodes within the brain as well as on the surface of the brain and a clinical EEG recorded from only surface electrodes. The last chapter, Chapter six, contains the conclusions resulting from this research and identifies questions and further research topics.

2. MEDICAL BACKGROUND

This chapter starts with a description, based on the anatomy of the brain, of how the potentials measured at electrode sites are generated. The discussion continues with a review of the terminology used to describe EEGs and to classify the activity within an EEG as abnormal or normal. This chapter also includes the criteria for the identification of the abnormal activity typical of the epileptic seizures. It is this distinctive signal with its temporal and spatial characteristics which the epileptologist desires to identify and isolate. An understanding of the temporal and spatial characteristics of the epileptiform activity is helpful to substantiate the new data dependent filtering method developed. The chapter concludes with a discussion of surface, subdural and depth electrodes.

The first section presents an overview of the genesis of bioelectric potentials from the brain and is a paraphrase of the material presented by J. W. Clark in Chapter 4 of the text Medical Instrumentation: Application and Design [Webster 1992]. The information contained in the remaining sections of this chapter is a brief review of the material presented in Chapters 10 and 14 from the book Fundamentals of EEG Technology [Tyner et al. 1983]. As the references are numerous, it can be assumed that unless otherwise specified the information can be credited to the authors of these two books.

Bioelectric Potentials from the Brain

The anatomical structures of the brain generate electric fields within the brain and thus allow for electric potentials to be measured throughout the brain. The three major parts of the brain, the brainstem, the cerebellum and the cerebrum, as identified in Figure 2.1, form a closed system. The brainstem, an extension of the spinal cord, provides the link between the cerebral cortex, the spinal cord and the cerebellum. The brainstem controls life sustaining processes such as breathing, circulation and digestion as well as regulation of various muscle reflexes. The cerebellum coordinates the voluntary muscle system and acts in conjunction with the brainstem and cerebral cortex to maintain balance and coordination of muscle movements. The cerebrum, the largest portion of the brain, is the portion to which the conscious functions of the nervous system can be localized.

The cerebrum is split into pairs, the right and left cerebral hemispheres with each hemisphere relating to the opposite side of the body. The outer layer, the cerebral cortex, is the convoluted surface extending underneath the brain into the centermost part of the head. Some parts of this layer receive sensory information from skin, eyes, ears, and other receptors throughout the body. The cerebral cortex is packed with nerve cells that appear gray in color, and consequently this volume is referred to as the gray matter. The gray matter surrounds a core of white matter which consists of bundles of mylinated nerve fibers, the axons. Deep within the

cerebral white matter are several masses of gray matter, the basal nuclei, consisting of neuronal cell bodies.

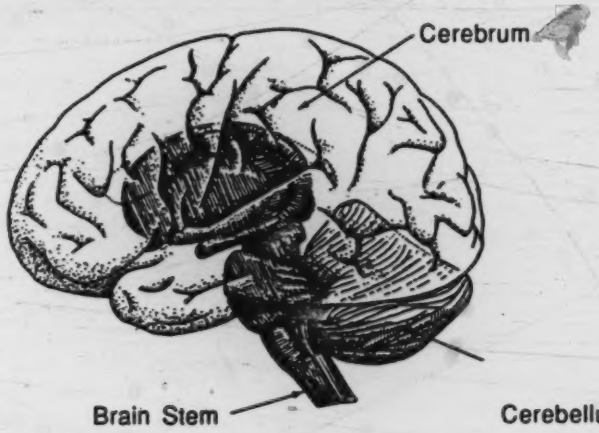

Figure 2.1 Parts of the Brain (From Medical Instrumentation Application and Design, JG Webster Editor, 1992, page 195)

The cerebral cortex, shown in Figure 2.2, is organized into a six layer stratification made up of mainly pyramidal cells and granule cells. The cortical neurons are not randomly distributed but instead are aligned along the axis normal to the cortical surface. This orderliness extends to both the distribution of cell types and their packing density. The normally oriented pyramidal cells, such as the one labeled a giant pyramidal cell in Figure 2.2, have long apical dendrites running parallel to one another.

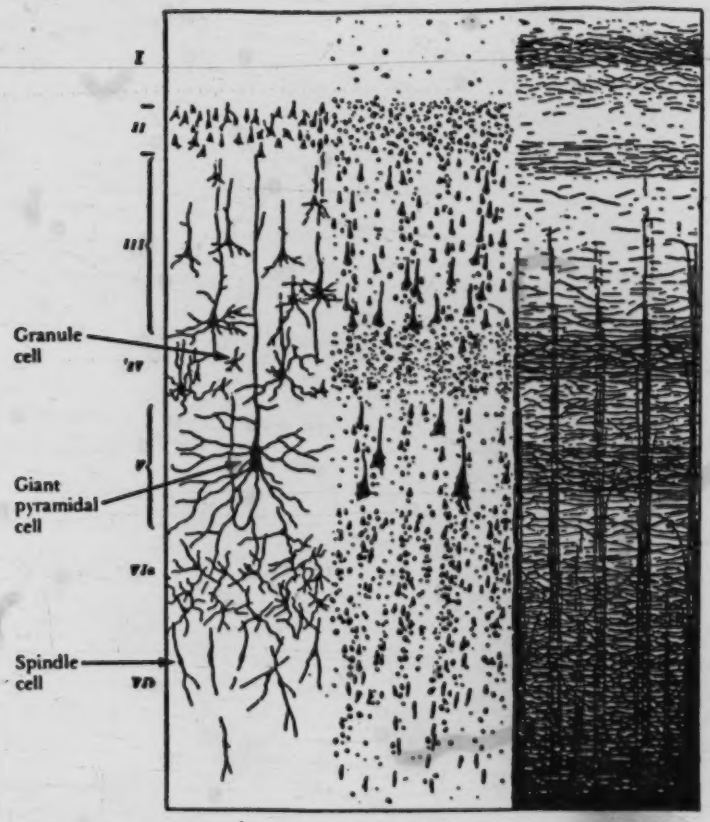

Figure 2.2 Cortical Layers (From Medical Instrumentation Application and Design, JG Webster Editor, 1992, page 202)

Differences in potentials can be measured in one part of a single cell body relative to another part. These differences in potentials create electric fields along which intercellular currents flow. The subthreshold current flows, as shown in Figure 2.3, in a closed path through the dendrites and cell body of the pyramidal cells, returning to the synaptic sites via the extracellular fluid. Due to the orderly alignment, the orientation of the cells, and if enough cells are synchronized, the potential difference can sometimes be measured at the cortical surface.

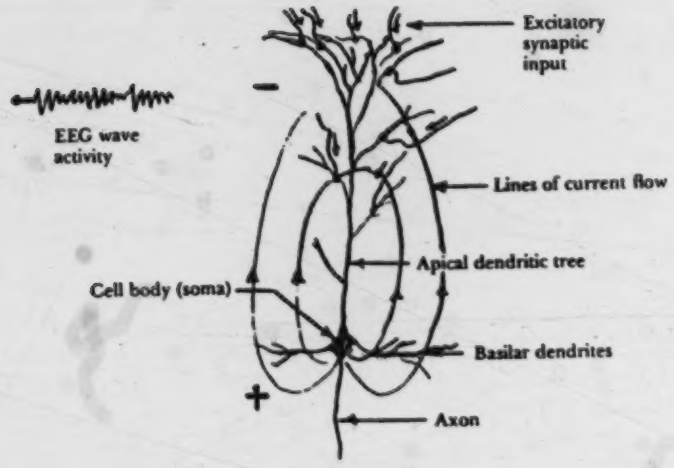

Figure 2.3 Cortical Dipole Field Potential (From Medical Instrumentation Application and Design, JG Webster Editor, 1992, page 205)

Although conducted action potentials in the axons are relatively significant in amplitude they contribute little to surface cortical records. Their net influence on the potential at the surface is negligible because these actions potentials occur asynchronously in a large quantity of axons, which run in many directions relative to the surface. But due to the alignment of each pyramidal cell, their current flow is additive within the system of cells. Thus a potential difference recorded at the surface results in the peaks and valleys, presenting an intricate signal attributed to the pyramidal potentials.

The resultant effect of this potential difference, referred to as a dendritic postsynaptic potential (PSP), depends on a combination of: the sign (excitatory (-) or inhibitory (+)), the orientation, and on the location relative to the potential measurement site. The effect

of each PSP may be regarded as creating an oriented dipole. The continuing synaptic input creates a series of potential dipoles and the resulting current flows are staggered but overlap in space and time. Thus, surface potentials can be generated by one population of presynaptic fibers and the cells on which they terminate.

Since the head is viewed as a large conductive medium of active elements [Gevins et al. 1991, Soong and Koles 1995, Nunez et al. 1991], a recorded potential change is a measure of the net potential difference between the electrode site and the reference electrode at that moment in time. Recordings can be taken from the inner surfaces of the brain, using subdural or depth electrodes, or from the scalp, using surface electrodes. The intensities of the brain waves recorded on the exposed surfaces of the brain, relative to a distant reference electrode such as the earlobe, range in values as large as 10 mV. Those recorded from the scalp have smaller amplitudes, approximately 100 μV, with frequencies ranging from 0.5 to 100 Hz. These oscillating electric potentials are referred to as brain waves and a recording of the potentials at multiple electrode sites is the electroencephalogram (EEG).

It appears as if brain waves are irregular and no general pattern can be observed, but distinct patterns do occur. The intensity and the patterns of the continuously oscillating electric activity is a measure of the functional activity of the brain. Some of the patterns can be recognized and are classified, based on the frequency per second, as belonging to one of four wave groups; alpha, beta, theta, and delta. These patterns under certain conditions and other patterns

not solely classified according to frequency can be attributed to specific abnormalities of the brain. Analysis of these patterns are crucial to the classification of EEGs.

EEG Descriptive Traits

EEGs are described in terms of their content, in that major patterns and changes in activity are referred to as they appear against a background. The background is the setting from which a change or pattern is distinguished and can be classified as normal or abnormal. EEG activity must be analyzed in reference to the patient's age and state of responsiveness; drowsy, awake and asleep. EEG activity can be described using a number of variables, those that are pertinent to this research are; frequency, amplitude, morphology, continuity and location.

A significant trait that is used to describe EEG activity is the stability of the frequency content, referring specifically to the rhythmic repetitive EEG activity. The pattern is rhythmic if the EEG activity consists of waves of approximately constant frequency. The EEG activity is arrhythmic if no stable rhythms are present. Dysrhythmic activity refers to rhythms and/or patterns of EEG activity which should not be present in a specific state in the healthy patients.

The voltage of an EEG is described in terms of amplitude level and attentuation. This term can be used in reference to either average voltage or peak voltage of EEG activity. A period of attenuation, the reduction of amplitude of EEG activity, has some

significance if the flattening of activity is seen prior to a burst of dysrhythmia. An increase in voltage and regularity of rhythmic activity implies an increase in the number of neural elements contributing to the rhythm. Both a normal or abnormal activity can emerge from the background with a rapid onset, and may reach a high voltage and end with an abrupt return to the underlying background activity.

Morphology refers to the shape of the waveform. The shape of the wave of the EEG pattern is determined by the frequencies that combine to make up the waveform and by their phase and amplitude relationships. Surface polarity is either negative or positive in reference to a particular activity or waveform at specific electrode locations. The terms monomorphic or polymorphic describe the number of dominant frequencies combined to form a simple or complex waveform. Sinusoidal refers to waves that resemble sine waves. A transient is a isolated event, a wave or pattern that is distinctly different from background activity such as a spike or sharp wave. A complex refers to a sequence of two or more waveforms, not necessarily of the same frequency, creating a pattern distinctly different from the background activity.

The specific EEG activity can be continuous, discontinuous or intermittent, regular and irregular. This term can be used to describe the continuity of a particular pattern or series of events.

Location of the EEG activity refers to the scalp distribution of that particular rhythm or pattern. The location is generalized if the activity is not limited to a specific area. The pattern is lateral or

lateralized if it appears to come from one side of the brain; or bilateral, if it comes from both sides. The term focal indicates the involvement of a specific part of the brain rather than the whole brain. The EEG activity is symmetrical when the pattern is equally distributed over structurally corresponding areas.

EEG Classifications

A significant element in the analysis of an EEG for the purposes of diagnosis is the change in activity from normal to abnormal. Most significant is the identification of the onset of the abnormal activity. Therefore the distinction between normal and abnormal activity is fundamental to the filter design method presented in the following chapters.

Normal EEG activity is defined as any distinctive activity that appears in the EEGs of large groups of people known to have no complaints, no symptoms, no neurological or other disease and no family history of neurological disease. Any EEG activity observed in this healthy group, the control group, is considered normal EEG activity. Abnormal EEG activity is defined as any of the EEG activities which do not appear in the EEGs of the control group.

Normal EEG activity is different for individuals who are awake and for those who are asleep. Awake activity typically consists of combinations of alpha, beta, theta activity, mu rhythm, lambda waves and posterior slow waves. Alpha activity has the frequency range of 8 to 13 Hz, but averages about 10 Hz. Beta activity is an activity with a frequency faster than 13 Hz, generally referring to

rhythmic activity in the 14 to 25 Hz range. Theta activity includes frequencies between 4 and 7.5 Hz. Mu rhythm is an archlike activity with average frequency of 9 Hz, but ranging from 7 to 11 Hz. Lambda waves are sharp waves with an equivalent frequency of 4 to 6 Hz which occur during drowsiness. Posterior slow waves of youth are delta, below 3.5 Hz, and alpha activity intermixed and sometimes resembles sharp and slow wave activity.

Abnormal EEG activity must have one or more of the following six conditions to be considered abnormal:

i) an increase or decrease of the frequency of the basic rhythm, in comparison to a similar aged control group, particularly if asymmetrical;

ii) an increase or decrease in amplitude of the particular EEG activity, in comparison to the control group, particularly if asymmetrical;

iii) a difference in the locations of various frequencies, in comparison to the control group;

iv) a difference in the morphology of the waveforms, compared to those encountered in the control group;

v) an appearance of distinctive elements with a delay between appearances, which is unusual for the age and state;

vi) an atypical response or loss of reactivity to stimulation.

Some specific abnormal EEG patterns include spikes, sharp waves, spike and wave complexes, sharp and slow wave complexes, rhythmic hypersynchronous activity, periodic discharges, triphasic waves, excessively slow activity, excessively fast activity, and excessively high amplitude activity.

As mentioned previously, the EEG does not represent only cerebral activity, but includes other electrical activity that is not of cerebral origin. This activity, referred to as noise or artifact, includes physiological effects such as electromyographic (EMG) or muscle artifact, electrocardiographic activity (pulse and pacemaker artifacts), eye movement, myogenic (jaw movement) and glossokinetic (tongue movement) potentials, respiration, tremor and electroretinogram. Other non-physiological artifacts such as those arising from the 60 Hz powerline, electrode noise, and body movement may also be present in an EEG.

The descriptions of normal and abnormal activity has been made in reference to activity recorded from groups of people. But similar distinctions can be made for segments within a single EEG record. Therefore, a single EEG record can contain a section of abnormal EEG activity and a section of normal EEG activity.

Epileptic Seizures

The term epileptic seizure is an abstract description as there are many different types of epileptic seizures. Each patient may have multiple seizures, each having different clinical signs and symptoms The seizure free period preceding a seizure and the

interval between seizures are termed the preictal period and the interictal period, respectively. These periods, during which the patient appears to be in her/his usual state, define the normal activity within a specific EEG. The interval of altered behavior, the ictus, includes the onset of the abnormal activity and the progression of that particular activity. The seizure onset may be focal or generalized and the duration of the ictus is variable in type and severity. There may be immediate and total loss of consciousness, partial impairment of consciousness or no impairment throughout the ictus. As the signs and symptoms of the seizure end, a postictal period begins during which a transient EEG abnormality may be present.

The abnormal neuronal activity during the ictal period of the EEG appears as a discharge with epileptiform characteristics. The observable epileptiform pattern generally consists of distinctive waves or complexes, which are distinguishable from background activity. The development of the observable seizure phenomena requires, even for the production of a focal seizure, the synchronized firing of a large population of cerebral neurons.

As described previously, with respect to general brain activity, the neurons of the brain normally function through orderly processes of excitation and inhibition; the resultant balance establishes the cerebral state and behavior. During an epileptic seizure, groups of cerebral neurons discharge in an uncontrolled, and abnormal manner, and the normal course of behavior is disrupted. Uncontrolled neuronal activity can be caused by three conditions; i) too much

excitation, ii) too little inhibition, and iii) the development of hyperirritable neurons that are either continuously or recurrently so close to their firing thresholds that they discharge spontaneously.

Typically, epileptic seizures are classified into three groups: partial seizures, generalized seizures and unclassified seizures. Partial seizures are characterized by symptoms with the onset limited to neurons in one part of the cerebral hemisphere. Simple partial seizures have no impairment of consciousness whereas complex partial seizures are those with altered consciousness. Generalized seizures are characterized by clinical behavior which may represent the initial involvement of both hemispheres with consciousness severely impaired and during which bilateral motor manifestation occur.

The Recording Electrodes

If generators within the brain are represented as dipoles with current flowing between the cell body, the source, and the dendrites, the sink. Placing an electrode in the electric field generated by this dipole will enable the potential difference between this electrode and a reference electrode to be measured. Electrodes placed at a significant distance, will not be able to pick up the field potentials of a single neuron since the potentials are too small and are also affected by the activity of adjacent neurons. Neurons arranged randomly in space and those which are activated randomly do not produce significant field effects because their activities cancel each other. Therefore, the potentials which are recorded at a

distance from the generators are the result of dipoles which are geometrically aligned and activated synchronously. As seen in Figure 2.4, a surface electrode (macroelectrode) generally reflects the activity of a large number of neurons when they are activated synchronously. A depth electrode (microelectrode) frequently reflects the activity of a small number of neurons which may not be representative of the majority of the neurons.

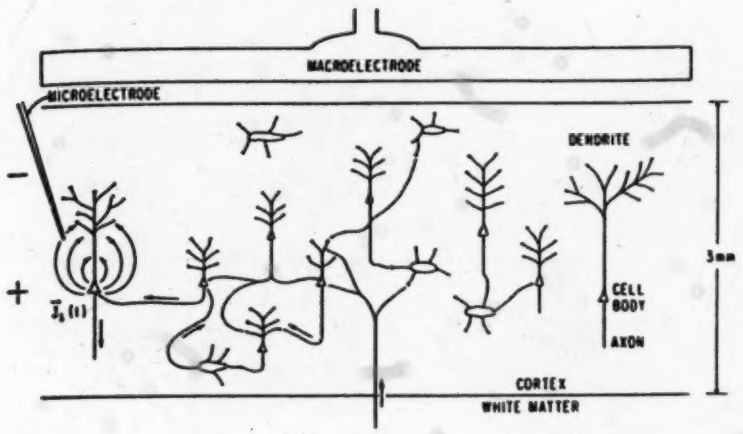

Figure 2.4 Cortical Tissue with Electrodes (From Electric Fields of the Brain, PL Nunez, 1981, page 77)

Non-invasive recording uses surface electrodes typically placed on the scalp following the International 10-20 System of electrode placement. Figure 2.5 displays the superior view of the electrode site locations and Table 2.1 identifies the label, specifying the appropriate channel, and the location of each electrode site.

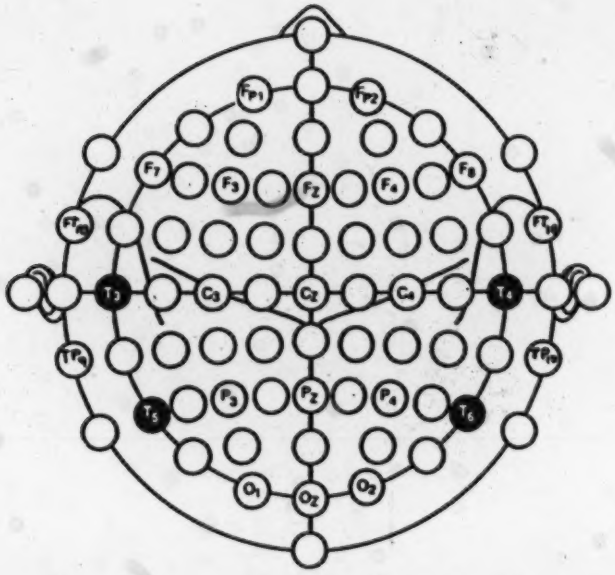

Figure 2.5 Electrode Positions- The Extended International 10/20 System (Adapted from Current Practice of Clinical Electroencephalography, DD Daly and TA Pedley Editors, 1990, page 47)

Label	Spin	Tip	Label	Spin	Tip
FP1	-108.00	90.00	FP2	-72.00	90.00
F3	-130.71	58.57	F4	-49.29	58.57
C3	-180.00	45.00	C4	0.00	45.00
P3	-229.29	58.57	P4	49.29	58.57
O1	-252.00	90.00	O2	72.00	90.00
F7	-144.00	90.00	F8	-36.00	90.00
T3	-180.00	90.00	T4	0.00	90.00
T5	-216.00	90.00	T6	36.00	90.00
Fz	- 90.00	45.00	Cz	-90.00	0.00
Pz	-270.00	45.00	Oz	90.00	90.00
LSPH or FT9	-162.00	112.50	RSPH or FT10	-18.00	112.50
LMAS or TP9	162.00	112.50	RMAS or TP10	18.00	112.50

Table 2.1 Electrode Angles (Adapted from working material of the Biomedical Engineering Department, University of Alberta, ZJ Koles, 1996)

In this system the electrodes are located on the top half of a perfect sphere. The center of the head is then assumed to be placed at the

center of the 3 dimensional coordinate system. Thus two angles, tip and spin specify the electrode site location. These angles are listed in Table 2.1 and depicted in Figure 2.6.

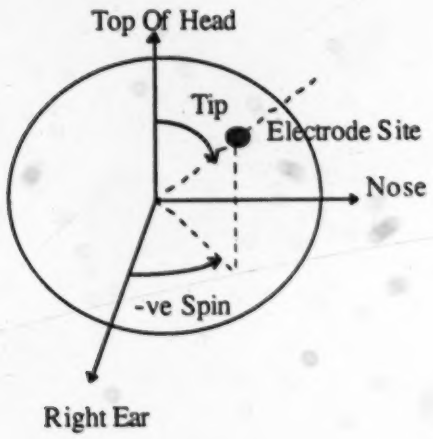

Figure 2.6 Tip and Spin (From working material of the Biomedical Engineering Department, University of Alberta, I Buclieu, 1996)

One of the limitations of recording from surface electrodes is the low amplitude of the electrical brain potentials. Therefore, contamination of the recording with noise and artifacts represents a significant difficulty especially when trying to record the extremely low amplitude potentials.

Invasive recording, using subdural or depth electrodes, allows for the elimination of some artifactual interference and the attentuation of the potentials due to the skull resistance. Another advantage of invasive recording is that the electrodes conduct potentials generated by a relatively small number of generators. Specifically, from those located deep in the brain, or from those oriented in such a way in the folds of the cortex that it makes it

difficult to pick up their activity from the surface. Therefore invasive techniques, with the electrodes placed closer to the generators, generally reflect the activity of a smaller number of neurons, those closest to the electrode.

Subdural electrodes are designed to provide cortical recordings. The electrodes are placed in a grid or in strips. The grid, a 2 dimensional array of electrodes, covers an extensive local area. The strip electrodes are slipped under the dura into the subdural space. The strip electrode sites range from the point of entry through to a desired location.

Depth electrodes are arrays of electrodes designed for introduction directly into the substance of the brain and the recording of subcortical structures. Depth EEG recordings usually demonstrate excellent signal-to-noise ratios, since the electrodes are not generally plagued with interference by muscle and movement artifacts and bypass the high-resistance of the skull. The morphology of the epileptiform activity recorded using depth electrodes can be considered the gold standard for the representation of the abnormal waveform. Although, the epileptiform activity originating in a particular depth electrode only indicates that this electrode location is closer than the others to the seizure focus. Thus, the ictal changes detected by this electrode do not necessarily begin in the structures from which the recording is obtained. Thus it is advantageous when invasively recording, to simultaneously record from multiple electrode types and locations, including from surface electrodes.

3. Mathematical Background

This chapter presents the mathematical background on which a data dependent filter design procedure is based. As described in Chapter 1, the filter is designed to extract seizure related ictal activity from recorded brain activity. This objective is split into three parts; first, the approximation of recorded brain activity, second, the decomposition of the brain activity into abnormal and normal activity, and third, the extraction of the epileptiform activity.

The mathematical background consists of mathematical principles and operations that are fundamental to the above stated objective. Initially, this chapter includes a brief review of the approximation of source potentials. The bulk of the chapter incorporates a detailed review of matrix algebra operations as applied to recorded data. These operations lead to the decomposition of the recorded data and aid in the separation of the epileptiform activity from extraneous ictal, artifactual and background activity.

Approximation of Source Potentials

The current dipole has been used as an acceptable model for the source of electrical activity within the brain [Nunez et al. 1991]. As described in Chapter 2, a group of synchronously acting neurons can be considered the source of the electrical activity. The potentials generated by current dipole sources have been used to approximate the electrophysiological processes of this group of neurons. The

electrical currents generated by these sources are volume conducted throughout the brain to the recording electrodes [Gevins et al. 1991, Soong and Koles 1995, Nunez et al. 1991]. Based on this, the potentials due to localized sources spread over various areas of the scalp. It follows that the potential measured at a scalp electrode site represents the summation of signals from many sources, including abnormal and normal sources [Gevins et al. 1991, Koles 1991].

This summation of the activity from multiple sources is an application of the linear superposition principle. This principle states that the composite electric field due to many sources can be expressed as a vector sum of the individual fields produced by each source [Hjorth et al. 1988]. Based on this, equations for the potentials measured at electrode sites can be written that combine both abnormal and normal source activity [Koles 1991]. These equations will be specified in a later section.

To summarize, three concepts of significant importance can be employed. The first concept is that each source can be modeled separately as a current dipole source. The second is that the summation of the separate source activities can be equated to the potential at each electrode site, The third concept, discussed in the previous chapter, is that of the utility of medical expertise and information. As presented in Chapter 2, this information can be used to identify the abnormal and normal patterns that may appear temporally and spatially within composite signals. The combination of these three concepts, as reported by Koles [1991], provide the

framework for the decomposition of the recorded EEG. Further, using this decomposition, the spatial and temporal information of the abnormal source(s) can be determined.

The application of these concepts are used to develop the potential equations representative of each channel recording. These equations and the basic matrix operations applied in previous research studies are presented in detail in the following sections.

EEG Data Matrix

Basic to signal processing is the fundamental concept of vectors and matrices. A matrix is an array of real or complex numbers. In the case of the EEG, the numbers correspond to digitally converted EEG signals [Harner 1990]. Most computerized analysis of EEGs utilize this concept [Koles 1991, Harner 1990, Hjorth 1989, Hjorth and Rodin 1988].

To this end, the multichannel EEG record can be viewed as a matrix of data points simultaneously sampled at different electrode sites at regular intervals [Koles 1991]. The T potential measurements taken from each of the N electrode sites can be formatted as an (NxT) data matrix:

(3.1)

$$\begin{bmatrix} V_{11} & V_{12} & V_{13} & \cdots & V_{1T} \\ V_{21} & V_{22} & V_{23} & \cdots & V_{2T} \\ V_{31} & V_{32} & V_{33} & \cdots & V_{3T} \\ & & \vdots & & \\ V_{N1} & V_{N2} & V_{N3} & \cdots & V_{NT} \end{bmatrix}$$

The above matrix can be viewed in each of its two dimensions; horizontal rows and vertical columns. The view of the data matrix, as a set of horizontal rows of data points is referred to as the temporal view. The rows of the matrix correspond to wave amplitudes as a function of time in each electrode recording [Harner 1990]. Therefore, each row provides a different measurement viewpoint of the underlying processes within the brain as they change over time.

The spatial view of the data matrix, is a set of vertical columns of data points. A single column of the measurement matrix contains one set of simultaneous potential measurements taken at each of the N electrode sites. This single column can be interpreted as a snapshot of the spatial distribution of the collective activity within the brain, at that specific moment in time.

Spatio-Temporal Decomposition

Hjorth et al. [1988] and Koles [1991] both base their analysis on the EEG data matrix viewed as a linear combination of source waveforms. As mentioned in a previous section, the linear superposition of the potentials generated by each source measured at each electrode site can be specified by a general equation. Thus, the potential measured at a specific electrode generated from p sources can be written as:

(3.2) $$V_i = \sum_{j=1}^{p} M_{ij} S_j$$

The index i identifies which of the N electrode recordings or which row of the data matrix is being defined. The index j specifies the particular source.

Using equation 3.2, each row of the data matrix presented in equation 3.1 can be approximated. Equation 3.3 presents this result in a general format that is typically referred to as the spatio-temporal decomposition of a data matrix.

$$\mathbf{V} = \mathbf{M}\,\mathbf{S} \tag{3.3}$$

The above equation presents the data matrix, **V**, decomposed into two matrices, the spatial matrix and the corresponding temporal waveform matrix [Koles et al. 1995, Koles 1991]. According to equation 3.2, the spatial matrix, **M**, consists of p columns. Each column is referred to as a spatial pattern. A spatial pattern is the distribution of the field strength of the corresponding temporal waveform across the N electrode sites. These values reflect the location of the source that generates the corresponding electrical activity [Hjorth et al. 1988]. The temporal waveform matrix, **S**, can be viewed as p rows of source waveforms. These source waveforms represent the variation in potential of each source within the brain as it changes through time. By convention the labels M and S are reserved for reference to the exact spatial patterns and temporal waveforms of sources that generate the brain activity. Other spatio-temporal decompositions will use other labels.

Using the format of equation 3.3, the spatial matrix can be viewed as a matrix specifying the electrode from which the electrical activity was recorded. The sampled potentials are

assigned the corresponding row in the temporal waveform matrix. Therefore, these two matrices provide both the spatial and temporal information responding to the questions "from where" and "what and when" with regard to the recorded data. These details are displayed in equation 3.4. The spatial matrix, in this case the identity matrix, identifying the specific electrode from which the data has been obtained. The temporal waveform matrix is the data measurement matrix shown in equation 3.1 and in this decomposition is equivalent to the data matrix **V**.

$$(3.4)\quad \mathbf{V} = \begin{bmatrix} 1 & 0 & 0 & \cdots & 0 \\ 0 & 1 & 0 & \cdots & 0 \\ 0 & 0 & 1 & \cdots & 0 \\ & & & \ddots & \\ 0 & 0 & 0 & \cdots & 1 \end{bmatrix} \begin{bmatrix} V_{11} & V_{12} & V_{13} & \cdots & V_{1T} \\ V_{21} & V_{22} & V_{23} & \cdots & V_{2T} \\ V_{31} & V_{32} & V_{33} & \cdots & V_{3T} \\ & & \vdots & & \\ V_{N1} & V_{N2} & V_{N3} & \cdots & V_{NT} \end{bmatrix}$$

The spatio-temporal decomposition of a particular data matrix is not unique. In fact any number of temporal waveform and spatial pattern matrices may be used to reconstruct the data matrix.

Basis Vectors

A set of spatial patterns that are linearly independent and span the space that embodies the data may be referred to as a basis set [Strang, 1976]. A set of vectors is linearly independent if none of the vectors can be written as a linear combination of the others [Strang, 1976]. Each of these spatial patterns can be referred to as a basis vector. Usually, but not necessarily, basis vectors are not only linearly independent but orthogonal. Orthogonal vectors are vectors that have a dot product of zero [Strang, 1976]. If the vectors are also

normalized, then the basis vectors have unit length and are referred to as being orthonormal [Strang, 1976].

Any data matrix can be expressed in terms of a linear weighted sum of basis vectors. These basis vectors can be non orthogonal, orthogonal or orthonormal. This concept can be expanded so that a particular set of basis vectors can be derived according to particular specifications.

Singular Value Decomposition

One such specification is to constrain the basis vectors to be not only orthonormal but also optimal with respect to the portion of total variance they each account for in the data matrix. The derivation of basis vectors meeting these constraints is termed singular value decomposition (SVD) analysis. This analysis is a linear expansion of the data matrix through the use of a minimal set of orthonormal basis vectors each constrained to account for maximum variance. [Hjorth et al. 1988, Hjorth 1989, Harner 1990, Koles 1991].

As presented by Koles, singular value decomposition expands a (NxT) data matrix, **V**, into three matrices;

$$\mathbf{V} = \mathbf{U}\,\lambda\,\mathbf{Q} \tag{3.5}$$

The columns of the (NxN) matrix **U** form the minimal set of orthonormal basis vectors, the eigenvectors of the covariance matrix $\mathbf{VV}'$. A following section discusses in detail this covariance matrix. The eigenvectors occur in descending order according to the

variance they account for in the data matrix. The first vector represents the most prominent, highly correlated and widespread feature of the original data matrix [Harner 1990]. The singular value matrix, λ, is a (NxT) matrix of singular values and is equal to the square root of the variance. The elements of the singular value matrix are zero except for the diagonal elements. The diagonal of λ_{NxN} is the vector $[\lambda_1, \lambda_2, \lambda_3, \ldots \lambda_N]$. The diagonal element, λ_j, corresponds to the j^{th} column vector and row vector of the matrices **U** and **Q** respectively. The matrix, **Q**, is a (TxT) orthonormal matrix of eigenvectors of the covariance matrix **V'V**. If **V** is a square data matrix then **UQ = I,** where **I** the identity matrix. In this case, **Q** can be shown to be the inverse of **U** as well as the transpose of **U**, and are termed unitary. The elements of matrices λ and **Q** are ordered corresponding to the order within **U.**

Although the matrix λ is of dimension (NxT), the rank of **V** will be equal to or less than N. The rank of a matrix is equivalent to the maximum number of nonzero singular values. Typically, the rank also represents the minimal number of orthogonal vectors required to span the space. In many cases, the data matrix, **V**, is overdetermined and the rank will be less than N. This means that the data matrix requires less than N orthogonal vectors to reconstruct the data matrix **V** [Hjorth et al. 1988, Harner 1990, Koles 1991]. But in general the rank of a matrix also indicates the number of linearly independent vectors in a basis set of vectors [Strang 1976]. This suggests that if a set of vectors can be found such that the difference in their direction is not zero but this set is of full rank

and spans the space then this set can also be referred to as a basis set for that space. It follows that these vectors are also linearly independent.

Linear Transformations

The results of the singular value decomposition of a data matrix can be equated to the results of a spatio-temporal decomposition of the same data matrix. If the temporal waveform matrix is defined as the rows of **Q** scaled by the singular values;

(3.6) $$\mathbf{Y} = \lambda \mathbf{Q}$$

and the spatial pattern matrix as the basis vector matrix **U**, then based on equation 3.3, a spatio-temporal decomposition of the data matrix, **V**, can be written as:

(3.7) $$\mathbf{V} = \mathbf{U}\,\mathbf{Y}$$

Basis Vectors ↵ ↓

Temporal Waveforms ↵

Since the basis vectors, the columns of **U** from the singular value decomposition, are orthonormal equation 3.7 can be inverted and rewritten as:

(3.8) $$\mathbf{Y} = \mathbf{U}'\,\mathbf{V}$$

It is this form of **Y** that can be viewed as a linear transformation of **V** where **U'** is the (NxN) transformation matrix [Fukunaga 1972] In the new coordinate system, the unit length basis vectors define the direction of the axes. The linear transformation can be thought of as the projection of the data matrix, **V**, onto the basis vectors,

resulting in the temporal waveforms, **Y**, that correspond to the distances along the new axes. In practice, if the basis vectors, **U**, and the data matrix, **V**, are known then equation 3.8 can be used to calculate the temporal waveforms **Y**. Each value in **Y** corresponds to an original data point in **V**.

Transformations can be used to reduce the dimension of the data set, as in the case when the data matrix is overdetermined. To accomplish this the transformation matrix is derived from a reduced set of basis vectors that span the same measurement space. A typical reduced set is based on the fact that the number of orthogonal basis vectors having a magnitude of any significance is always much smaller than the number of electrodes contained in the original EEG [Harner 1990, Hjorth et al. 1988]. Hjorth and Rodin also report that since a few eigenvalues stand out significantly from the general noise level of the remaining eigenvalues, then these eigenvalues represent the choice of eigenvectors and temporal waveforms to be studied.

For example, if a set of basis vectors, $\mathcal{B}$, and a corresponding set of temporal waveforms, $\mathcal{C}$, are derived by some linear transformation of **U** and **Y** respectively, then the data matrix, **V**, can be constructed using $\mathcal{B}$ and $\mathcal{C}$. If the basis vectors, $\mathcal{B}$, are unitary then equation 3.7 can be used. But if the set of basis vectors are derived such that $\mathcal{B}\mathcal{B}' \neq \mathbf{I}$, then the inverse is used instead of the transpose in the construction of **V**:

(3.9) $$V = (\mathcal{B}')^{-1} C$$

Basis Vectors ↵ ↓

Temporal Waveforms ↵

Further, should the matrix of basis vectors, $\mathcal{B}$, be of the dimension that is traditionally non-invertible then the psuedo-inverse can be used in place of the inverse in equation 3.9.

In the above example, based on the naming convention established in equation 3.7, equation 3.9 also depicts a spatio-temporal decomposition of the data matrix **V**. Therefore matrix transformations can be used to derive other spatio-temporal decompositions of an EEG. The goal in this research is to find a spatio-temporal decomposition that isolates, to a minimal number of basis vectors, the abnormal patterns that may or may not be apparent from the recorded data samples.

Covariance Matrix

Transformations can also be used to enhance specific features. One such transformation makes use of the covariance of the data. The covariance matrix describes relational information among the EEG channels based mainly on the waveform but also taking into account the amplitudes [Harner 1990]. An estimate of the spatial covariance matrix of any data matrix can be obtained from the product of the data matrix and its transpose [Hjorth et al. 1988, Koles 1991]. Thus the covariance matrix of **V**, $\mathbf{R}_V$ can be written as:

(3.10) $$R_V = V\,V'$$

where R_V is a (NxN) matrix containing, on the diagonal, a measure of the variance of each of the rows of **V** and, off diagonal, a measure of the covariance between all possible rows [Koles 1991]. If the data matrix **V** is expressed in terms of a singular value decomposition then the covariance equation can be written as:

(3.11) $$R_V = (U\,\lambda\,Q)\,(U\,\lambda\,Q)'$$

$$= U\,\lambda\,(Q\,Q')\,\lambda\,U'$$

$$= U\,\lambda^2\,U'$$

Therefore, the singular value decomposition of a general (NxN) covariance matrix can be written in the following format:

(3.12) $$R = U\,\Lambda\,U'$$

This means that any covariance matrix, **R**, can be decomposed into a matrix of orthonormal basis vectors, **U**, the transpose matrix, **U'**, and a diagonal matrix of eigenvalues, Λ. The diagonal elements of Λ are the square of the singular values, λ^2, of **V**.

Applying this result, the covariance matrix of **Y**, where **Y** is a linearly transformed data matrix, can be determined. Based on equation 3.8 and 3.10, the covariance matrix R_Y, is:

(3.13) $$R_Y = Y\,Y'$$

$$= U'\,V\,V'\,U$$

$$= U'\,(R_V)\,U$$

The covariance of the original data matrix, R_v, can be further expanded using the spatio-temporal decomposition of equation 3.11:

$$R_v = U' (U \lambda^2 U') U$$

$$= \lambda^2$$

$$= \Lambda$$

From this result the covariance matrix, R_v, is as a diagonal matrix. In summary, a linear transformation matrix that will diagonalize the covariance matrix of data points in a new coordinate system is the transpose of the basis vectors derived from the covariance matrix of the data points in the old coordinate system [Fukunaga, 1972]. The diagonal matrix indicates that the transformed data elements, **Y**, are uncorrelated [Hjorth 1989] whereas the original data elements, **V**, are typically correlated. Since the orthonormal basis vectors, the columns of **U**, are linearly independent, each column can be used as a mutually perpendicular axis in the new coordinate system.

Whitening Transformation

Transformations can be used to enhance, identify and separate the data points. One such transformation is the whitening transformation [Fukunaga 1972, Koles 1991]. The whitening transformation matrix, **W**, that transforms the data matrix **V** into the whitened data matrix, **Z**, can be defined as:

(3.14) $$W = \Lambda^{-1/2} U'$$

where the eigenvalue matrix, Λ, and the basis vector matrix, **U**, are derived from the decomposition of a covariance matrix as shown in equation 3.12. The transformation equation can be written as:

$$\mathbf{Z} = \Lambda^{-1/2}\,\mathbf{U}'\,\mathbf{V} = \mathbf{W}\,\mathbf{V} \tag{3.15}$$

Although applied as a unit, the whitening transformation matrix can be subdivided into the two linear transformation matrices, **U'** and $\Lambda^{-1/2}$. To clarify the effect of the application of each of these transformations they are analyzed separately. First as defined in equation 3.16 the linear transformation, **Y**, is a projection of the data matrix into another coordinate system,

$$\mathbf{Y} = \mathbf{U}'\,\mathbf{V} \tag{3.16}$$

where any data matrix **V** is transformed into **Y**, the corresponding temporal waveforms in the new coordinate system. As previously mentioned, the covariance of the linearly transformed matrix **Y** results in a diagonalized covariance matrix, Λ:

$$\mathbf{R}_Y = \mathbf{U}'\,\mathbf{R}\,\mathbf{U} = \mathbf{U}'\,(\mathbf{U}\,\Lambda\,\mathbf{U}')\,\mathbf{U} = \Lambda \tag{3.17}$$

The second transformation, the scaling of the basis vectors by $\Lambda^{-1/2}$ will modify the covariance matrix, $\mathbf{R}_Y$, to equal the diagonal identity matrix, **I**:

$$\mathbf{R}_Z = \Lambda^{-1/2}\,\mathbf{U}'\,\mathbf{R}\,\mathbf{U}\,\Lambda^{-1/2} = \Lambda^{-1/2}\,\Lambda\,\Lambda^{-1/2} = \mathbf{I} \tag{3.18}$$

Therefore, the whitening transformation matrix, **W**, shown in equation 3.14, scales the basis vectors, **U**, to be inversely proportional to the square root of the corresponding eigenvalue in Λ.

Although R_Z remains diagonal, the use of the scaling matrix in the whitening transformation does not preserve orthonormality [Fukunaga 1972] since:

$$(\Lambda^{-1/2}\ U')'\ (\Lambda^{-1/2}\ U') \neq I.$$

In summary, the whitening transformation, Z, can be viewed as a projection of the data matrix onto the scaled axes of the new coordinate system. As described later, the simultaneous diagonalization of two covariance matrices incorporates this whitening transformation [Fukunaga 1972].

Composite Covariance Matrix

If an EEG record contains both abnormal and normal segments then this information can be used to derive the axes of a new coordinate system that embodies data from both segments [Koles 1991]. The technique, reported by Koles, that can be used to derive a common set of basis vectors, U_c, for two EEGs is the singular value decomposition of a composite covariance matrix. The composite covariance matrix, R_c, is built from the covariance matrices of both an abnormal segment, V_A, and a normal segment, V_N. Each segment, V_A and V_N can be portrayed using the same format as equation 3.1.

The composite covariance matrix is defined as:

$$R_C = R_A + R_N \tag{3.19}$$

where the covariance matrices, R_A and R_N, are initially calculated as defined in equation 3.10 but are also normalized. Each matrix is normalized, as shown in equation 3.20, using the trace of the

appropriate covariance matrix. The trace of a matrix is the sum of the diagonal values.

(3.20) $$R_A = V_A \, V_A' \; / \; \text{trace}(V_A \, V_A')$$

$$R_N = V_N \, V_N' \; / \; \text{trace}(V_N \, V_N')$$

The normalization accommodates the different magnitudes of the potentials from the two different data segments and allows the two covariance matrices to be added without amplitude bias [Koles 1991].

The square composite covariance matrix, R_c, can then be expanded into three matrices by singular value decomposition.

(3.21) $$R_c = U_c \, \Lambda_c \, U_c'$$

These orthonormal basis vectors U_c can be used as the axes in a new coordinate system that encompass data from both the abnormal and normal EEG.

Simultaneous Diagonalization

The technique of simultaneous diagonalization pulls together two transformations that enable the partitioning of the elements of an EEG data matrix into abnormal and normal EEG data matrices. First, the composite covariance matrix provides the whitening transformation elements to derive a set of scaled basis vectors that can be used as a set of axes in a new coordinate system. This new coordinate system encompasses data from both the abnormal and normal EEG data matrices. Second, a whitened covariance matrix

provides a set of basis vectors which can be used to transform the data points in the new coordinate system into a partitionable space. This section is a review of an application of simultaneous diagonalization as reported by Koles [1991].

To this end, the whitening transformation matrix, **W**, is built using the matrices derived from the singular value decomposition of the composite covariance matrix as shown in equation 3.21. Thus, the two transformed data matrices, Z_A and Z_N, can be obtained from the linear transformation of the abnormal and normal data matrices, V_A and V_N:

(3.22)
$$Z_A = \Lambda_c^{-1/2} U_c' V_A = W V_A$$
$$Z_N = \Lambda_c^{-1/2} U_c' V_N = W V_N$$

Next, the whitened covariance matrices, R_{WA} and R_{WN}, can be derived using equation 3.13 for the covariance matrix of a linearly transformed data matrix. Further, each whitened covariance matrix can be expanded into 3 matrices by singular value decomposition [Koles, 1995]. Thus,

(3.23)
$$R_{WA} = W R_A W' = B \psi_A B'$$
$$R_{WN} = W R_N W' = B \psi_N B'$$

where

(3.24)
$$\psi_A + \psi_N = I$$

The matrix **B** is a set of common basis vectors and ψ_A and ψ_N are the corresponding abnormal and normal diagonal eigenvalue matrices

[Fukunaga 1972]. The label common refers to the fact that the basis vectors, **B**, are common to both the abnormal and the normal subspaces. The eigenvalues, ψ_A and ψ_N, represent the percentage of combined variance that each basis vector in **B** accounts for in the abnormal and normal EEG respectively. The combined variance is the sum of the diagonal elements of the eigenvalue matrix. Equation 3.24 specifies that the sum of each corresponding abnormal and normal eigenvalue equals 1. This indicates that the eigenvector that accounts for the maximum variance in the abnormal EEG is the eigenvector that accounts for the minimum variance in the normal EEG, and vice versa.

This result implies that a transformation matrix can be designed to simultaneously diagonalize both whitened covariance matrices, $\mathbf{R}_{WA}$ and $\mathbf{R}_{WN}$. The linear transformation matrix that accomplishes this is the transpose of the common basis vectors, **B**:

$$\mathbf{C} = \mathbf{B}' \mathbf{Z} \tag{3.25}$$

If this transformation is applied to $\mathbf{Z}_A$ and $\mathbf{Z}_N$, then the diagonalized covariance matrices, $\mathbf{R}_{CA}$ and $\mathbf{R}_{CN}$, of the transformed abnormal and normal data matrices can be written as:

$$\mathbf{R}_{CA} = \mathbf{B}' \mathbf{R}_{WA} \mathbf{B} = \mathbf{B}' (\mathbf{B} \psi_A \mathbf{B}') \mathbf{B} = \psi_A \tag{3.26}$$

$$\mathbf{R}_{CN} = \mathbf{B}' \mathbf{R}_{WN} \mathbf{B} = \mathbf{B}' (\mathbf{B} \psi_N \mathbf{B}') \mathbf{B}' = \psi_N$$

In conclusion, the whitening transformation, **W**, and the linear transformation, **B**, can be written as a single transformation applied to a general data matrix, **V**:

(3.27) $$C = B' (W V) = (W' B)' V$$

The diagonalized covariance matrices in equation 3.26 indicate that any data vectors transformed by $(W' B)'$ will be uncorrelated. Although, the use of the linear whitening transformation does not preserve orthogonality. As well, equation 3.24 indicates that the order of the eigenvalues in the diagonalized matrices suggest the partitioning of these uncorrelated transformed data vectors.

Using equation 3.27, a reconstructed data matrix V can now be written using the spatio-temporal decomposition format:

(3.28) $$V = ((W' B)')^{-1} C = (B_w')^{-1} C$$

Basis Vectors — $(W' B)'$; *Temporal Waveforms* — C

The inverse, rather than transpose, is used in equation 3.28 since the basis vectors are not unitary due to the fact that the whitening transformation does not preserve orthogonality. Should R_c be ill-conditioned or for estimation purposes be less than full rank, then W would be computed using only the significant eigenvalues [Koles 1991] and the psuedo inverse can be used in equation 3.28 in place of the inverse. When the matrix, $(B_w')^{-1}$, is not reduced for ease of calculation, it is of full rank, invertible and spans the measurement space of containing both the abnormal and normal data. Therefore, this matrix can be termed a basis set. Using the spatio-temporal decomposition naming convention the columns of $(B_w')^{-1}$

can be referred to as the basis vectors and can be considered linearly independent. The rows of **C** are referred to as the corresponding temporal waveforms.

In summary, two results are significant. First, the simultaneous diagonalization of abnormal and normal covariance matrices, R_{CA} and R_{CN}, result in both the abnormal and the normal subspaces being spanned by a common set of basis vectors, $(B_w')^{-1}$. This means that these basis vectors can be used as axes for the new coordinate system. Thus, any signal that is a member of the combined space can be written in terms of these basis vectors. The proportion of each basis vector required to construct the signal, in the new coordinate system is determined by projecting the signal onto each basis vector. The matrix that contain these proportions is the transformed data matrix **C**.

Second, the simultaneous diagonalization transformation orders the eigenvalues, ψ_A and ψ_N, and the corresponding basis vectors. This is significant since the eigenvalues, indicate whether the signal is relatively more normal or abnormal. Therefore, the abnormality of a basis vectors can be quantified according to the percentage of variance accounted for in the abnormal EEG. The basis vectors that account for maximal variance in the abnormal EEG also account for minimal variance in the normal EEG. The projection of the data matrix onto this set of common basis vectors can be thought of as a transformation that enables the partitioning of the data matrix into abnormal and normal subspaces.

4. METHOD

This chapter describes a filtering method used to isolate the abnormal activity within an EEG recorded from an epileptic patient. The three filter method separates the selected abnormal activity from normal background activity, any extraneous abnormal activity, noise components and other artifacts. Two of the three filters used are designed following the data dependent filter design procedure outlined within this chapter. Also included is an overview, a presentation of naming conventions and a summary of equations. The final three sections of the chapter detail the application of the filter design procedure to a generic EEG recorded from an epileptic patient.

Method Overview

The filtering method eliminates the undesirable information, utilizing three forms of filtering; temporal bandpass, temporal pattern and spatial pattern filtering. Each filter eliminates distinctly different content from the EEG. The method begins with bandpass filtering to remove the base line shifts, 60 Hz power line interference, any high frequency artifacts and noise. Next, the temporal pattern filter design procedure derives an optimal set of temporal basis vectors, also known as temporal patterns, from a selected electrode recording. Then the EEG is filtered, using a temporal pattern filter designed from a reduced set of temporal basis vectors. The temporal basis vectors, included in this reduced

set, incorporate the epileptiform activity and account for maximum variance in the abnormal segment. Finally, spatial pattern filtering decomposes the temporally filtered EEG into an optimal set of spatial basis vectors, commonly referred to as spatial patterns, and a corresponding set of temporal waveforms. The abnormal portion of the temporally and spatially filtered EEG is reconstructed from the abnormal spatial patterns and the corresponding temporal waveforms. The abnormal spatial patterns are those that isolate the epileptiform activity. The method is successful if the epileptiform activity is isolated to a minimal number of temporal waveforms. The spatial patterns corresponding to these few temporal waveforms can then be used to the estimate the source location. [Koles et al, 1995]

Data Dependent Filter Design Procedure

Both the temporal pattern and the spatial pattern filters are designed using the same filter design procedure. The steps of the procedure are as follows:

Step 1. **Basis Vectors:** This step determines the optimal basis vectors that span a measurement space and account for both the normal and the abnormal activity in the EEG. The simultaneous diagonalization of a composite covariance matrix results in a set of common basis vectors. The temporal and spatial basis vectors are derived from different data matrices.

Step 2. **Temporal Waveforms:** The temporal waveforms corresponding to the basis vectors are calculated using the linear transformation matrix that is the transpose of the basis vectors.

Step 3. **Partitioning of Matrices:** The basis vector matrix is partitioned into those that span the abnormal subspace and those that span the normal subspace. The calculated temporal waveform matrix is correspondingly partitioned.

Step 4. **Filter Design and Application:** The basis vectors that account for significantly more variance in the abnormal segment than in the normal segment are used for the filters. This process is different for temporal pattern and spatial pattern filters.

Naming Conventions

The naming conventions for specific vectors and matrices used in the remaining of this chapter are listed in Table 4.1. The labels temporal and spatial and the subscripts, t and s, when used in reference to basis vectors, refer to the type of filter. The terms temporal and spatial filters are also associated with the aspect of the EEG that is being processed. In general, all the basis vectors in Table 4.1 are either temporal or spatial basis vectors. But for clarity and historical consistency, the specific terms temporal basis vectors and spatial basis vectors are reserved for $\mathbf{P}_t$ and $\mathbf{P}_s$. These basis vectors relate to the spatio-temporal decomposition of the corresponding data matrices, **D** and **V**. The use of the terms

temporal patterns and spatial patterns for these vectors, is intended to prevent any ambiguity from arising.

Table 4.1 Filter Design Naming Conventions

Temporal Pattern Filtering		Spatial Pattern Filtering	
Label	Name	Label	Name
D	Data matrix	V	Data matrix
U_{tc}	Basis vectors	U_{sc}	Basis vectors
B_t	Common basis vectors	B_s	Common basis vectors
W_t	Whitening transformation matrix	W_s	Whitening transformation matrix
$B_{tw} = W_t' B_t$	Whitened common basis vectors	$B_{sw} = W_s' B_s$	Whitened common basis vectors
$B_{tw}' = (W_t' B_t)'$	Transformation matrix	$B_{sw}' = (W_s' B_s)'$	Transformation matrix
$P_t = ((W_t' B_t)')^{-1}$	Temporal basis vectors or Temporal patterns	$P_s = ((W_s' B_s)')^{-1}$	Spatial basis vectors or Spatial patterns
C_t	Temporal Pattern Filtered (TPF) temporal waveforms	C_s	Spatial Pattern Filtered (SPF) temporal waveforms

Equation Summary

Table 4.2 contains a summary of the equations for the temporal and spatial pattern filtering procedure. The equations are listed in order that they appear during the application of the filter design procedure. Table 4.2 includes the references to equations developed in Chapter 3 and to the equations in the remaining sections of Chapter 4.

Table 4.2 Comparative Summary of Filter Design Equations

Temporal Pattern Filter Design Equations	Spatial Pattern Filter Design Equations
Composite Covariance Matrices:	Equation References: 3.19, 3.20, 3.21
$U_{tc}\Lambda_{tc}U_{tc}' = R_{tc} = \frac{D_A D_A'}{\text{trace}(D_A D_A')} + \frac{D_B D_B'}{\text{trace}(D_B D_B')}$	$U_{sc}\Lambda_{sc}U_{sc}' = R_{sc} = \frac{V_A V_A'}{\text{trace}(V_A V_A')} + \frac{V_B V_B'}{\text{trace}(V_B V_B')}$
Whitening Transformation Matrices:	Equation References: 3.14, 3.22, 4.3, 4.20
$W_t = \Lambda_{tc}^{-1/2} U_{tc}'$	$W_s = \Lambda_{sc}^{-1/2} U_{sc}'$
Whitened Covariance Matrices:	Equation Reference: 3.23
$B_t \Psi_{tA} B_t' = R_{twA} = W_t R_{tA} W_t'$	$B_s \Psi_{sA} B_s' = R_{swA} = W_s R_{sA} W_s'$
Abnormal Whitened Eigenvalue Matrices:	Equation Reference: 3.23
$\Psi_{tA} = (W_t B_t)' R_{tA} (W_t B_t)$	$\Psi_{sA} = (W_s B_s)' R_{sA} (W_s B_s)$
Whitened Basis Vectors:	Equation References: 3.28, 4.4, 4.21
$B_{tw} = W_t' B_t$	$B_{sw} = W_s' B_s$
STEP 1: Basis Vectors:	Equation References: 3.28, 4.5, 4.6, 4.22, 4.23
$P_t = (B_{tw}')^{-1} = U_{tc}\Lambda_{tc}^{1/2} B_t$	$P_s = (B_{sw}')^{-1} = U_{sc}\Lambda_{sc}^{1/2} B_s$
STEP 2. Temporal Waveforms:	Equation References: 3.27, 3.28, 4.7, 4.24
$C_t = B_{tw}' D$	$C_s = B_{sw}' V_{tf}$
Spatio-Temporal Decomposition:	Equation References: 3.28, 4.8, 4.26
$D = (B_{tw}')^{-1} C_t$	$V_{tf} = (B_{sw}')^{-1} C_s$
STEP 3. Partitioning of Matrices:	Equation References: 4.10, 4.11, 4.25, 4.27
$D = P_t C_t = \left[P_{tA}\ P_{tB}\right]\begin{bmatrix} C_{tA} \\ C_{tB} \end{bmatrix}$	$V_{tf} = P_s C_s = \left[P_{sA}\ P_{sB}\right]\begin{bmatrix} C_{sA} \\ C_{sB} \end{bmatrix}$
STEP 4. Filter Design and Application:	Equation References: 4.17, 4.18, 4.28
$V_{tf} = (P_t)_{tA}\ B_{twA}' \otimes V_{spf}$	$V_{sf} = P_{sA} C_{sA}$

In comparing the two sets of design equations in Table 4.2 the similarity between the 2 columns can be easily identified with a few exceptions. First, the original data matrices for the two filtering techniques are different. This is seen in the pair of equations in the first row and the rows labeled Step 2 and Step 3. A second more obvious difference is between the pair of equations for Step 4. Lastly, a trivial exception is the naming convention subscripts purposely added to delineate between the spatial and temporal aspects.

The remaining 3 sections of this chapter describe the step by step application of temporal bandpass filtering, temporal pattern filtering and spatial pattern filtering to a generic EEG recorded from an epileptic patient. Table 4.2 can be used as an outline of the presentation contained within the last two sections.

Temporal Bandpass Filtering

The filtering method starts with a bandpass filter to eliminate those frequencies outside the bounds of the epileptiform activity, such as the 60 Hz artifact and any dc level base line shifts. The bandpass filter is designed using conventional data independent digital filter design techniques. Low-pass and high-pass filters are combined to form the desired bandpass filter.

The N channel EEG record containing T sample measurements is represented by the data matrix **V**. The time domain or impulse response of the bandpass filter is represented by the vector F_{bp} in the following equation. The symbols $\mathcal{F}$ and $\mathcal{F}^{-1}$ represent the Fourier

transformation and the inverse Fourier transformation respectively. The bandpass filter can be applied to the data matrix, **V**, in the frequency domain creating a (NxT) bandpass filtered data matrix, labeled V_{bpf}.

(4.1) $$V_{bpf} = \mathcal{F}^{-1}(\mathcal{F}(F_{bp}) \cdot \mathcal{F}(V))$$

Temporal Pattern Filtering

The (NxT) data matrix, V_{bpf}, can be viewed as N rows of data points with a spatio-temporal decomposition as shown in equation 3.4. Each row is a different perspective of all the activity within the brain. Abnormal activity in the EEG will be most evident in the rows that correspond to electrode sites closest to the sources of this activity. If the amplitude of the abnormal activity is large in comparison to the normal or background activity the abnormal temporal activity will dominate the data points. It is this temporal activity that will be isolated.

In some EEGs this temporal activity may be obscured. The amplitude of the source potential of the abnormal activity may be equal to or smaller than the normal activity. In these cases, traditional methods of temporal filtering may not isolate the frequency components of the abnormal temporal activity. The temporal filter design, using the method of simultaneous diagonalization of autocovariance matrices from both abnormal and normal EEGs, is used to isolate the desired frequency components.

The temporal pattern filter is designed following the general data dependent filter design procedure. The specific equations are summarized in Table 4.2. This procedure is adapted from the spatial pattern filtering method developed by Koles [1991]. The filter is based on the temporal basis vectors that account for maximum variance in the abnormal EEG and minimum variance in the normal EEG. The temporal pattern filter that results matches the specific abnormal temporal activity contained within a single row of the EEG data matrix. Based on the linear superposition principle as applied to the EEG activity, presented in Chapter 3, this activity is assumed to be present to some extent in each tracing of the EEG. Therefore when the frequency response of the filter is applied to an EEG this abnormal temporal activity will be enhanced within each of the N electrode recordings.

Step 1. Temporal Basis Vectors:

The first step consists of determining a set of temporal basis vectors that span the measurement space. These basis vectors are derived from the decomposition and transformation of two data matrices. These data matrices are derived from two segments of a single row of data points in the EEG. The two segments are chosen from the normal and the abnormal sections of the recording.

Data Matrices:

The temporal pattern filter design begins with the selection of an electrode recording, V_e, from the bandpass filtered data matrix, V_{bpf}. The selected recording must contain at least 3 seconds of persistent abnormal activity and at least 3 seconds of normal

activity. Chapter 2 describes the criteria for identification of abnormal and normal activity and is used in the selection of the two segments. Denoted by the vectors V_{eA} and V_{eN}, these segments are used to form the abnormal and the normal data matrices, D_A and D_N.

The data matrices, are derived from data points in each segment as:

$$\begin{bmatrix} V_1 & V_2 & V_3 & \cdots & V_L \\ V_2 & V_3 & V_4 & \cdots & V_{L+1} \\ V_3 & V_4 & V_5 & \cdots & V_{L+2} \\ \vdots & & & & \\ V_M & V_{M+1} & V_{M+2} & \cdots & V_{L+M-1} \end{bmatrix} \qquad (4.2)$$

In this data matrix, the row vector $[V_1\ V_2\ V_3 \ldots V_L]$ contains the first L data points of a selected data segment. The data matrices, D_A or D_N, are formed such that each of the M rows is a shifted selection of L data points from the original segments, V_{eA} or V_{eN}. Since L > M, the length of the original segment, $[V_1\ V_2\ V_3 \ldots V_{L+M-1}]$, must be at least twice the number of shifts, M. The data matrix, D_A, includes both the abnormal and normal data points, whereas the data matrix, D_N, contains only the normal data points. This distinction allows for the partitioning of the data points into normal and abnormal subspaces.

Autocovariance Matrices:

The matrices, R_{tA} and R_{tN}, derived from the data matrices D_A and D_N are an estimate of the autocovariance of V_{eA} and V_{eN}. These autocovariance matrices are calculated with the data matrices D_A and D_N replacing V_A and V_N in equation 3.20. The autocovariance defines the dependence of the data points within a segment on each other. The autocovariance matrices, R_{tA} and R_{tN}, enable the different

temporal patterns in the vector segments V_{eA} and V_{eN} to be identified. The differences in these temporal patterns are quantified so that the measurement space can be partitioned into abnormal and normal subspaces. This quantification is obtained through the simultaneously diagonalizing of the two autocovariance matrices. For this purpose, the composite autocovariance matrix, R_{tC}, is derived based on equation 3.19.

Whitening Transformation Matrix:

The second step towards simultaneously diagonalizing R_{tA} and R_{tN} is the derivation of the whitening transformation matrix.

$$W_t = \Lambda_{tC}^{-1/2} U_{tC}' \qquad (4.3)$$

The transformation matrix components Λ_{tC} and U_{tC}, in equation 4.3 are derived from the singular value decomposition of the composite autocovariance matrix, R_{tC}, as shown in equation 3.21.

Whitened Basis Vectors:

The common basis vectors, B_t, are derived from the singular value decomposition of either the whitened autocovariance matrices R_{tWA} or R_{tWN} as shown in equation 3.23. The whitened common basis vectors, B_{tw}, as the name suggests can be viewed as the common basis vectors, B_t, transformed by the whitening transformation matrix, W_t, and can be written as:

$$B_{tw} = W_t' B_t \qquad (4.4)$$

The detailed derivation of the whitening transformation matrix and the whitened common basis vectors, B_{tw}, are detailed in the simultaneous diagonalization section of Chapter 3.

Temporal Patterns:

The temporal basis vectors, the columns of $(B_{tw}')^{-1}$ also referred to as temporal patterns, P_t, are given by:

$$P_t = (B_{tw}')^{-1} = ((W_t' B_t)')^{-1} \quad (4.5)$$

The inverse is used in equation 4.5 instead of the transpose due to the fact that the use of the whitening transformation matrix, W_t does not preserve orthonormality [Fukunaga 1972]. Should R_{tc} be ill-conditioned or for estimation purposes be of less than full rank, then W_t would be computed using the psuedo-inverse in place of the full inverse [Koles 1991]. For computational purpose equation 4.5 is written as:

$$P_t = U_{tc} \Lambda_{tc}^{1/2} B_t \quad (4.6)$$

Each of the temporal patterns, P_t, are common to each data segment and are ordered according to the percentage of variance each accounts for in the abnormal or normal EEG segments respectively. The abnormal and normal eigenvalue matrices, ψ_{tA} and ψ_{tN}, that contain this information are derived in a previous calculation from the singular value decomposition of the whitened autocovariance matrices R_{tWA} and R_{tWN} based on equation 3.23.

Step 2. TPF Temporal Waveforms:

Any data matrix **D**, built from a data segment in the form of equation 4.2, can be transformed, using the temporal basis vectors, into a partitionable coordinate system. As a result of this transformation the data points within the data matrix **D** in the old

coordinate system correspond to the temporal waveforms in the new coordinate system. To this end, the linear transformation required to derive the temporal waveforms can be viewed as the projection of the data matrix onto each of the transposed whitened common basis vectors.

The equation for this transformation is

$$C_t = (W_t' B_t)' D = B_{tw}' D \tag{4.7}$$

where the transformation matrix, B_{tw}', transforms the data matrix **D** into the temporal waveforms, C_t. Using this transformation each of the temporal waveforms corresponding to the temporal patterns in P_t can be calculated. Equation 4.7 can also be viewed as a filtering process where the original data segment used to create the data matrix is filtered by each temporal pattern. To this end the data matrix, **D**, can be viewed as a convolution matrix of the data segment. Therefore based on this perspective the rows of C_t are referred to as temporal pattern filtered (TPF) temporal waveforms.

Spatio-Temporal Decomposition:

The transformation that enables the partitioning of the data matrix used in this research is equation 4.7. Rewriting this equation according to the convention of spatio-temporal decomposition the data matrix **D** can be written as:

$$D = (B_{tw}')^{-1} C_t \tag{4.8}$$

Temporal Basis Vectors ↵ ↓
or Temporal Patterns ↵
TPF Temporal Waveforms ↵

It is from this form of the transformation that the labels temporal basis vectors, temporal patterns and TPF temporal waveforms are assigned.

Step 3. Partitioning of Matrices:

As discussed in Chapter 3, since $(B_{tw}')^{-1}$ is invertible the whitened common basis vectors, B_{tw}, are linearly independent. The whitened common basis vectors, B_{tw}, are also ordered corresponding to the order of the eigenvalues and therefore can be partitioned as follows:

(4.9) $$B_{tw} = \left[B_{twA}\ B_{twN}\right]$$

Because P_t is inversely related to B_{tw} and can be written in terms of the diagonal matrices and matrices of linear independent vectors as expressed in equation 4.6, the temporal patterns can also be similarly partitioned into abnormal and normal subsets. It follows as a result of equation 4.7 that the transformed data matrix, C_t, corresponding to the data points in **D**, can also be partitioned into two sets of TPF temporal waveforms. Each waveform is a member of either an abnormal subspace or a normal subspace in the new coordinate system.

The reconstruction of the data matrix given by equation 4.8, using the temporal patterns, P_t, and the derived TPF temporal waveforms, C_t is:

(4.10) $$D = P_t C_t$$

Therefore, the partitioned equation for the reconstruction of the data matrix is:

$$D = \begin{bmatrix} P_{tA} & P_{tN} \end{bmatrix} \begin{bmatrix} C_{tA} \\ C_{tN} \end{bmatrix} \qquad (4.11)$$

It follows that the abnormal and normal subspaces are spanned by temporal patterns, P_{tA} and P_{tN}, respectively. In practice the partitioning is accomplished by a visual inspection of C_t and is guided by the percentage of variance each temporal pattern accounts for in the abnormal data matrix. The percentage of variance accounted for in the abnormal data matrix corresponding to each temporal pattern is the corresponding element in the eigenvalue matrix, Ψ_{tA}.

Step 4. Filter Design and Application:

The definition of a data matrix, **D**, using equation 4.2 indicates that the first row, D_1, of the data matrix is the first L data points of the original segment from a electrode tracing, V_{ss}. An equation for this row can be written using the form of equation 4.10 for D_1 and then substituting equation 4.8 for C_t:

$$D_1 = (P_t)_1 \; C_t = (P_t)_1 \; (B_{tw}' \; D) = ((P_t)_1 \; B_{tw}') \; D \qquad (4.12)$$

Equation 4.12 indicates that the first row, D_1, referred to as the data segment, V_{ss}, can be viewed as the product of the row vector, F_t, and the data matrix, **D**,

$$V_{ss} = F_t \; D \qquad (4.13)$$

where the vector F_t is defined as

(4.14) $$F_t = ((P_t)_1 \; B_{tw}')$$

Using the partitioning of equations 4.9 and 4.11 in equation 4.14 the vector F_t can then be similarly partitioned into abnormal and normal submatrices:

(4.15) $$F_t = F_{tA} + F_{tN} = \left[(P_t)_{1A} \; (P_t)_{1N}\right] \begin{bmatrix} (B_{twA})' \\ (B_{twN})' \end{bmatrix}$$

Instead of recombining all the temporal patterns, as suggested by equation 4.13, a subset can be used. In particular, those temporal patterns that represent only the abnormal activity can be recombined to reconstruct the abnormal portion of the electrode recording. Thus, the segment from the single electrode recording, V_{ss}, can be viewed as the sum of the abnormal activity, V_{tA}, and the remainder.

(4.16) $$V_{ss} = V_{tA} + V_{tN} = F_{tA}\, D + F_{tN}\, D$$

Although the remainder is labeled normal, V_{tN}, this signal segment typically is composed of any combination of normal background activity, irrelevant abnormal activity and artifacts.

Using equation 4.15, the abnormal temporal pattern, F_{tA}, is derived from a linear reconstruction of the rows of abnormal whitened common basis vectors, B_{twA}, that contain the epileptiform activity, and the corresponding temporal pattern coefficients, $(P_t)_{1A}$:

$$(4.17) \qquad F_{tA} = (P_t)_{1A}\, B_{twA}' = \left[(P_t)_{11} \cdots (P_t)_{1a} \right] \begin{bmatrix} B_{tw1}' \\ \vdots \\ B_{twa}' \end{bmatrix}$$

The index **A** represents the row elements, [1 ... a], that have been identified as abnormal. The reconstructed vector, F_{tA}, is a template for the abnormal activity specifically the epileptiform activity for the particular selection of normal and abnormal segments. This template is referred to as the temporal pattern filter.

Although the abnormal activity is derived from the decomposition of a single electrode recording, the principle of linear superposition states that this abnormal activity is present in each electrode recording to some degree. Even though in some electrode recordings this activity may be swamped by other stronger normal signals and is not as clearly apparent. Therefore, the subspace that contains the abnormal data points from the single electrode recording should be the same subspace that contains the abnormal data points from the complete EEG. As a result, similar abnormal components within the EEG can be determined by temporally filtering the complete EEG with the same temporal pattern filter.

Temporal filtering can be performed in either the time domain or in the frequency domain. In the time domain, the temporal pattern filter, F_{tA}, can be convolved with the bandpass filtered EEG, V_{bpf}, to create the temporally filtered EEG, V_{tf}. The convolution function is represented by the symbol $\otimes$.

$$(4.18) \qquad V_{tf} = F_{tA} \otimes V_{bpf}$$

The filtering can be accomplished in the frequency domain by multiplication of the frequency response of both the bandpass filtered EEG and the temporal pattern filter. In this domain both temporal filters can be applied in a single calculation:

$$V_{tf} = \mathcal{F}^{-1}(\mathcal{F}(F_t) \cdot \mathcal{F}(F_{bp}) \cdot \mathcal{F}(V)) \qquad (4.19)$$

Equation 4.19 includes the process described by equation 4.1.

Spatial Pattern Filtering

Similar to temporal pattern filtering, spatial pattern filtering utilizes two data segments, abnormal and normal, from a single EEG record. One difference is that while temporal pattern filtering uses a single electrode recording, spatial filtering use all N electrode recordings. Following the method developed by Koles [1991] the data dependent design process for a the spatial pattern filter begins with the derivation of an optimal set of spatial basis vectors. Following this, the corresponding common temporal waveforms are calculated and the abnormal and the normal spatial patterns and their corresponding temporal waveforms are separated. Finally, a data matrix is spatially filtered when the abnormal spatial patterns and the corresponding common temporal waveforms are recombined. Fundamental to this process, the technique of simultaneously diagonalizing of a composite covariance matrix is described in detail in Chapter 3 and is outlined here for completeness and to specify the equations with appropriate labeling. The specific equations are also summarized in Table 4.2.

Step 1. Spatial Basis Vectors:

The first step in the spatial pattern filter design consists of determining the spatial basis vectors of the N channel temporally filtered EEG data matrix.

Data Matrices:

The two data matrices, V_A and V_N, used for this purpose are data segments selected from the N channel temporally filtered data matrix, V_{tf}. Each (N x T) data matrix contains at least 3 seconds of persistent abnormal or normal activity and has a spatio-temporal decomposition as shown in equation 3.4.

Covariance Matrices:

The covariance matrices of the data matrices V_A and V_N are calculated as shown in equation 3.20. The covariance matrices, relabeled as R_{sA} and R_{sN}, enable the differences between the spatial patterns in the EEG segments V_A and V_N to be identified. These differences are used to separate the activity in the measurement space into abnormal and normal subspaces according to the locations the sources. The composite covariance matrix, R_{sC}, is calculated as in equation 3.19.

Whitening Transformation Matrix:

The whitening transformation matrix, W_s, as defined in equation 3.14, is created from the eigenvalues and eigenvectors of the composite covariance matrix and is relabeled in equation 4.20.

(4.20) $$W_s = \Lambda_{sC}^{-1/2} U_{sC}'$$

Whitened Basis Vectors:

The common basis vectors, B_c, are the eigenvectors of the whitened normal or abnormal covariance matrices, R_{cA} or R_{cN}. The whitened common basis vectors are given by the equation:

$$B_{cw} = W_c' B_c \tag{4.21}$$

Spatial Patterns:

The spatial basis vectors, the columns of $(B_{cw}')^{-1}$, commonly referred to as spatial patterns, are derived from the whitened common basis vectors calculated as in equation 4.21 and can be written as:

$$P_c = ((W_c' B_c)')^{-1} \tag{4.22}$$

For computational purpose equation 4.22 is written as:

$$P_c = U_{cc} \Lambda_{cc}^{1/2} B_c \tag{4.23}$$

The inverse is used in equation 4.22 instead of the transpose due to fact that the use of the whitening transformation, W_c does not preserve orthonormality. Should R_{cc} be ill-conditioned or for estimation purposes be of less than full rank, then W_c would be computed using only the significant eigenvalues and the psuedo-inverse used in place of the inverse [Koles 1991]. Each spatial basis vector is common to both data matrices and accounts for maximum variance, ψ_{cA}, in the abnormal EEG segment while accounting for minimum variance, ψ_{cN}, in the normal EEG segment.

Step 2. Temporal Waveforms:

Similar to temporal pattern filtering, spatial pattern filtering utilizes the linear transformation of equation 3.27 to derive the temporal waveforms, C_s.

(4.24) $$C_s = (W_s' B_s)' V_{tf}$$

To distinguish these temporal waveforms from the temporal waveforms derived during temporal pattern filtering they are referred to as spatial pattern filtered (SPF) temporal waveforms. Equation 4.24 can also be viewed as a form of filtering where the data matrix is filtered by each spatial pattern. The linear transformation, given by equation 4.24 can be used to calculate the SPF temporal waveforms of any data matrix, V_{tf}.

Spatio-Temporal Decomposition:

The temporally filtered data matrix, V_{tf}, can be reconstructed using the spatial patterns and their corresponding SPF temporal waveforms using the spatio-temporal decomposition format:

(4.25) $$V_{tf} = P_s C_s$$

Spatial Basis Vectors ↓

SPF Temporal Waveforms ↓

A more specific equation can be obtained by substituting equation 4.22 for P_s:

(4.26) $$V_{tf} = ((W_s' B_s)')^{-1} C_s = (B_{sw}')^{-1} C_s$$

Step 3. Partitioning of Matrices:

As a result of the ordering of the eigenvectors within the spatial patterns, P_s, the calculated SPF temporal waveforms are correspondingly ordered and the partitioning of the matrices is possible. The partitioning of the data matrix, V_{tf}, can be viewed as rows of composite signals that are composed of abnormal signals, V_{fA}, and the remainder. The remaining activity labeled, V_{fN}, may consist of any combination of normal background, extraneous abnormal activity or artifacts. The partitioning of the spatial patterns and the corresponding waveforms is most easily accomplished by identifying those SPF temporal waveforms that contain the epileptiform activity. Labeled as abnormal, these SPF temporal waveforms typically are those that also account for a significant percentage of the variance in the abnormal EEG. Using this partitioning the data matrix can be written as follows:

(4.27) $$V_{tf} = \begin{bmatrix} P_{sA} & P_{sN} \end{bmatrix} \begin{bmatrix} C_{sA} \\ C_{sN} \end{bmatrix}$$

Step 4. Filter Design and Application:

The complete set of spatial patterns can be used to reconstruct the temporally filtered data matrix, V_{tf}, as shown by equation 4.27. But using the partitioning, the abnormal and normal submatrices can now be defined as:

(4.28) $$V_{fA} = P_{SA}\, C_{SA} \qquad V_{fN} = P_{SN}\, C_{SN}$$

Therefore, the filtered EEG, V_{fA}, shown in equation 4.28, is the result of the recombination of the abnormal spatial patterns, P_{SA}, and their corresponding SPF temporal waveforms, C_{SA}.

Since the data matrix, V_{tf}, in equation 4.27 is a temporally filtered EEG, the partial reconstruction, V_{fA}, results in a new EEG data matrix that is both temporally and spatially filtered. This filtered EEG should exhibit both an enhanced view of the seizure onset and the distribution of the abnormal activity over the surface of the brain at the electrode sites. It follows that the abnormal activity contained within the temporally and spatially filtered EEG, V_{fA}, can be attributed to a subset of the total sources active within the brain. The number of sources in the subset is less than or equal to the number of abnormal spatial patterns used in the reconstruction.

In conclusion, temporal and spatial filtering is used to elicit the abnormal source activity from the EEG separating it from any extraneous activity. This method results in information about i) the number of possible abnormal sources active in the abnormal EEG segment, ii) the associated abnormal spatial patterns and iii) the corresponding SPF temporal waveforms. The enhanced seizure onset and the evolution of the abnormal source potentials through time can be easily identified visually in both the abnormal SPF temporal waveforms and abnormal EEG. Spatial mapping will give a coarse indication of the source location. The actual source locations inside the brain can be determined by using the spatial patterns as input to source localization techniques [Koles et al. 1995].

5. RESULTS

The 3 filter method described in the previous chapter was applied to more than 60 clinical EEGs and numerous simulated EEGs. This chapter assembles three sets of results; one simulated EEG and two clinical EEGs. These results will be used to validate the data dependent temporal and spatial pattern filter design procedure.

The chapter begins with the detailing of suitable values for the parameters used in the temporal and spatial pattern filter design procedure and the EEG analyses follow. The first set of results, the analysis of the simulated EEG included in this chapter has been chosen to exhibit the temporal and spatial filtering concept using clearly defined abnormal data. Since the spatial pattern corresponding to the seizure activity is known for the simulated EEG, the error will be calculated between the known and estimated spatial patterns resulting from different filter designs.

The next two sets of results are from the analysis of clinical data. The clinical EEGs that have been analyzed can be separated into two groups; those which include both invasive and non-invasive simultaneous electrode recordings and those with only non-invasive electrode recordings. An example EEG presented from the first group, recorded using Telefactor equipment at New York University, illustrates the effectiveness of a temporal pattern filter designed using a surface electrode recording in comparison to a gold standard of a depth electrode recording. The third EEG analysis is an example of the filtering method applied to an EEG from the second group, the

non-invasive clinical EEGs. This EEG was recorded from surface electrodes using BMSI equipment in the Long Term EEG Monitoring Unit at the University of Alberta Hospital.

Filter Parameters

The step by step filter design method detailed in Chapter 4 identified several parameters. The majority of these parameters are defined by the specific EEG data analyzed. Table 5.1 presents values used for the 3 EEGs analyzed in this chapter. The first 2 parameters, number of shifts and length of data segments, are related to the effectiveness of the temporal pattern filter. These settings were determined experimentally, resulting in filters that were effective for a range of abnormal activity.

Table 5.1 Filter Design Parameters

VARIABLES	Label	Simulated	Patient 1	Patient 2
Number of Shifts	M	100	100	100
Number of Samples in Data Matrix	L	500	500	500
Sampling Frequency (samples/sec)	fs	200	200	200
Length of Data Segment (Number of samples)	T	600	600	600
Abnormal (Ictal) Onset	V_{eA}	5 seconds	27.5 seconds	30 seconds
Normal (Preictal) Onset	V_{eN}	0 seconds	23 seconds	20 seconds
Number of Electrodes	N	24	27	24
Selected Electrode	V_e	T4	Surface: f10 Depth: B6	T3

The first parameter, the number of shifts, is fundamental to the temporal pattern filter design. The temporal pattern filter design procedure is based on the autocovariance matrices of the 2 selected signal segments. An autocovariance matrix was estimated using the covariance of a data matrix comprised of shifted versions of an electrode recording segment as shown in equation 4.2. The number of shifts, M, used to create the data matrix, D, is related to the frequency resolution of the data matrix. With a sampling frequency, f_s, of 200 Hz, a 0.5 second segment of the data is equivalent to 100 data samples. Therefore if the number of shifts is 100, the minimum frequency which can be resolved is 2 Hz. The maximum frequency is determined by the Nyquist frequency, $f_s/2$, of 100 Hz.

The use of a rectangular data matrix, (MxL), rather than a square (MxM) matrix, improves the estimate of the autocovariance and thus increases the effectiveness of the filter design. Therefore, the shifted data matrix, D, as described in equation 4.2, is a (MxL) matrix where the number of samples in the data matrix, L, the second parameter in Table 5.1, is set to be T-M-1. T, the length of the data segment, has been set at 600 samples, since the epileptiform activity is defined to be abnormal activity which persists for 3 seconds,

The abnormal data segment was chosen from the portion of the epileptiform activity within the selected electrode recording that contains the identifiable activity of the seizure. The normal data segment was chosen from the portion of the selected electrode recording that reflects the background and artifact activity. The

beginning of both abnormal and normal data segments and the selected electrode recording used for each EEG are listed in the Table 5.1

Simulated Data

The simulated EEG consists of eyeblink artifact, epileptiform activity, noise and normal background activity. These 4 types of brain activity are attributed to separate sources. The corresponding source waveforms, shown in Figure 5.1, form the (5x2000) matrix S in equation 5.1.

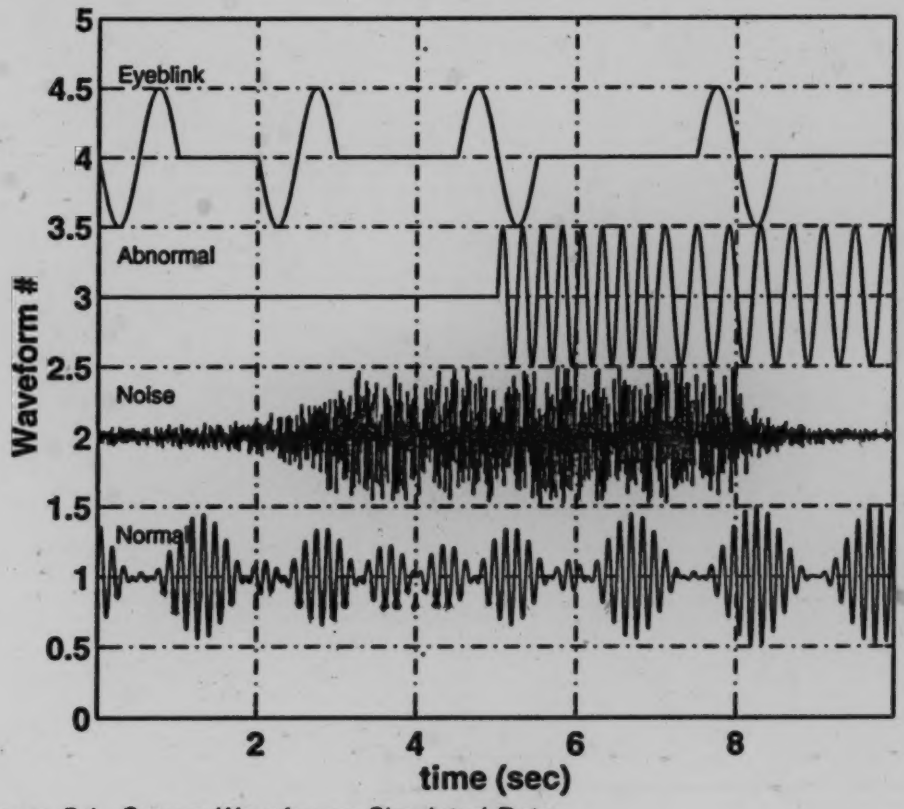

Figure 5.1 Source Waveforms; Simulated Data

Since the fundamental frequency of the epileptiform activity may change during the ictal period, the abnormal source waveform mimics this behavior. The abnormal waveform displays a seizure depicted by a sinusoid with an initial frequency of 4 Hz, between 5 and 7 seconds, which changes to the second frequency of 2.5 Hz at 7 seconds. The normal activity is the result of a combination of 3 sinusoidal waveforms with significant strength to be visible throughout the 10 second segment. The noise source waveform consists of random values scaled to obscure the seizure onset. The eyeblink artifact source waveform consists of segments of a 2 Hz sine waveform.

The columns of the (24x5) matrix, **M**, contain spatial patterns, normalized using the Euclidean norm, that correspond to the source waveforms. The spatial patterns of the simulated EEG that specify the distribution strengths of the source waveforms associated with each of the 24 electrode sites are listed in Table 5.2. The spatial pattern for the eyeblink artifact activity is a vector of surface potentials generated by placing, within a three spherical shell model, two unit dipoles at a radius of 0.7 at the locations defined by a tip angle of 90 degrees and spin angles of -110 and -70 degrees with the dipole orientation defined by pitch and yaw angles of 0 degrees. This general location is underneath the frontal and frontal-polar electrode sites. The spatial pattern corresponding to the epileptiform activity focuses the source location underneath a point half way between the T4 and F8 electrode sites in the right anterior temporal lobe. The spatial pattern is a vector of potentials generated by a unit dipole placed at a radius of 0.4 at a location

defined by the tip and spin angles of 90 and -18 degrees with the dipole orientation defined by pitch and yaw angles of 0 degrees.

Table 5.2 Spatial Patterns; Simulated Data

Electrode	Eye Blink	Abnormal	Noise	Normal
FP1	0.5971	0.0345	0.0299	-0.2475
FP2	0.5971	0.2292	0.0180	-0.2283
F3	0.2245	-0.0329	0.0212	-0.2304
F4	0.2245	0.2858	0.1488	-0.1769
C3	0.0430	-0.0833	0.0608	-0.1797
C4	0.0430	0.2464	0.1278	-0.0158
P3	-0.0155	-0.0891	0.3072	-0.0607
P4	-0.0155	0.1206	0.3267	0.3889
O1	-0.0307	-0.0699	0.2856	0.0467
O2	-0.0307	0.0345	0.0141	0.3889
F7	0.2247	-0.0699	0.1082	-0.2440
F8	0.2247	0.4451	0.2967	-0.1718
T3	0.0499	-0.1125	0.1443	-0.2149
T4	0.0499	0.4451	0.1819	-0.0331
T5	-0.0106	-0.1125	0.0641	-0.1383
T6	-0.0106	0.2292	0.3083	0.2719
Fz	0.2229	0.0828	0.2612	-0.2080
Cz	0.0365	0.0224	0.1893	-0.1037
Pz	-0.0199	-0.0155	0.2722	0.1430
LSPH	0.1029	-0.0907	0.2961	-0.2364
LMAS	0.1029	0.4098	0.1651	-0.1411
RSPH	0.0132	-0.1102	0.0718	-0.1951
RMAS	0.0132	0.3029	0.1647	0.0023
Oz	-0.0328	-0.0273	0.3084	0.2091

The spatial pattern for the noise is a vector of random potentials. The spatial pattern corresponding to the normal activity is a vector of potentials generated by a unit dipole placed at a radius of 0.6 at a location defined by a tip angle of 75 degrees and a spin angle of 60 degrees with the dipole orientation defined by pitch and yaw angles of 0 degrees. This general location is underneath a point half way between the O2 and P4 electrode sites in the right occipital lobe. Refer to Figures 2.5 and 2.6 for descriptions of angle definition and electrode site locations.

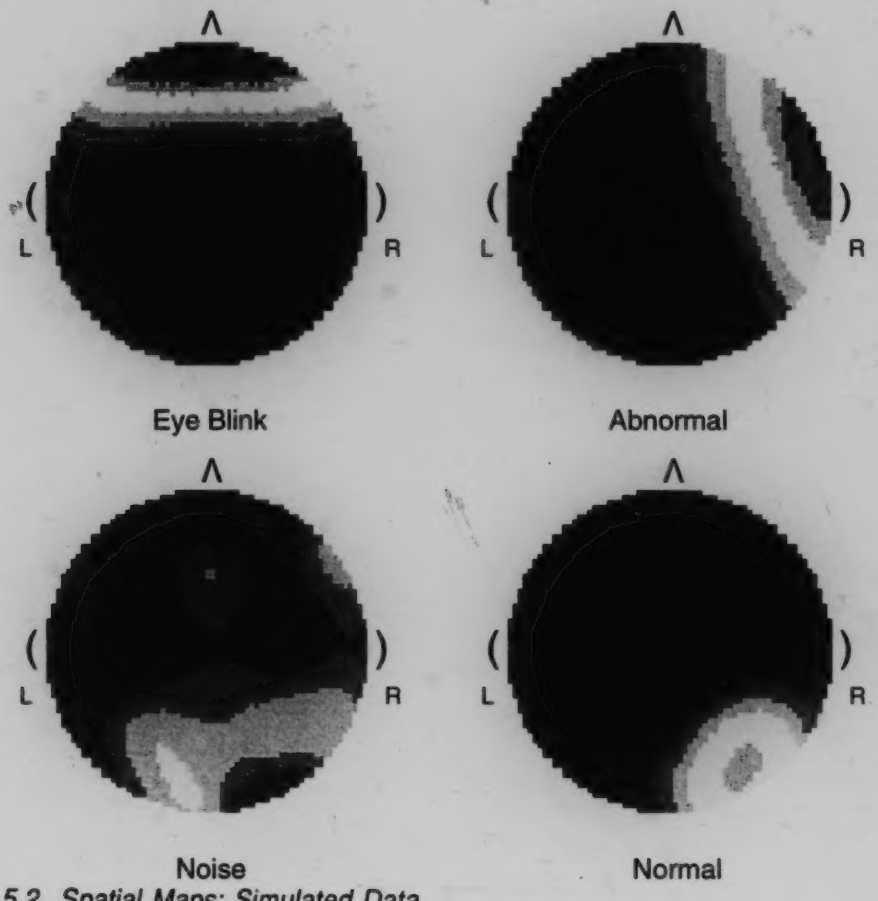

Figure 5.2 Spatial Maps; Simulated Data

The spatial maps corresponding to each of the source waveforms are shown in Figure 5.2. A spatial map is a visual depiction of a spatial pattern. The map is a quantized superior view of potentials on the surface of a sphere with the potentials at the electrode sites corresponding to the spatial pattern. The value of the spatial distribution between the electrode sites is determined using spherical harmonic interpolation [Soong et al. 1993].

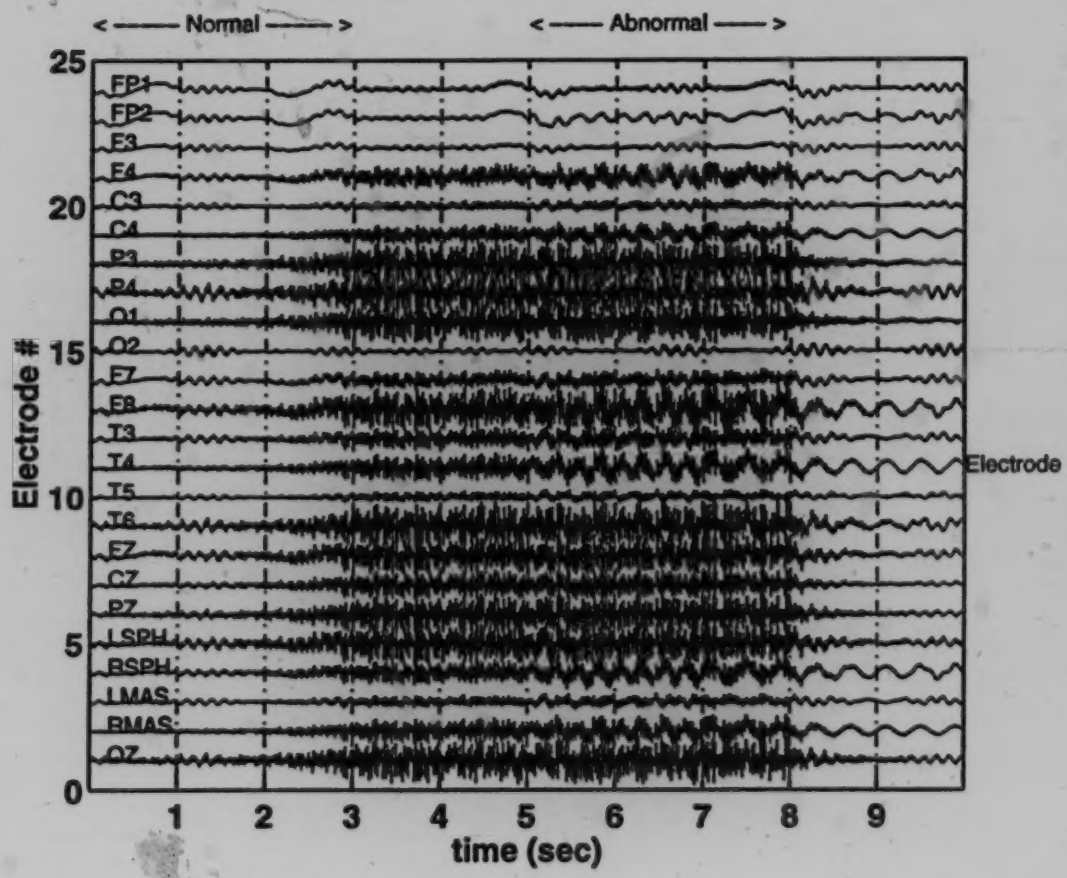

Figure 5.3 Raw EEG; Simulated Data

Data Matrix Construction

The two matrices, **S** and **M**, were combined to create the simulated data matrix, **V**, using the spatio-temporal decomposition matrix equation;

$$V = M S \qquad (5.1)$$

The simulated data matrix, **V**, is presented in EEG form in Figure 5.3. The selected electrode, $V_{\bullet}$, the abnormal, $V_{\bullet A}$, and the normal, $V_{\bullet N}$, segments that are specified in Table 5.1, are also identified in Figure 5.3. The data points corresponding to the selected electrode, T4, within the abnormal (5 seconds to 8 seconds) and the normal (0 seconds to 3 seconds) segments are used to form the data matrices, D_A and D_N.

Temporal Filtering

The temporal pattern filter design procedure, described in Chapter 4, was followed using the parameters set according to the values in Table 5.1. The first result of the procedure is the matrix of temporal pattern filtered (TPF) temporal waveforms corresponding to each of the temporal patterns derived from step 2 of the procedure. This result is useful when selecting the temporal patterns to be used in forming the temporal pattern filter. The complete set of TPF temporal waveforms, C_t, shown in Figure 5.4, are the result of a data matrix, $D_{\bullet}$, projected onto each of the temporal patterns, P_t. The data matrix, $D_{\bullet}$, was created, using the form of equation 4.2, from 10 seconds of the selected electrode recording, T4, from the simulated EEG.

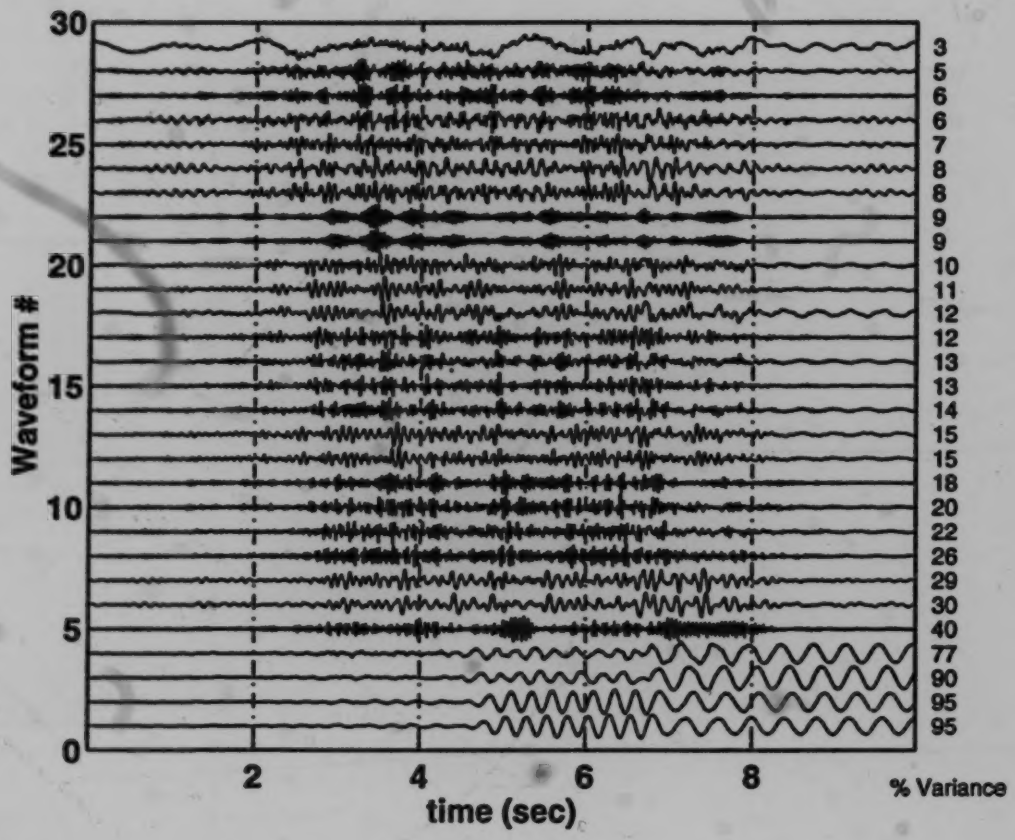

Figure 5.4 TPF Temporal Waveforms; Simulated Data

Each of the TPF temporal waveforms can be viewed as a temporally filtered version of the 10 second data segment from the selected electrode recording. Each waveform was the result of the data matrix, $\mathbf{D}_o$, projected onto a single temporal pattern. The selected electrode recording, T4, can be viewed as the linear summation of all the TPF temporal waveforms. The percentage of variance that each temporal pattern accounts for in the abnormal segment from the selected electrode recording is listed to right of the corresponding TPF temporal waveforms. The top waveform

corresponds to the temporal pattern which accounts for the minimum variance in the abnormal segment while accounting for maximum variance in the normal segment. The activity seen in the normal and background activity in the raw EEG in Figure 5.1 and in the source waveforms in Figure 5.3 can be identified in the top few TPF temporal waveforms. The bottom waveform corresponds to the temporal pattern which accounts for the maximum variance in the abnormal segment while accounting for minimum variance in the normal segment. As designed, the abnormal activity in this TPF temporal waveform is most visually pronounced in the abnormal segment (5-8 seconds) and least pronounced in the normal segment (0-3 seconds).

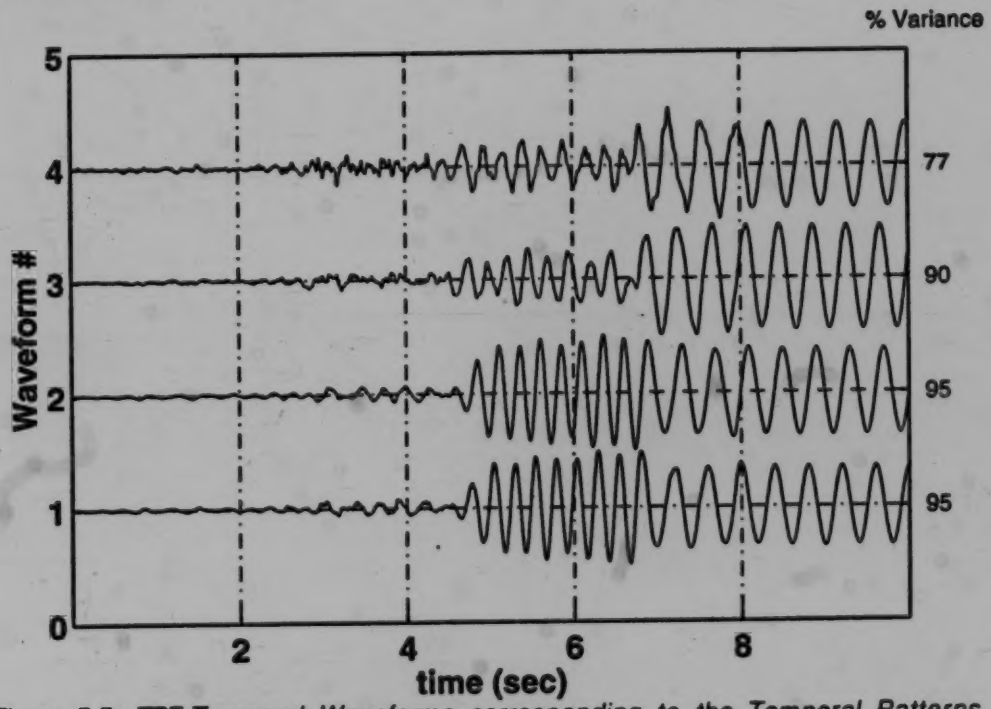

Figure 5.5 TPF Temporal Waveforms corresponding to the Temporal Patterns which account for the four largest variances in the abnormal segment; Simulated Data.

For clarity Figure 5.5 shows the bottom four TPF temporal waveforms. In this example, the TPF temporal waveforms appear to be in pairs, each pair containing the dominant frequencies of the abnormal source waveform. The second pair also contains more of the noise and normal activity which is reflected in the reduced variance. The temporal pattern that corresponds to the bottom TPF temporal waveform was used to form the temporal pattern filter applied in this analysis. Figure 5.6 shows the frequency response of the temporal filter used in this example.

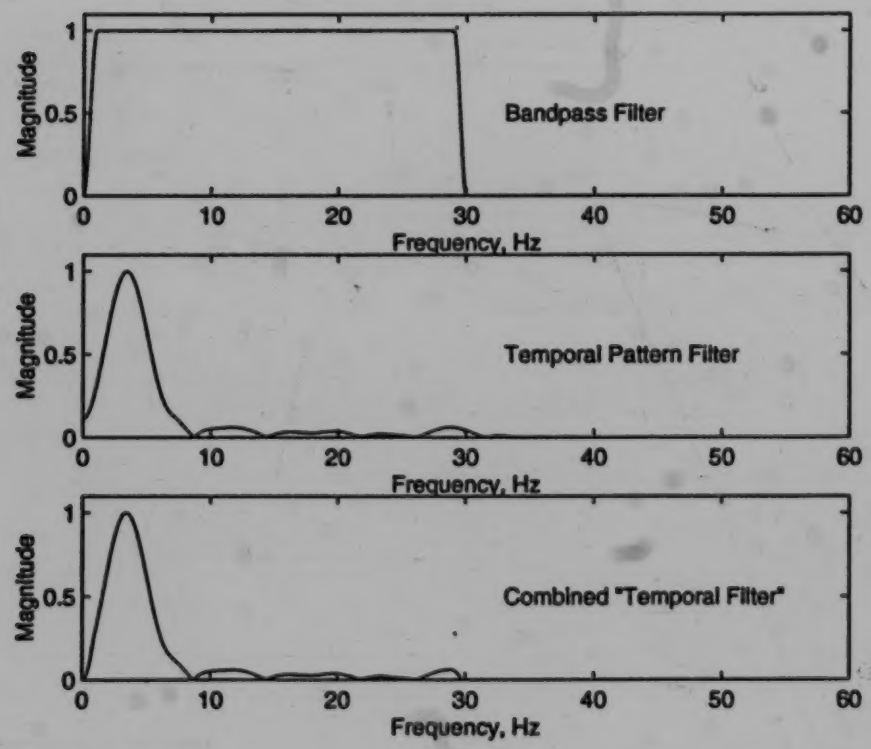

Figure 5.6 Temporal Filter Frequency Response; Simulated Data

The top plot in Figure 5.6 shows the frequency response of the temporal bandpass filter. The bandpass temporal filter, for the simulated EEG, passes frequencies between 1 Hz and 29 Hz untouched, and removes any frequencies above 30 Hz. The middle plot in Figure 5.6 shows the frequency response of the temporal pattern filter, based on equation 4.17 and following the procedure described in Chapter 4. The result of the combination of the temporal bandpass filter and the temporal pattern filter based on equation 4.19, is shown in bottom plot. The bandpass filtered EEG, filtered using only the temporal bandpass filter, is shown in Figure 5.7.

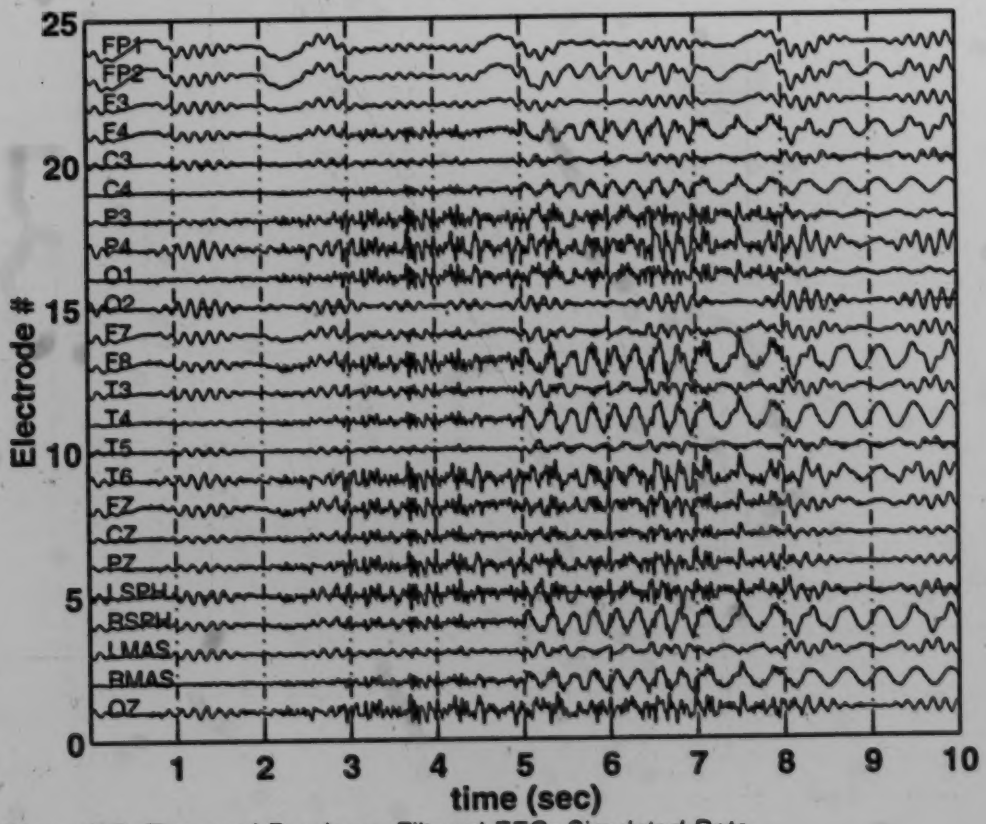

Figure 5.7 Temporal Bandpass Filtered EEG; Simulated Data

The temporally filtered EEG, using the combined bandpass and temporal pattern filter, is shown in Figure 5.8. The epileptiform activity is clearly displayed in this filtered EEG. This temporally filtered EEG clearly reveals the seizure onset at 5 seconds as well as lateralizes the seizure to the right hemisphere. (Note even numbered electrodes are located on the right hemisphere.)

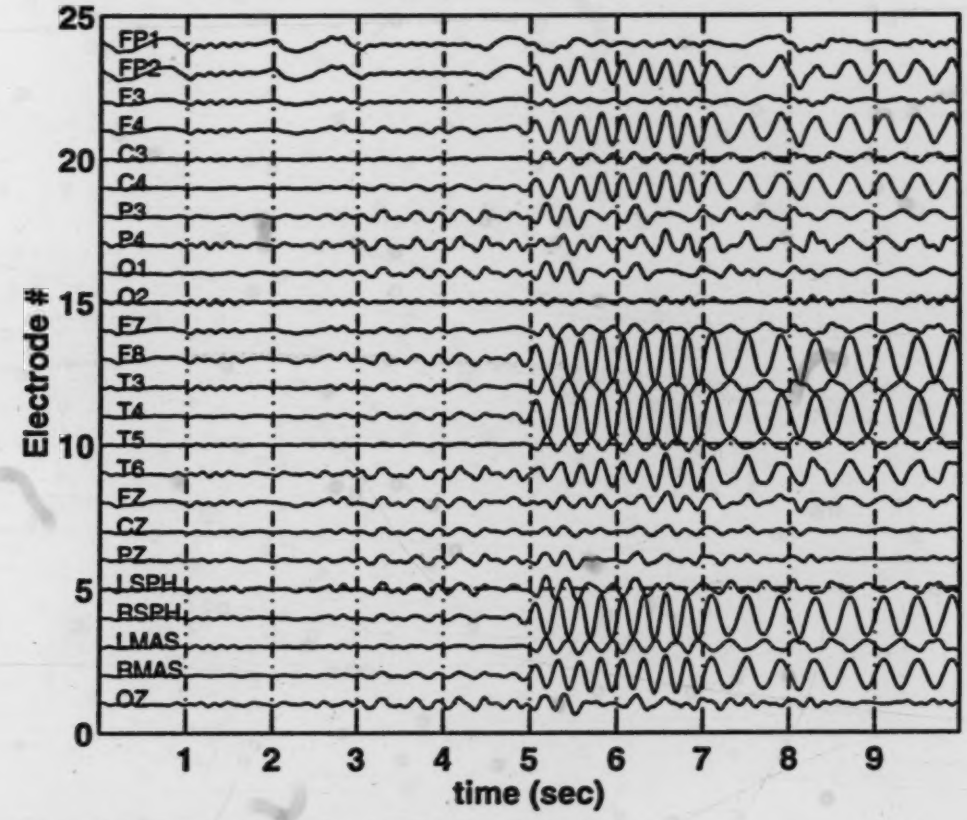

Figure 5.8 Temporally Filtered EEG; Simulated Data

Spatial Filtering

The procedure continues with the design of the spatial pattern filter. Spatial filtering results in further separation of the remaining activity within the temporally filtered EEG into abnormal and background spatial patterns and corresponding temporal

waveforms. The spatial pattern filtered (SPF) temporal waveforms derived by projecting the data matrix, V_{tt}, onto the spatial patterns are displayed in Figure 5.9. The percentage of variance each spatial pattern accounts for in the abnormal EEG segment is listed to the right of the corresponding SPF temporal waveform.

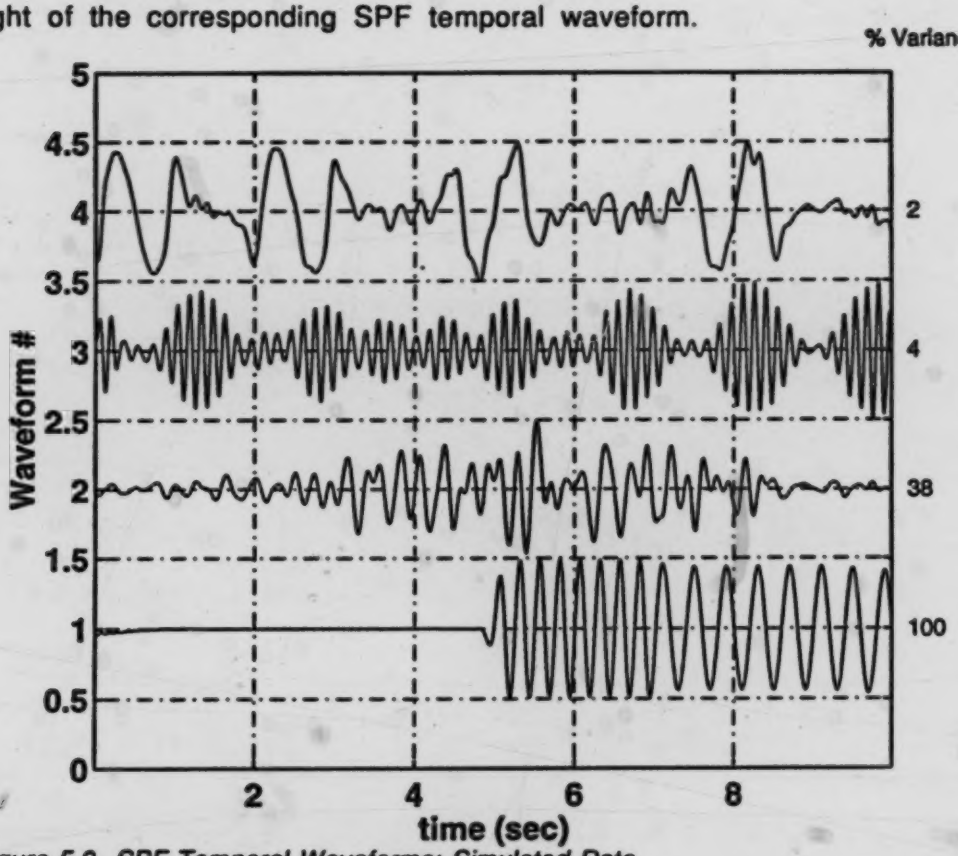

Figure 5.9 SPF Temporal Waveforms; Simulated Data

From these waveforms, it can be seen that the abnormal activity was isolated to a single SPF temporal waveform, waveform # 1 which corresponds to the spatial pattern that accounts for the largest variance in the abnormal EEG segment. In fact, the normal activity was also isolated to a separate SPF temporal waveform, waveform #3. Although most of the noise was eliminated using the

temporal filter the remaining noise and eyeblink artifact can also be identified in the remaining two SPF temporal waveforms, waveform #2 and 3 respectively.

Table 5.3 Common Spatial Patterns, Simulated Data

Electrode Site	Waveform # 1	Waveform # 2	Waveform # 3	Waveform # 4
FP1	0.0248	0.0239	-0.1214	-0.4943
FP2	0.2105	0.0296	-0.1133	-0.4944
F3	-0.0345	0.0349	-0.0998	-0.1812
F4	0.2679	-0.0588	-0.0845	-0.1901
C3	-0.0807	-0.0264	-0.0747	-0.0326
C4	0.2330	-0.0607	-0.0135	-0.0424
P3	-0.0879	-0.1532	-0.0366	-0.0011
P4	0.1118	-0.1658	0.1385	-0.0191
O1	-0.0691	-0.1441	0.0070	0.0088
O2	0.0332	-0.0114	0.1528	0.0104
F7	-0.0707	-0.0382	-0.1090	-0.1855
F8	0.4183	-0.1323	-0.0890	-0.1984
T3	-0.1094	-0.0672	-0.0924	-0.0415
T4	0.4218	-0.0871	-0.0229	-0.0504
T5	-0.1077	-0.0316	-0.0565	0.0107
T6	-0.2155	-0.1556	0.0933	-0.0178
Fz	0.0733	-0.1146	-0.1015	-0.1935
Cz	0.0189	-0.0911	-0.0503	-0.0369
Pz	-0.0173	-0.1374	0.0448	-0.0032
LSPH	-0.0909	-0.1392	-0.1095	-0.0934
LMAS	0.3876	-0.0747	-0.0664	-0.0901
RSPH	-0.1060	-0.0336	-0.0800	-0.0076
RMAS	0.2869	-0.0810	-0.0068	-0.0200
Oz	-0.0288	-0.1566	0.0696	0.0033

The normalized common spatial patterns from which the common spatial pattern filter was derived are listed in Table 5.3 and are shown as spatial maps in Figure 5.10. The comparison of the spatial maps in Figure 5.10 to those in Figure 5.2 show that the first (100% Variance) spatial map in Figure 5.10 can clearly be identified with the abnormal spatial map in Figure 5.2. It follows that the spatial maps of the normal activity, the eyeblink artifact and to some extent the noise activity in Figure 5.2 can also be associated with the third (4% Variance), fourth (2% Variance) and second (38% Variance) spatial maps in Figure 5.10 respectively.

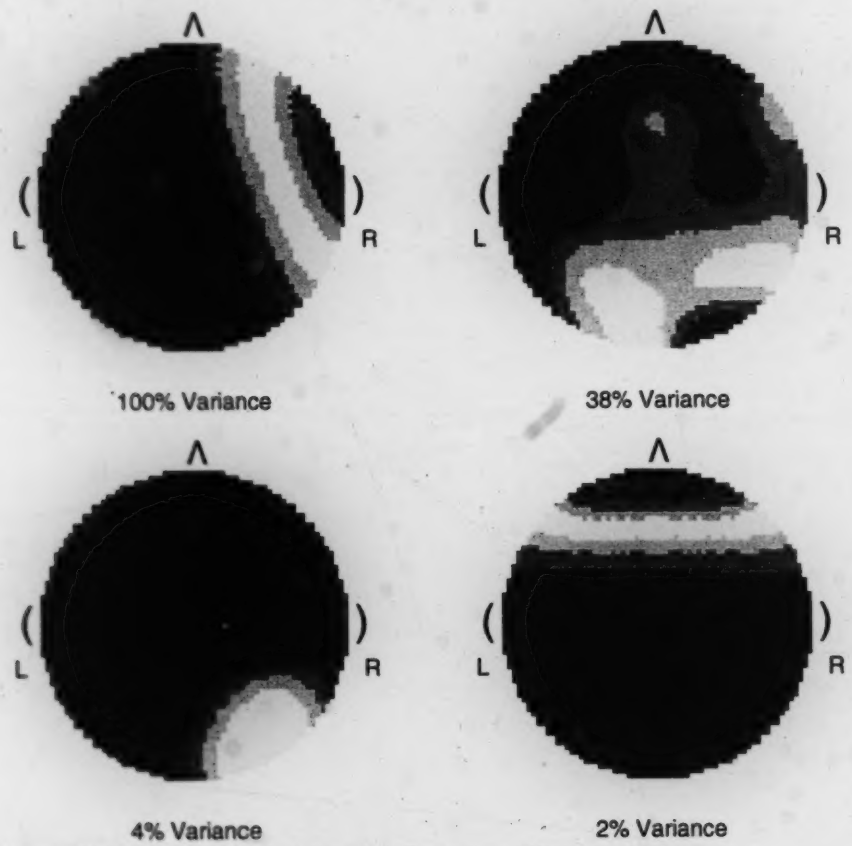

Figure 5.10 Mapping of Derived Spatial Patterns; Simulated Data

Even though the maps in Figures 5.10 and 5.2 look very similar, some inaccuracy is apparent when the SPF temporal waveforms and source waveforms are compared. Although, another choice of temporal pattern filter may provide a better visual isolation of the activity into the SPF temporal waveforms, the abnormal spatial pattern presented is the most accurate out of the filter design choices tested. The comparison of a few alternative filter designs are discussed later in this chapter.

The first spatial pattern which accounts for the maximum variance in the abnormal EEG corresponds to the bottom SPF temporal waveform in Figure 5.9. This spatial pattern was identified as abnormal and was used to spatially filter the temporally filtered data matrix. The temporally and spatially filtered simulated EEG was the result of the reconstruction of the abnormal spatial pattern and the corresponding SPF temporal waveform. The temporally and spatially filtered EEG, with enhanced epileptiform activity, is shown in Figure 5.11.

The strongest temporally and spatially filtered simulated electrode recordings, as seen in Figure 5.12, are F8, T4 and RSPH which are associated with the right temporal lobe. This is reflected as the bright red area in the first spatial map of Figure 5.10 and is confirmed by the corresponding values in Table 5.3. It is clear that the source of the activity in the temporally and spatially filtered simulated EEG has been localized to a single focus between the F8 and T4 electrodes. This can be seen by the amplitude comparisons of the temporally and spatially filtered electrode recordings and by the

quantization of these amplitudes in the spatial map. The seizure onset at 5 seconds is clearly confirmed in the temporally and spatially filtered EEG.

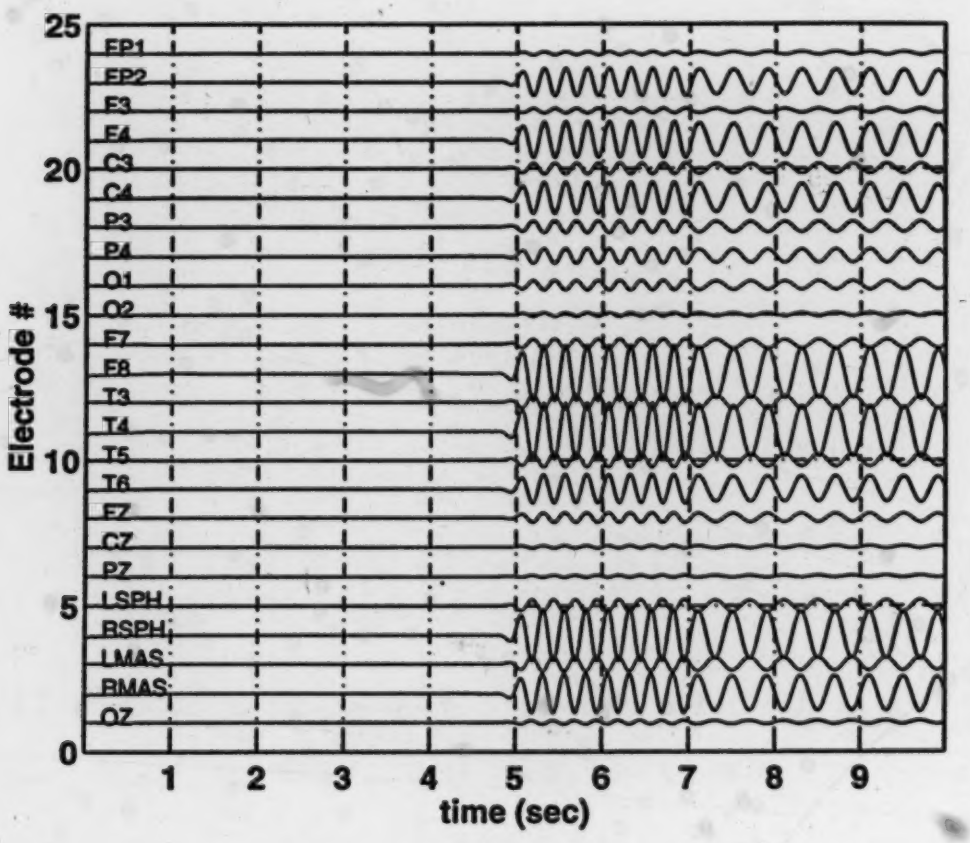

Figure 5.11 Temporally and Spatially Filtered EEG; Simulated Data

Filter Design Comparison

Since a spatial pattern is a basis vector, the spatial pattern defines an axis in the new coordinate system. The accuracy of the filter design can be quantified using the difference in the alignment between two spatial patterns. Thus, the angle between the assigned

spatial pattern and the derived spatial patterns can be defined as the error in the alignment of the derived spatial pattern. This error is an indication of how well the isolation of the abnormal subspace has been achieved.

The simulated EEG was analyzed using many variations in filtering. Figure 5.12 shows the frequency response of 7 temporal pattern filters which correspond to various combinations of the four TPF temporal waveforms shown in Figure 5.5. The top four plots are the frequency responses of filters designed using each of the first four temporal patterns separately. The next three frequency responses correspond to the temporal pattern filters created from combinations of temporal patterns.

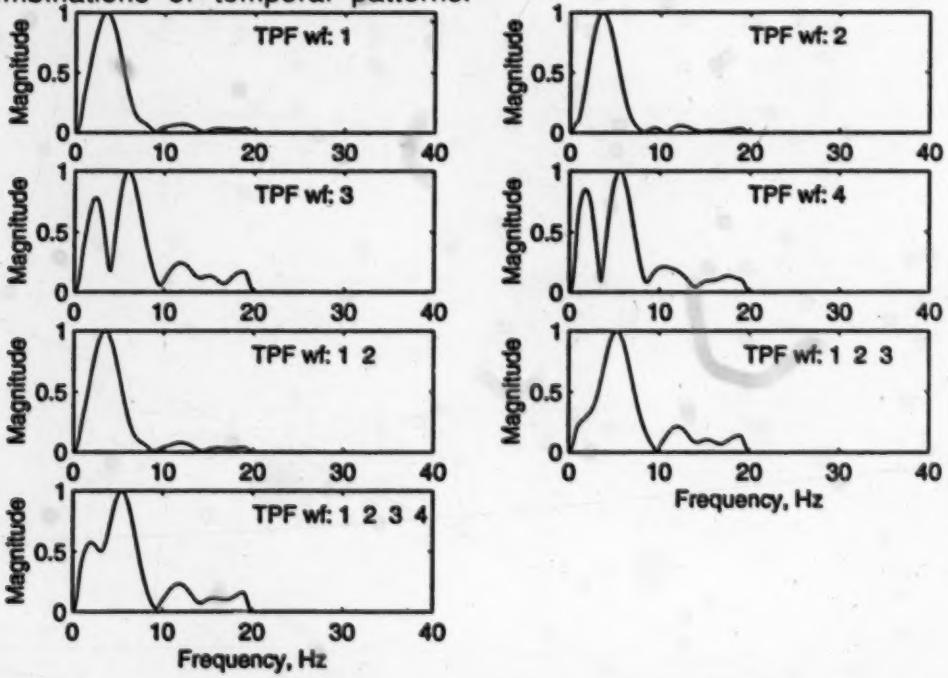

Figure 5.12 Frequency Response for 7 Temporal Pattern Filters; Simulated Data

The error between the assigned and the derived abnormal spatial patterns resulting from 8 different temporal pattern filter designs are shown in Table 5.4. The first variation used temporal bandpass filtering followed only with spatial filtering. The following rows show the errors in alignment resulting from temporal and spatial filtering, incorporating the different combinations of temporal pattern filters. The temporal pattern filter was designed using the temporal patterns corresponding to the boxes in Table 5.4 marked with an "X". Rows 2 through 5 show the results when a single temporal pattern is used. Rows 6 through 8 show the result using two, then three temporal patterns, until the last row where the all four temporal patterns are used. The errors in degrees, α_i, between the normalized derived abnormal spatial patterns $\mathbf{C}_i$ and the normalized assigned abnormal spatial pattern $\mathbf{M}_a$ are listed in the final column of the table. The error defined in radians can be calculated using the following equation:

$$\alpha_i = \cos^{-1}(\mathbf{M}_a' \mathbf{C}_i) \qquad (5.2)$$

The index i refers to each of the derived abnormal spatial patterns and the corresponding alignment angle.

The results shown in Table 5.4 suggest that the temporal pattern filter using only the first temporal pattern provides the maximum accuracy in deriving the abnormal spatial pattern. The filter design using the temporal pattern that accounts for maximum variance in the abnormal segment is the design criterion applied to the remaining EEG analyses presented in this thesis.

Table 5.4 Alignment Error Comparisons, Simulated EEG

Temporal Pattern Filter Design	No Temporal Pattern Filtering	Temporal Waveform # 1	Temporal Waveform # 2	Temporal Waveform # 3	Temporal Waveform # 4	Error (degrees)
1	X					1.1109
2		X				0.9848
3			X			1.0824
4				X		3.2429
5					X	3.1574
6		X	X			1.0153
7		X	X	X		1.5854
8		X	X	X	X	1.3332

In summary, prefiltering with a temporal pattern filter before spatial filtering an EEG improved source localization. The temporal and spatial pattern filter design procedure creates filters that are able to decompose an EEG into accurate spatial patterns and temporal waveforms.

Clinical Data

In this section, the two EEGs analyzed were recorded from patients diagnosed with epileptic disorders. The first EEG consists of simultaneous depth, subdural and surface recordings. In this case, the abnormal activity enhanced by the temporal pattern filter which was designed using a surface electrode recording can be compared against a standard. The standard used is the abnormal activity which was recorded using a depth electrode placed closer to the source. The second EEG discussed in this section is typical of those analyzed during an informal clinical trial. In this trial, the temporal and spatial filter design procedure was applied to clinical EEGs recorded using only surface electrodes. The results are representative are those typically presented at the weekly Epilepsy Seizure Conference at the University of Alberta Hospital.

Clinical Validation Results

The data dependent filter design process was applied to EEGs from patients diagnosed with mesial temporal sclerosis. The EEGs contained combinations of simultaneously recorded depth, subdural and surface electrodes. This data was recorded using Telefactor recording equipment at the Epilepsy Center at Yale School of Medicine from Patient 1. Figure 5.13 shows the outlines of MRI images of Patient 1's brain and identifies the locations of the electrode sites. For this analysis, the 64 simultaneous electrode recordings have been reformatted into a montage of 3 sets of electrode recordings. These sets include 8 depth recordings (B, RPT,

right depth electrode), 5 subdural strip recordings (F, RAT, right subdural anterior temporal electrode strip) and 14 surface recordings (f9, f7, t3, f3, c3, f10, f8, t4, t6, f4, c4, fpz, cz, and oz).

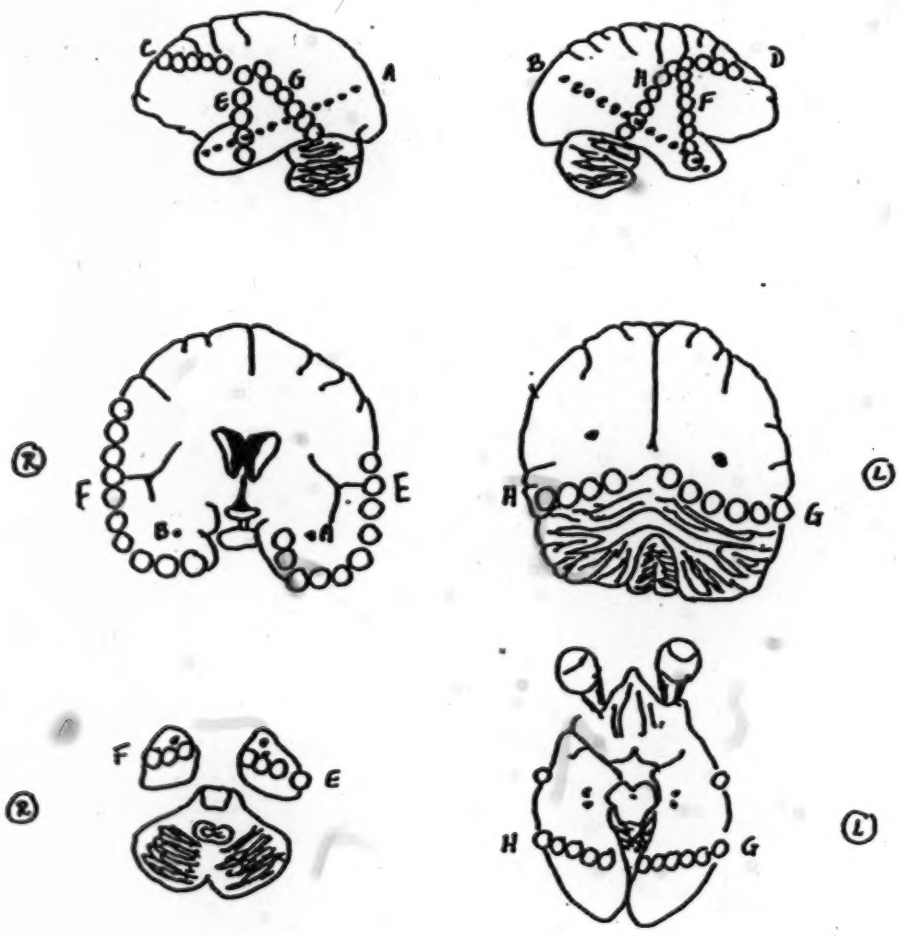

B = RPT, Right Depth Electrode

F = RAT, Right Anterior Temporal Subdural Electrode Strip

Figure 5.13 MRI Tracing of Electrode Locations; Patient 1

Figure 5.14 shows a 10 second portion of these electrode recordings from the raw EEG. Each of the depth, subdural and surface

electrode recordings, in Figure 5.14, are labeled with the appropriate identifier corresponding to the labels specified in Figure 5.13. Each of the sections, the depth, subdural and surface electrodes were scaled independently so that the activity in each set is visible. In comparing the three groups of electrode recording the apparent spikes of the seizure onset are evident in the surface electrode recordings. Although it is important to note that based on these raw surface EEG recordings alone the seizure onset can not be confidently identified and the sources of the epileptiform activity cannot be lateralized.

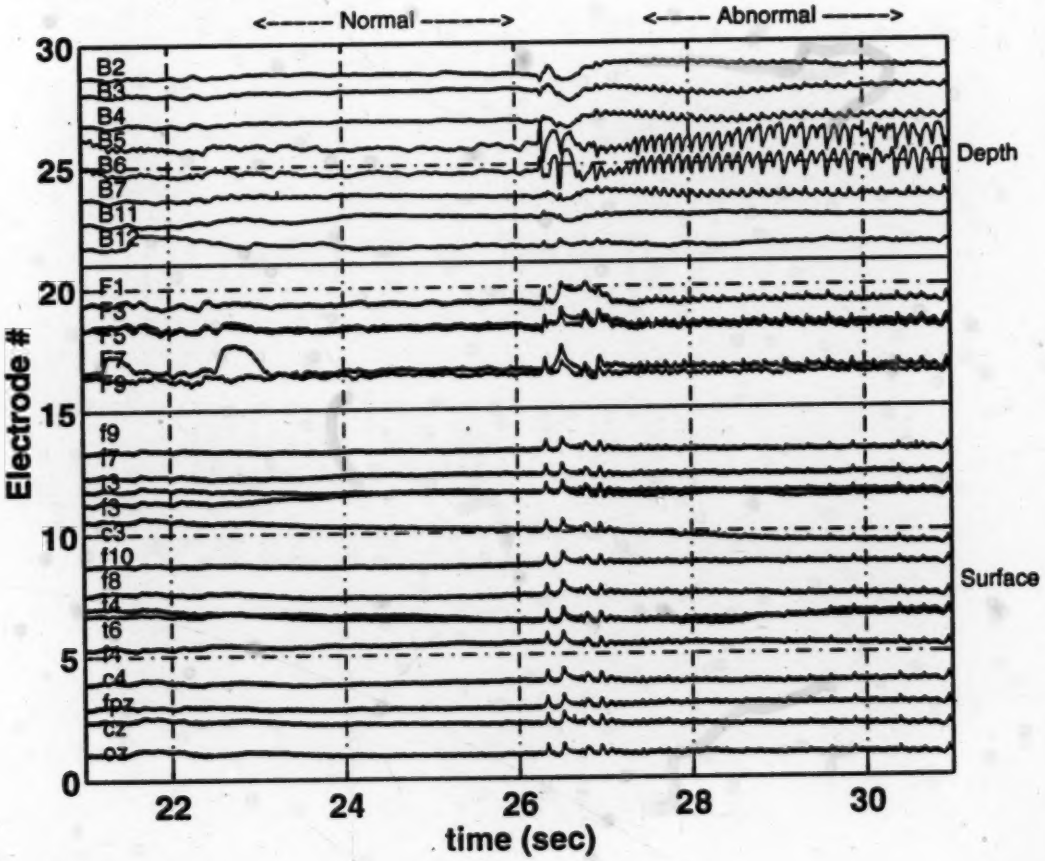

Figure 5.14 Raw EEG; Patient 1

Temporal Filtering

EEG recordings from depth electrodes which were invasively inserted into the brain provides the closest facsimile of the true abnormal activity. Depth recordings typically, are not obscured by muscle artifact or other extraneous activity as the abnormal activity prevails over the background or other activity [Tyner et al. 1983]. Therefore, a depth electrode recording can be used as the standard to which the results can be compared. The temporal and spatial filtering of simultaneously recorded surface and depth electrode recordings enables a comparison of a test set of results to a standard set of results. The test set of filtered recordings was obtained using a temporal pattern filter designed from a surface electrode recording. The standard set of filtered recordings was obtained using a temporal pattern filter designed from a depth electrode recording. These two filters are referred to as the surface and the depth designed temporal filters, respectively.

The two temporal pattern filters were designed using the selected depth and surface electrode recordings identified in Figure 5.14 as B6 and f10, respectively. Also indicated on Figure 5.14 are the abnormal and the normal segments selected from each of the depth and surface electrode recordings identified in Table 5.1. Recall from Chapter 2 the terms ictal and preictal. The abnormal segment incorporates the ictal activity which is defined as a change, that persists for a period of 3 seconds, from the normal frequency or waveform pattern. The normal segment incorporates the preictal activity and was selected from an EEG segment where the apparent ictal components are not present. In this case, the period between

27.5 seconds and 30.5 seconds was chosen as the abnormal segment and the period between 23 seconds and 26 seconds was chosen as the normal segment.

The results of applying a temporal bandpass filter to the 10 second portion of the raw EEG is shown in Figure 5.15 with the 3 separate sections scaled independently. The (0-1-30) temporal bandpass filter consists of low frequency cut off set at 0 Hz with the high frequency cut off set at 30 Hz. The DC bias has been removed from the data and thus the B6 depth electrode recording and the f10 surface electrode recording can be more clearly identified.

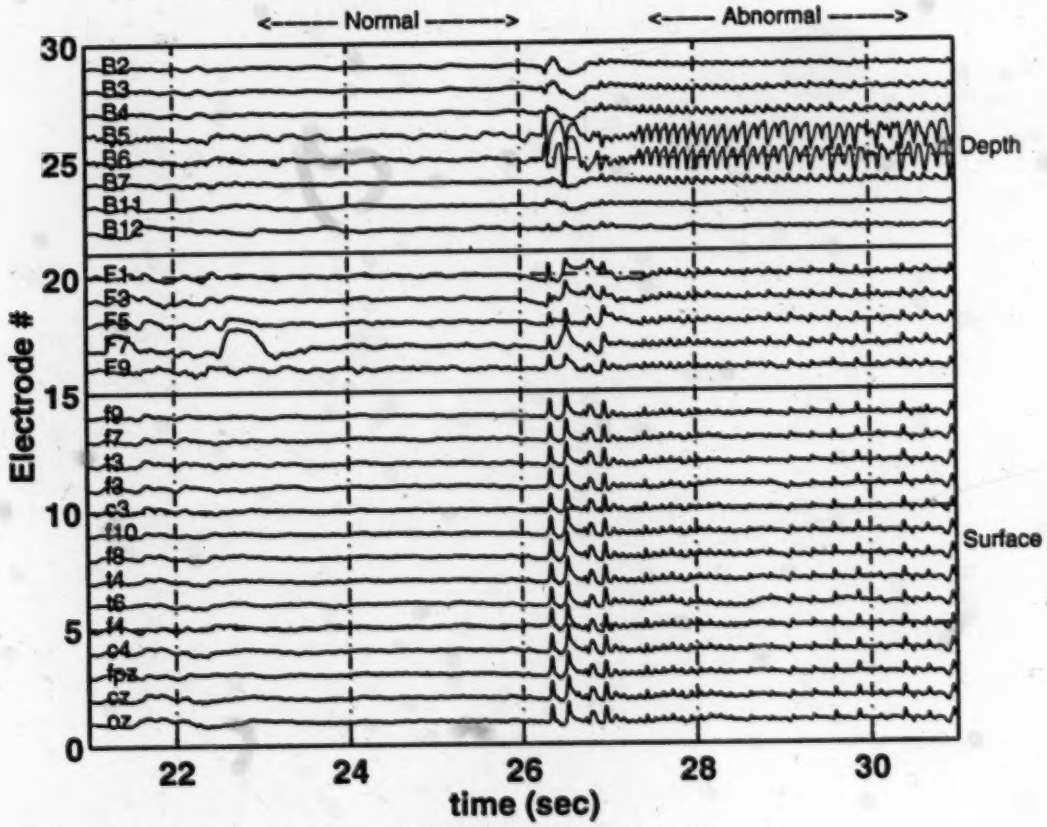

Figure 5.15 Temporal Bandpass Filtered EEG; Patient 1

At this point the temporal patterns and the TPF temporal waveforms were derived using both the selected depth and surface electrode recordings. The depth and surface designed TPF temporal waveforms, shown in Figure 5.16 and 5.17, can be viewed as a decomposition of the depth and surface electrode recording, respectively. The column of numbers on the right side of the waveforms are the corresponding percentage of variance that each temporal pattern accounts for in the abnormal segment of the selected electrode recording. The TPF temporal waveforms that correspond to the temporal pattern which account for maximum variance in the abnormal segment and the minimum variance in the normal segment are displayed at the bottom of the figures. Figure 5.16, displays the TPF temporal waveforms corresponding to each of the depth designed temporal patterns. According to the design criterion, established in the Simulated Data section of this chapter, the first temporal pattern which accounts for 97% variance in the abnormal segment was used in the depth designed temporal filter. Figure 5.17, displays the TPF temporal waveforms corresponding to each of the surface designed temporal patterns. The first temporal pattern which accounts for 98% variance in the abnormal segment was used in the surface designed temporal filter. The low frequency (approximately 8 Hz) that is apparent in the raw B6 depth recording is clearly evident in the bottom TPF temporal waveforms in both figures.

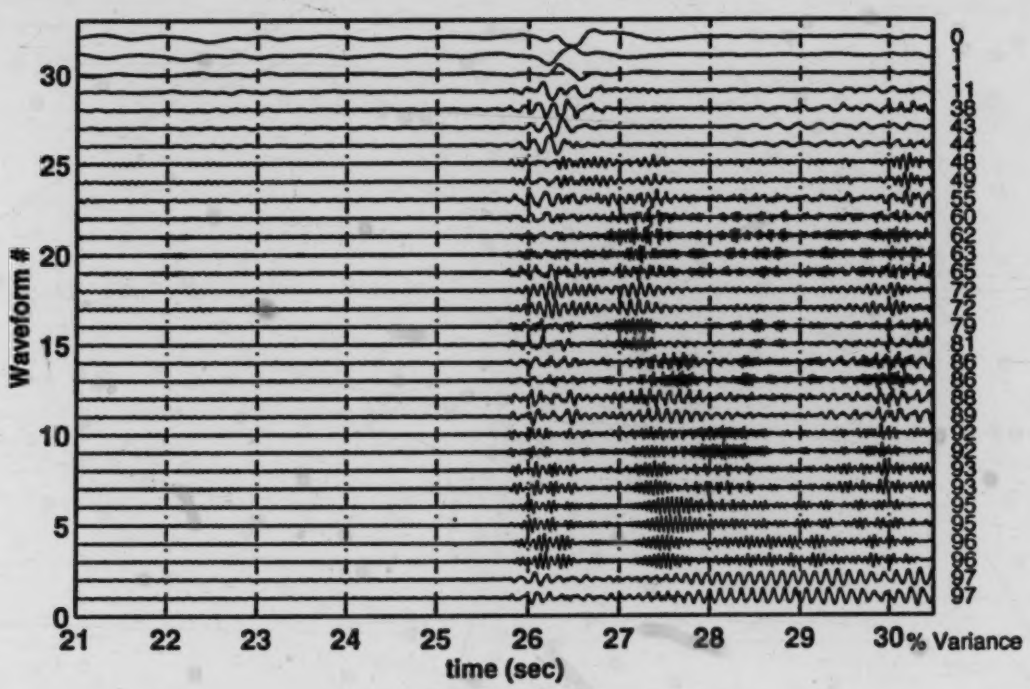

Figure 5.16 TPF Temporal Waveforms for Temporal Pattern Filter Designed Using a Depth Electrode; Patient 1

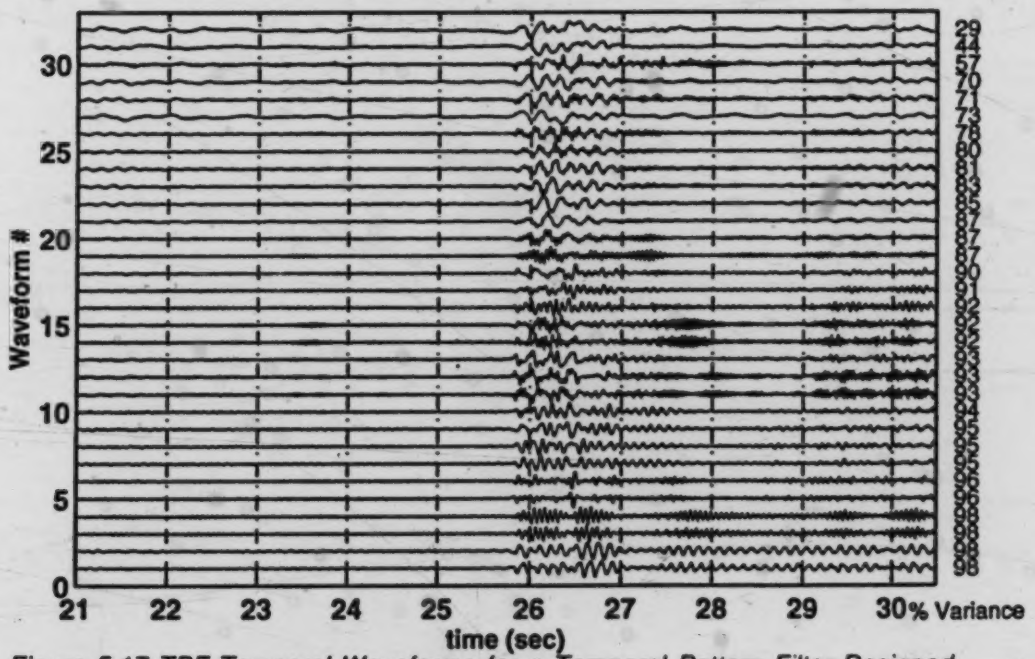

Figure 5.17 TPF Temporal Waveforms for a Temporal Pattern Filter Designed Using a Surface Electrode; Patient 1

Figure 5.18 presents the frequency response of the temporal bandpass, the temporal pattern and the combined temporal filter for the depth and surface designed temporal filters. The comparison of the frequency responses for the two combined temporal pattern filters indicates that the surface and the depth designed temporal filter both consist of similar fundamental frequency content under 10 Hz.

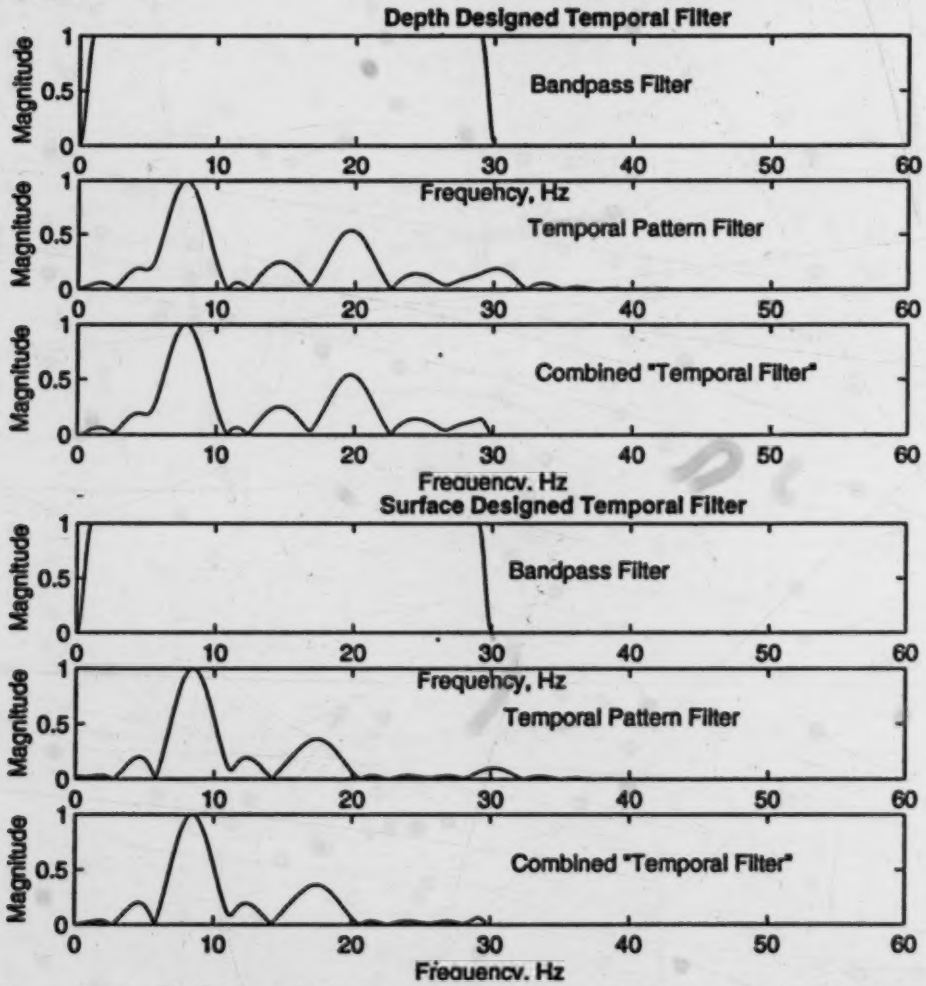

Figure 5.18 Frequency Response for Depth and Surface Designed Temporal Filters; Patient 1

Figures 5.19 and 5.20 exhibit the temporally filtered EEGs using the depth designed temporal filter and the surface designed temporal filter, respectively. The filters were applied to the 10 second portion of the raw EEG data shown in Figure 5.14. Each group of electrode recordings within these figures was independently scaled. The application of both temporal filters to the raw EEG data, resulted in the enhancement of the selected ictal components within the depth, subdural and surface electrodes.

Reviewing the surface electrode recordings alone, in both temporally filtered EEGs, the seizure onset can be easily identified. The correlation of the seizure onset, indicated by the consistent presence of an increased amplitude of the rhythmic low frequency at approximately 5 seconds, is clearly seen in all three sets of electrode recordings. Even though the seizure onset is visible in the temporally filtered surface recordings the seizure cannot be visually lateralized. Although in Figure 5.20, in the 27.5 to 28.5 sec interval, the amplitude of the temporally filtered electrode recordings, f9, f7, t3 and f3 are not as large as the amplitude of the temporally filtered electrode recordings f10, f8, t4 and t6 suggesting a right temporal lobe focus.

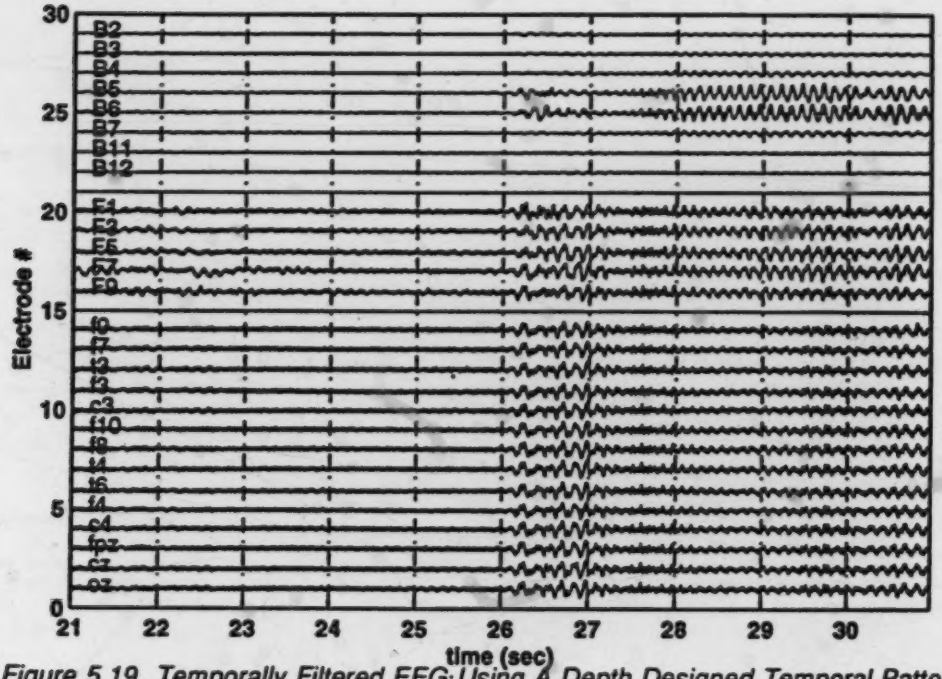

Figure 5.19 Temporally Filtered EEG Using A Depth Designed Temporal Pattern Filter; Patient 1

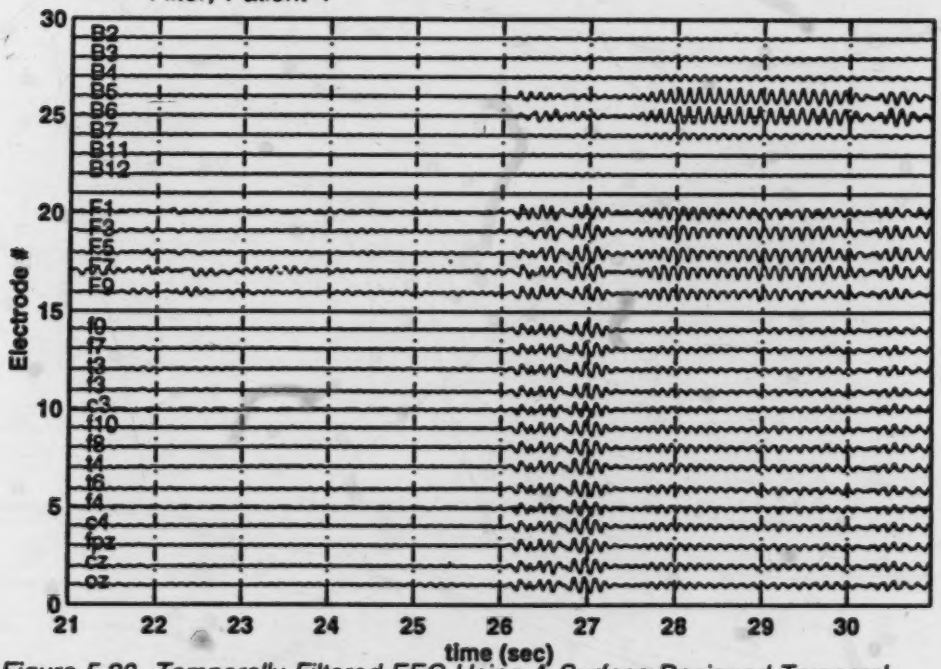

Figure 5.20 Temporally Filtered EEG Using A Surface Designed Temporal Pattern Filter; Patient 1

Spatial Filtering

The analysis continues with the design of a spatial pattern filter following the procedure outlined in Chapter 4. Only the surface electrode recordings were used in the spatial pattern filtering. Figures 5.21 and 5.22 present the SPF temporal waveforms which correspond to the spatial patterns of the temporal filtered surface electrode recordings using the depth and surface designed temporal filters. In both cases, the abnormal activity was isolated to the SPF temporal waveform which accounts for maximum variance in the abnormal surface electrode recordings. According to equation 4.28 the corresponding spatial pattern and SPF temporal waveform and filtered EEG can be now labelled as abnormal.

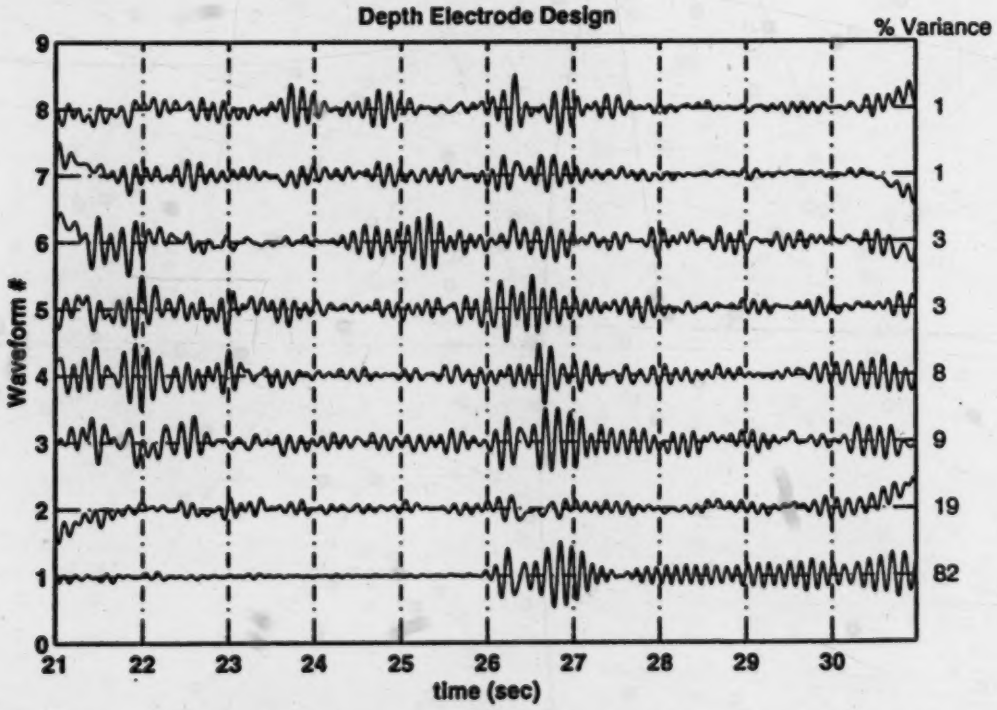

Figure 5.21 SPF Temporal Waveforms of Surface Electrode Recordings Using A Depth Designed Temporal Filter; Patient 1

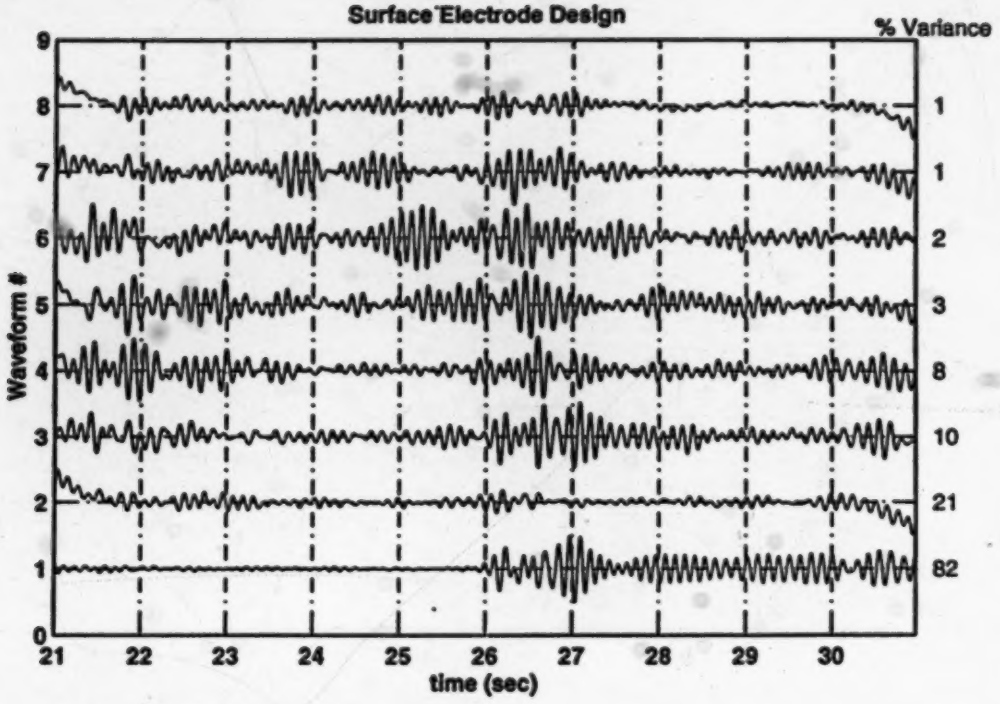

Figure 5.22 SPF Temporal Waveforms of Surface Electrode Recordings Using A Surface Designed Temporal Filter; Patient 1

Recombining the abnormal SPF temporal waveform and the corresponding spatial pattern for surface electrodes creates the temporally and spatially filtered surface electrode recordings. The filtered EEGs derived from use of the depth and surface designed filters are shown in Figures 5.23 and 5.24. These filtered EEGs are scaled according to the minimum weight within the spatial pattern (C=C-min(C)) to distribute the difference between the weightings. Although the complete set of surface electrodes are not used, both filtered EEGs confirm the seizure onset at 26 seconds and lateralize the seizure to the right temporal lobe.

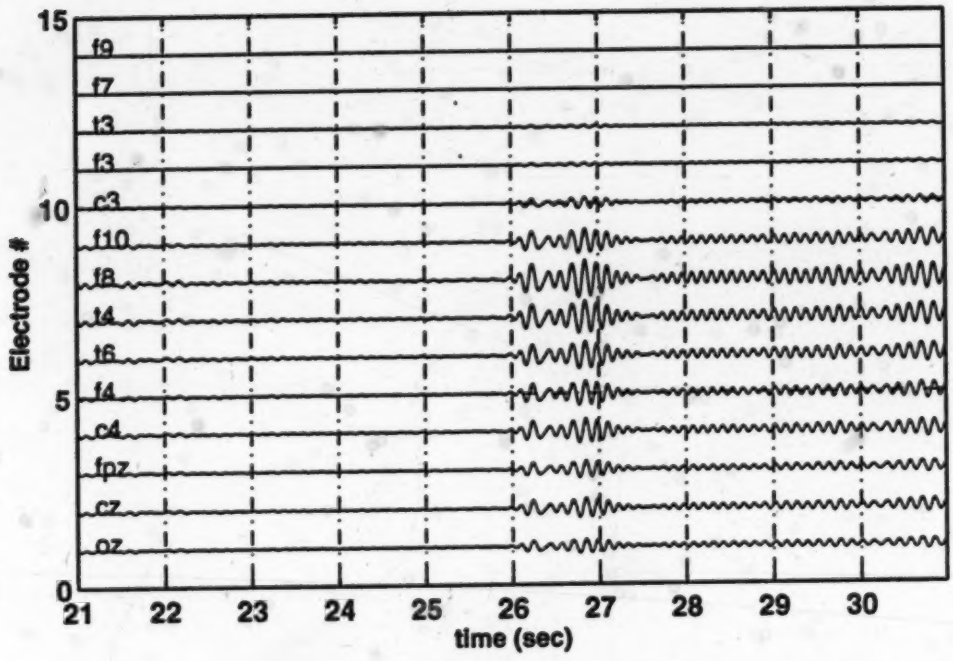

Figure 5.23 Scaled Temporally and Spatially Filtered Surface Electrode Recordings Using A Depth Designed Temporal Filter; Patient 1

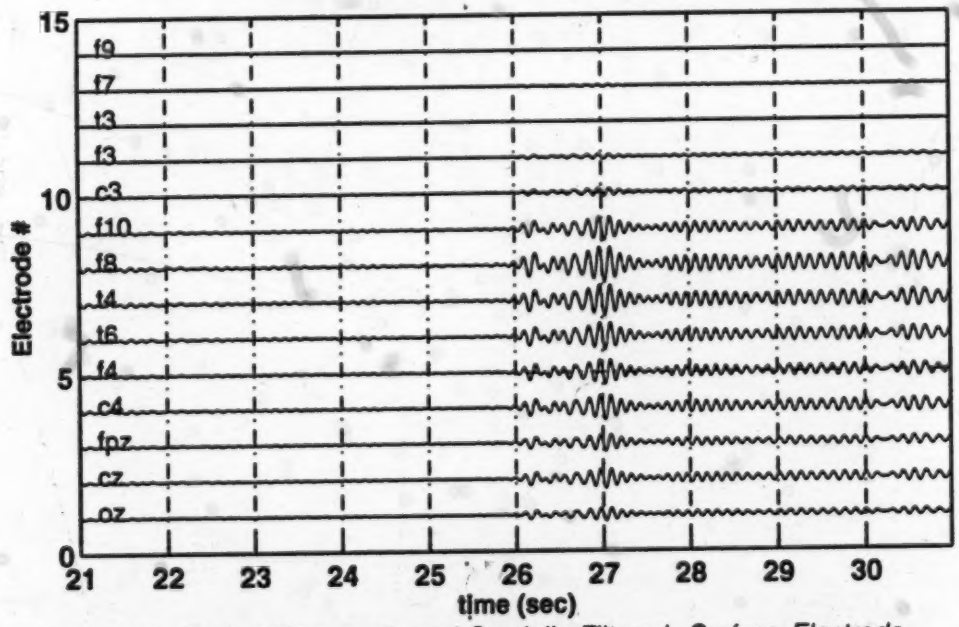

Figure 5.24 Scaled Temporally and Spatially Filtered Surface Electrode Recordings Using A Surface Designed Temporal Filter; Patient 1

Filter Design Comparisons

To evaluate the effectiveness of the temporal pattern filter an analysis of the EEG was completed without a temporal pattern filter. Figure 5.25 presents the SPF temporal waveforms using only the temporally bandpass filtered surface electrodes. In this case different segments were selected from those used for the surface and depth designed spatial temporal filters. The abnormal and normal segments, of 25 seconds to 30 seconds and 22 seconds to 25 seconds respectively, were selected to improve the results for spatial pattern filtering without temporal pattern filtering. In fact, in this case the burst between 26 and 27 seconds had to be included.

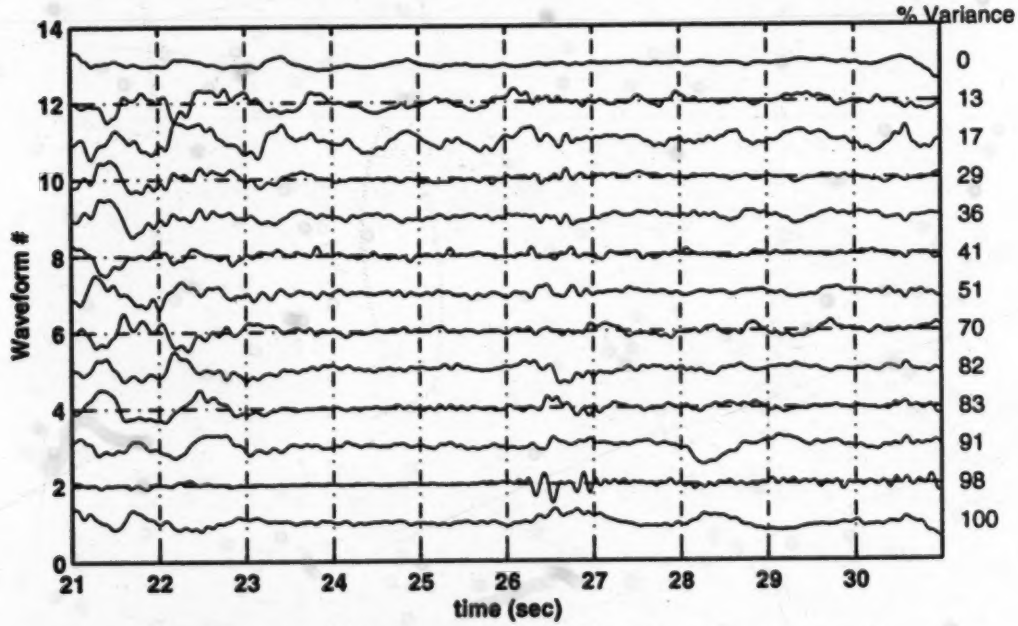

Figure 5.25 SPF Temporal Waveforms for a Filter Designed without a Temporal Pattern Filter; Patient 1

The second SPF temporal waveform was selected as the abnormal SPF temporal waveform containing epileptiform activity. However, the abnormal activity can not be confidently attributed to an

epileptic seizure. The SPF temporal waveforms, compared to those in Figures 5.21 and 5.22, indicate that prefiltering with a temporal pattern filter improves the isolation of the abnormal activity.

Quantifying the comparisons of the effectiveness of the filter designs, Table 5.5 lists the normalized abnormal spatial patterns for temporally and spatially filtered surface electrode recordings using three temporal filter options. The three temporal filter options are the surface designed temporal filter, the depth designed temporal filters and no temporal pattern filter but using a bandpass temporal filter.

Table 5.5 Comparison of Abnormal Spatial Patterns; Patient 1

Electrode Site	Depth Designed Filter	Surface Designed Filter	No Temporal Pattern Filter
f9	0.2223	0.2165	0.2503
f7	0.2258	0.2219	0.2332
t3	0.2291	0.2167	0.2394
f3	0.2320	0.2300	0.2572
c3	0.2491	0.2407	0.2319
f10	0.2827	0.2865	0.2869
f8	0.3149	0.3216	0.3123
t4	0.3042	0.3091	0.2937
t6	0.2900	0.2981	0.2618
f4	0.2841	0.2873	0.2679
c4	0.2873	0.2900	0.2862
fpz	0.2628	0.2652	0.2868
cz	0.2734	0.2729	0.2693
oz	0.2616	0.2533	0.2500
Angle Error	0.0°	1.3114°	3.5293°

The filters designed using the surface designed temporal filter and the design without a temporal pattern filter are compared to the filter design using the depth designed temporal filter. A narrower bandpass filter (0-1-10) was applied to focus the spatial filters on the rhythmic low frequency pattern and to improve accuracy of the design without a temporal pattern filter. The error between the spatial patterns, shown on the last line of Table 5.5, is a quantified measure of the improvement in filter design. The errors were calculated using equation 5.2.

The mapping of the abnormal spatial patterns corresponding to the filter design using the depth and surface designed temporal filters and the design without a temporal pattern filter are displayed in Figure 5.26. Comparing the three abnormal spatial patterns, the spatial maps corresponding to the surface and depth designed filters are very similar, as confirmed by the low errors. The design without a temporal pattern filter appears to focus more anterior in the right temporal region. The irregularity of the distribution in the left hemisphere indicates that the spatial pattern corresponds to activity that originates from more than one source. This is an indication that the filter design has not totally isolated the abnormal source. But in general, all 3 spatial maps pin point the source underneath the right anterior temporal electrodes. The wide spread distribution of the abnormal source indicates that the source is deeper than if the distribution was more highly focused. This location is confirmed by the location of the depth electrode site, B6, as seen in Figure 5.13. Thus, through the use of temporal and spatial

filtering the abnormal activity can be lateralized using only the surface electrode recordings.

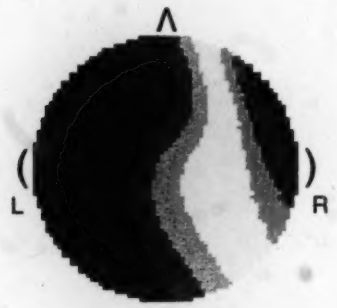

Depth Electrode Design

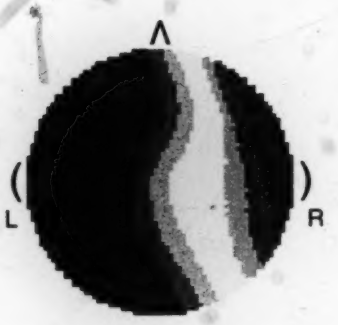

Surface Electrode Design

No Temporal Pattern Design

Figure 5.26 Mapping of Abnormal Spatial Patterns for Depth and Surface Designed Temporal Filters and a Filter without a Temporal Pattern Filter; Patient 1

Another measure of accuracy is achieved through the comparisons of frequency spectra. In this case, the correlation of the low frequency in both the temporally filtered surface recordings using the depth designed and the surface designed temporal filters is corroborated in Figure 5.27. This figure presents a visual comparison of the sets of filtered electrode recordings. The insets display the cross spectral densities of the paired recordings. The cross spectrum identifies the frequency components that the two recordings have in common during the one second interval. The

interval analysed is identified by the sequence of stars above the time axis. The top cross spectral density is the comparison between the bandpass filtered B6 depth electrode recording and the temporally and spatially filtered f10 surface electrode recording using the depth designed temporal filter. The bottom cross spectral density is between the bandpass filtered B6 depth electrode recording and the temporally and spatially filtered f10 surface electrode recording using the surface designed temporal filter. The graphs are labeled with the peak frequency that is most common between the pair of electrode recordings.

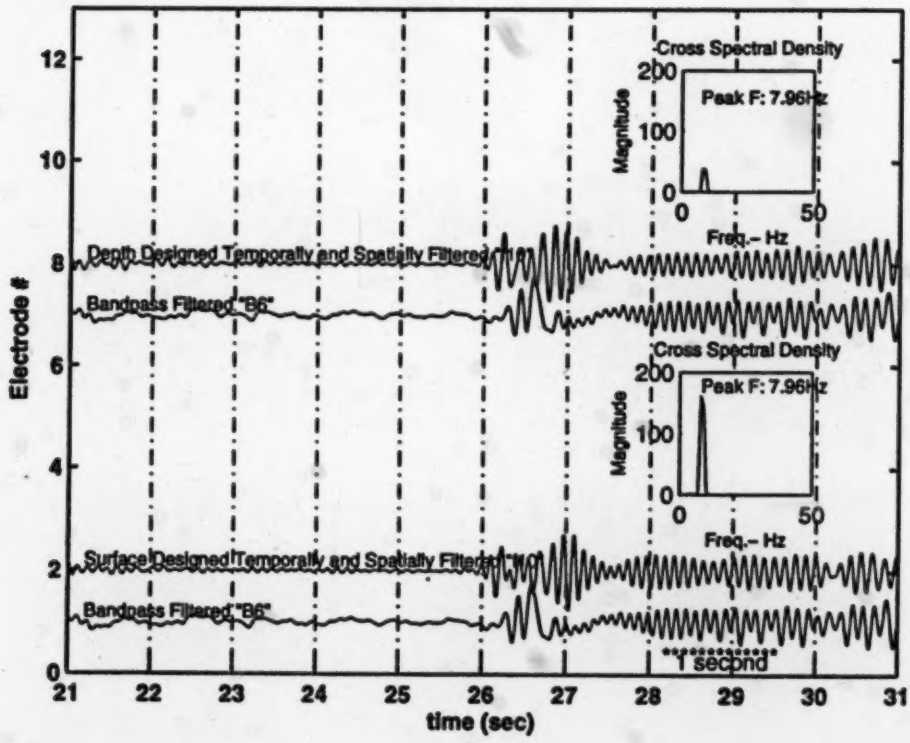

Figure 5.27 Comparison of Filtered Electrode Recordings Resulting from Depth and Surface Designed Temporal Filters; Patient 1

A comparison of the 2 cross spectral densities shows a strong correlation at the peak frequency of 7.96 Hz. This indicates that this low frequency is the strongest frequency component in the bandpass filtered depth recording, B6, and the temporally and spatially filtered surface recording, f10, using both the depth and surface designed temporal filter. The fact that the bottom cross spectral density has a higher peak frequency density is not surprising since the magnitude of this frequency in the frequency response of the surface designed temporal pattern filter is higher than the magnitude of this frequency in the depth designed temporal pattern filter frequency response. Refer to the middle plots of Figure 5.18. The significant fact which is quantified by the cross spectral density comparisons is that both pairs of electrode recordings have the same peak frequency. This suggests that the same information can be derived through the temporal and spatial filtering of the non-invasive surface electrode recordings as can be derived from the invasive depth electrode recordings.

In summary, the simulated EEG analysis suggests that the temporal pattern filtering is a useful procedure and an improvement over spatial filtering alone. The analysis of the Patient 1's EEG indicates that temporal and spatial pattern filtering is able to provide seizure onset and lateralization results from surface electrode recordings alone which are comparable to those results derived from depth electrode recordings.

Clinical Trial Results

During the ongoing informal clinical trial, temporal bandpass, temporal pattern and spatial pattern filtering was applied to an EEG recorded from an adult patient, Patient 2, admitted for Long Term Monitoring at the University of Alberta Hospital under the care of Dr. M. Javidan. The data was recorded as a required element of the patient's diagnosis and treatment under the Comprehensive Epilepsy Program. The patient data was recorded on BMSI equipment with surface electrodes using an extended 10/20 electrode placement system. Refer to Figure 2.5 and Table 2.1. The standard 20 electrodes were supplemented with 4 extra electrodes placed on the left and right temporal lobes in the FT10, FT9, TP10, and TP9 positions. These 4 electrodes are referred to as RSPH, LSPH, RMAS and LMAS respectively. The standard surface reference electrode was placed at Cpz, half way between Cz and Pz.

The results presented are representative of the analysis of patient EEGs completed prior to the weekly epilepsy seizure conference. The EEG from this patient has preictal activity that is similar in frequency content to the ictal activity and as such this EEG does not easily and clearly depict the seizure onset, either temporally or spatially. The questions that are posed regarding this particular EEG are:

- What effect does this level of preictal activity have on the filtering method?
- At what time does the seizure really start?

- What impact does the 6 Hz waveform pattern, during the 30 to 32 second interval in the right temporal electrode recordings, have on the seizure onset?
- Does the epileptiform onset activity consist solely of the 3 Hz activity seen in the left temporal electrode recordings?
- Is there seizure activity between 28 and 30 seconds? Is it overshadowed by other activity as seen in the temporal (LSPH, RSPH, LMAS and RMAS) electrode recordings

The segment of the EEG which has been analyzed has been extended to 20 seconds so that the first bursts of epileptiform activity can be identified. Figures 5.28a and 5.28b present the raw EEG, showing the normal (20 to 23 seconds) and abnormal (30 to 33 seconds) segments as well as the selected electrode (T3).

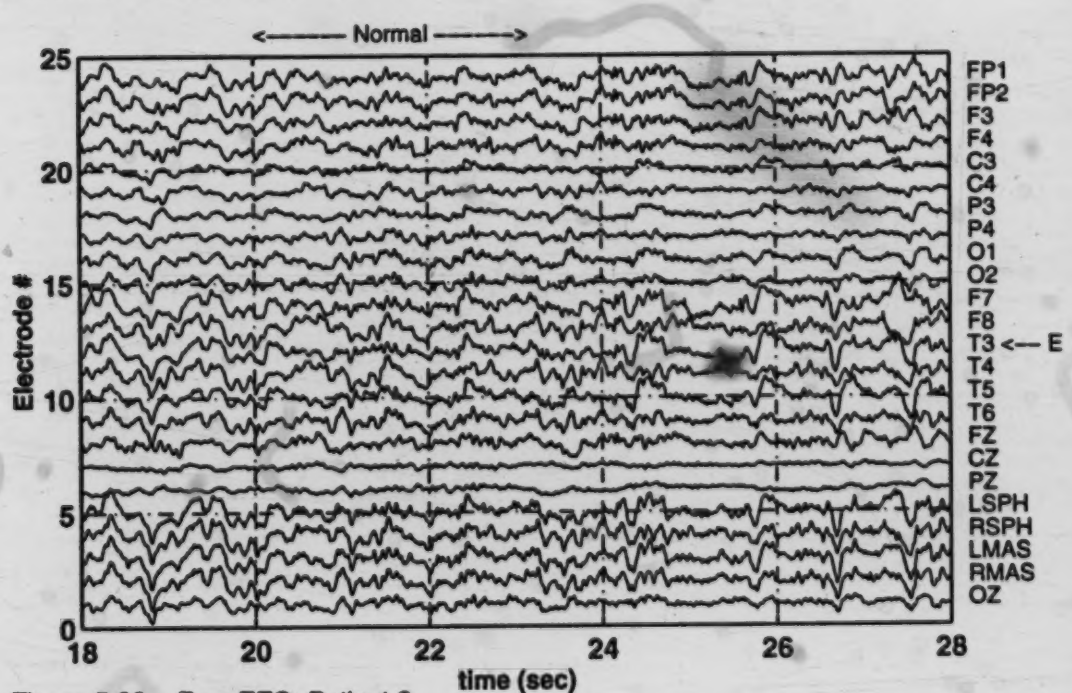

Figure 5.28a Raw EEG; Patient 2

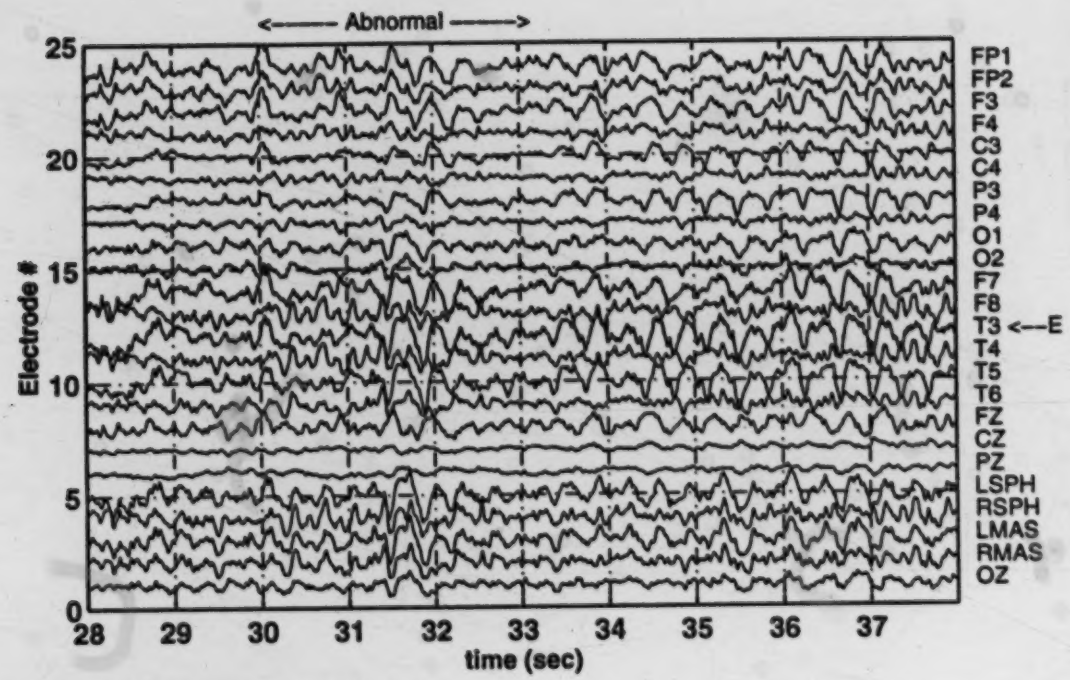

Figure 5.28b Raw EEG; Patient 2

The fully developed epileptic seizure activity (33.5 to 38 seconds) can be lateralized to the left temporal regions but the identification and lateralization of the seizure onset is not clear.

Temporal Filtering

Figures 5.29a and 5.29b display the bandpass filtered EEG. The bandpass filter (0-1-20) was chosen. Figures 5.30a and 5.30b present the TPF temporal waveforms. The temporal pattern filter was created using the first temporal pattern. The frequency response of the temporal filter shown in Figure 5.31 shows that the dominant frequencies of the temporal pattern filter are below 10Hz. A 5-6 Hz waveform pattern can be seen in the normal TPF temporal waveforms 3 to 6. The frequency response of the combined temporal filter, shown in Figure 5.31, contains broad based peaks which

suggest that both the 6 Hz and 3 Hz frequencies will be enhanced in the temporally filtered EEG.

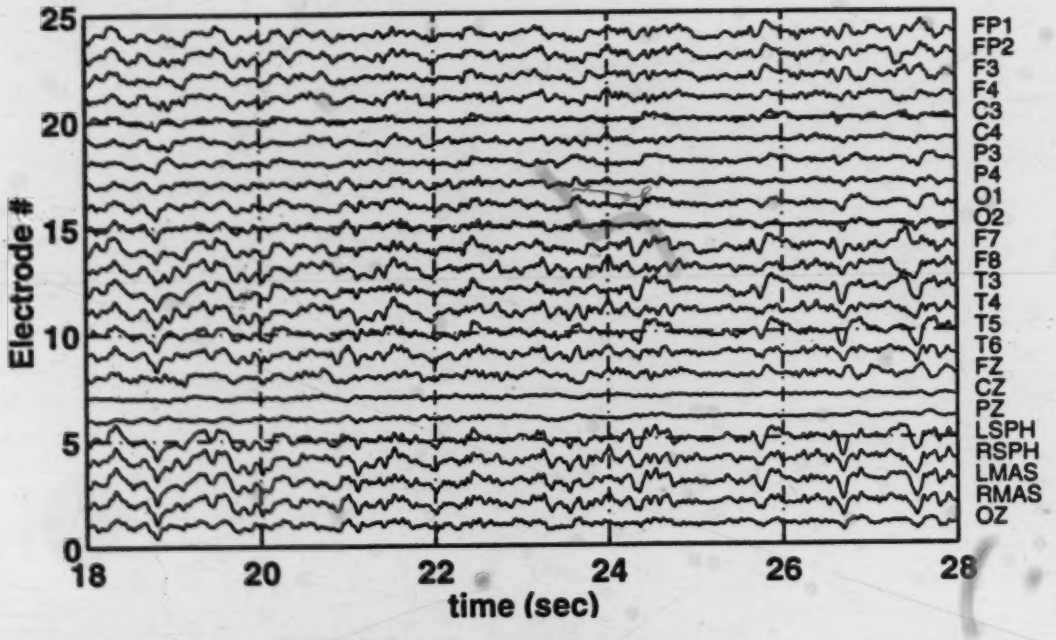

Figure 5.29a Temporally Bandpass Filtered EEG, Patient 2

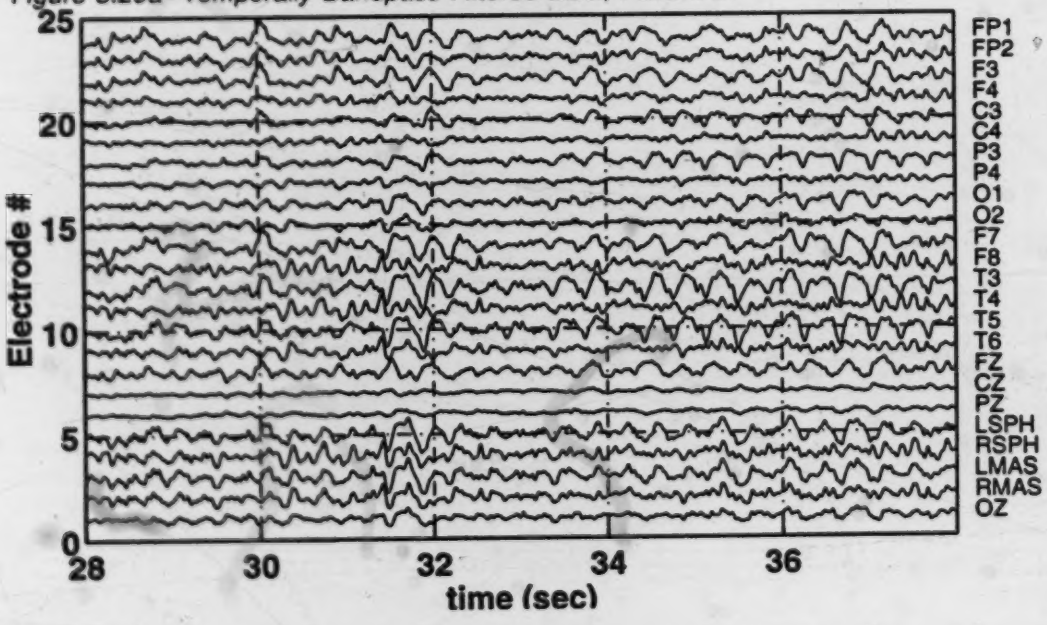

Figure 5.29b Temporally Bandpass Filtered EEG, Patient 2

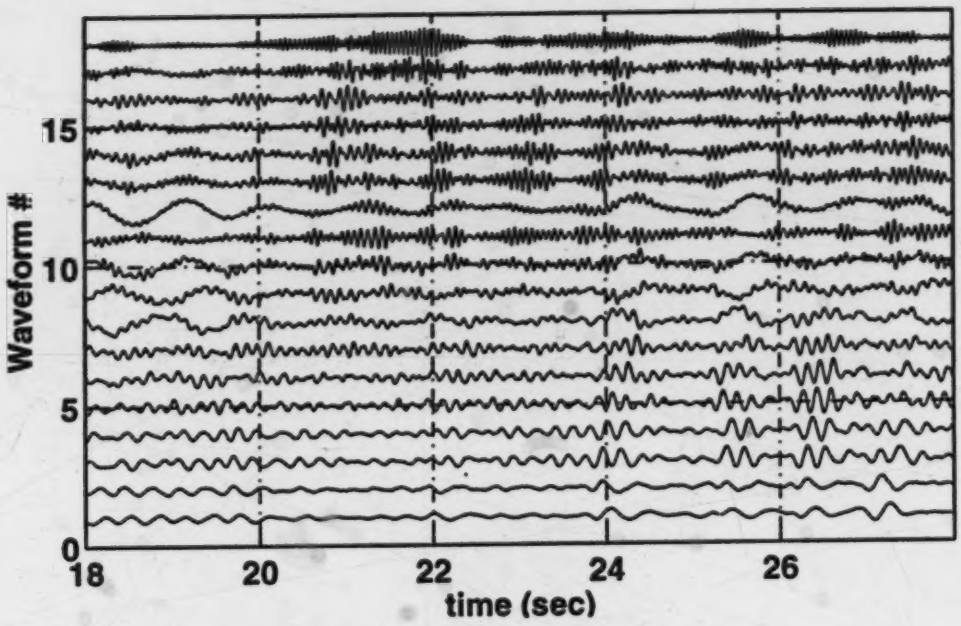

Figure 5.30a TPF Temporal Waveforms; Patient 2

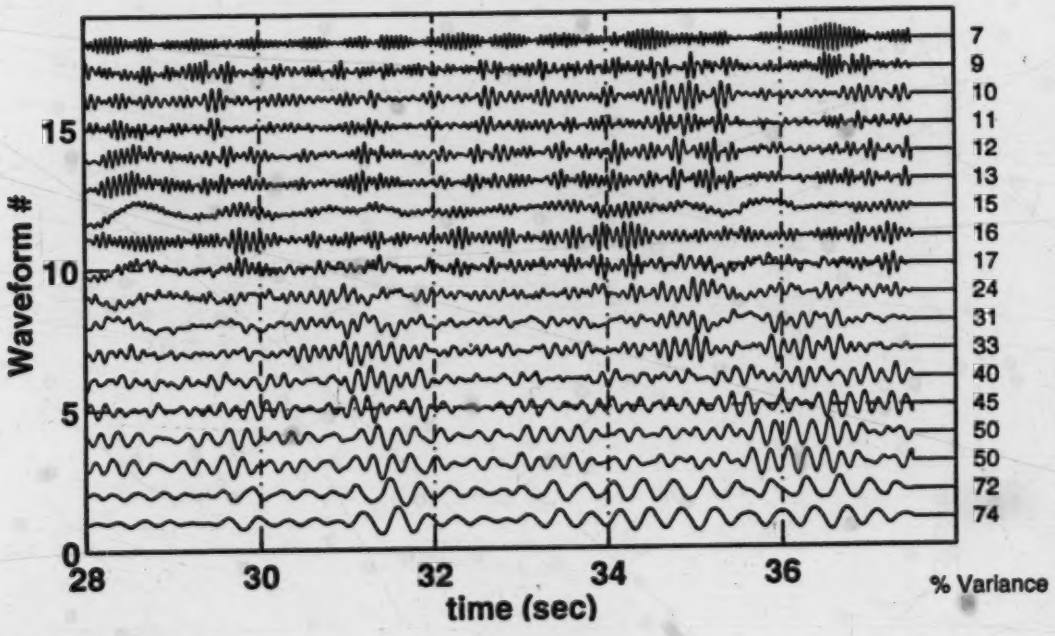

Figure 5.30b TPF Temporal Waveforms; Patient 2

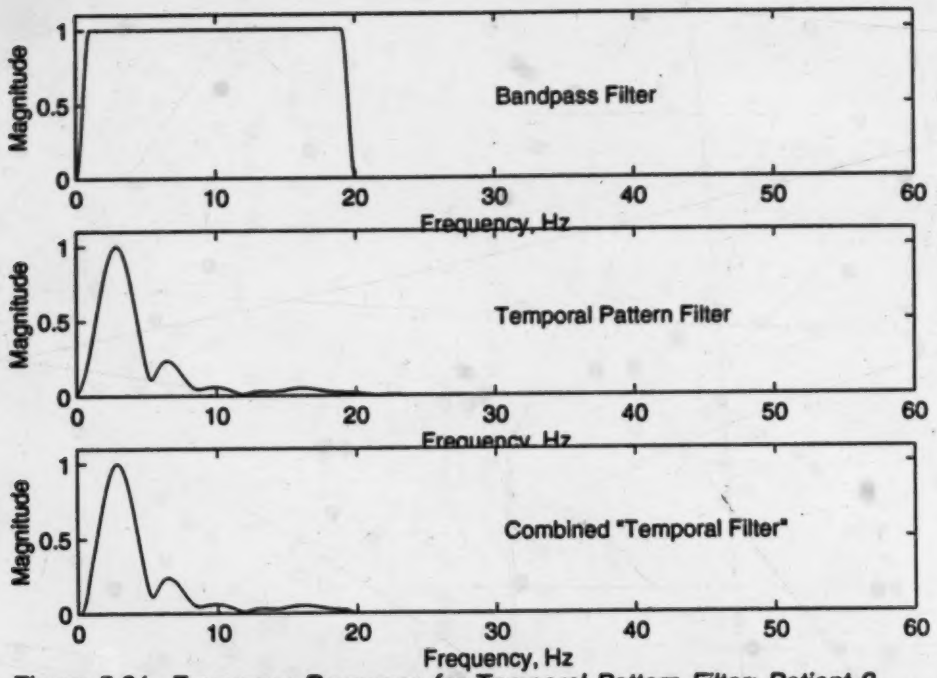

Figure 5.31 Frequency Response for Temporal Pattern Filter; Patient 2

Figures 5.32a and 5.32b display the result of the raw EEG filtered both with the bandpass filter and the temporal pattern filter. As expected, the 3 Hz left temporal activity is more clearly presented. The 6 Hz right temporal activity, in the 30 to 32 second interval, has been suppressed. The activity in the temporally filtered EEG appears to begin to be lateralized to the left hemisphere at 24 seconds with short bursts or waves of the same frequency as the fully developed seizure activity. Although, the left and right temporal electrode recordings, in the 28 to 30 second interval, still contain similar activity

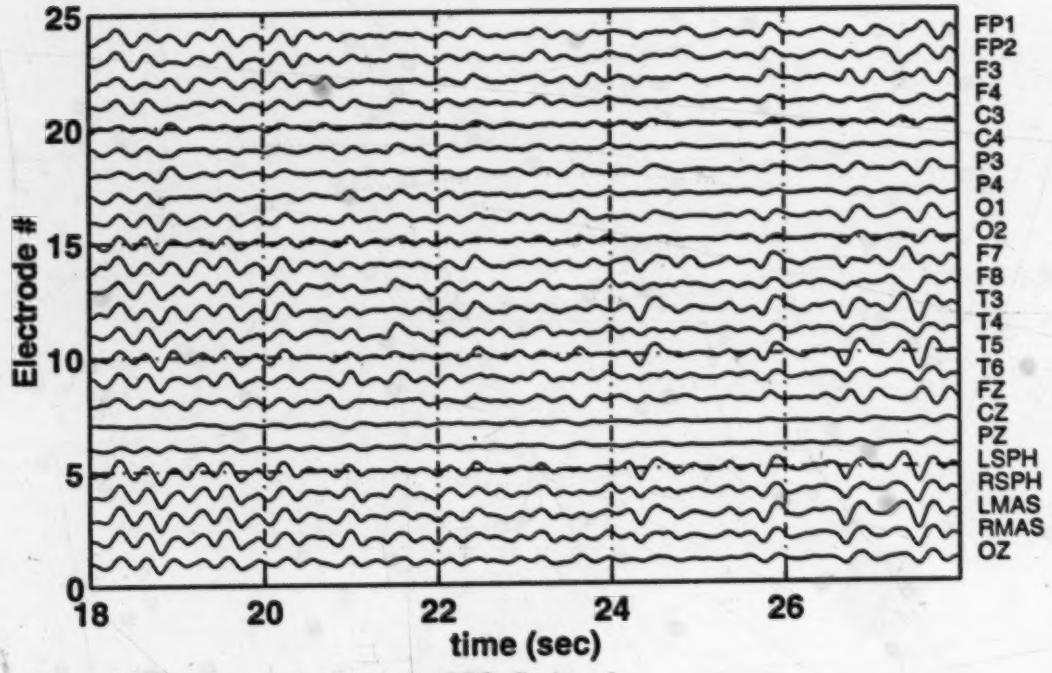

Figure 5.32a Temporally Filtered EEG; Patient 2

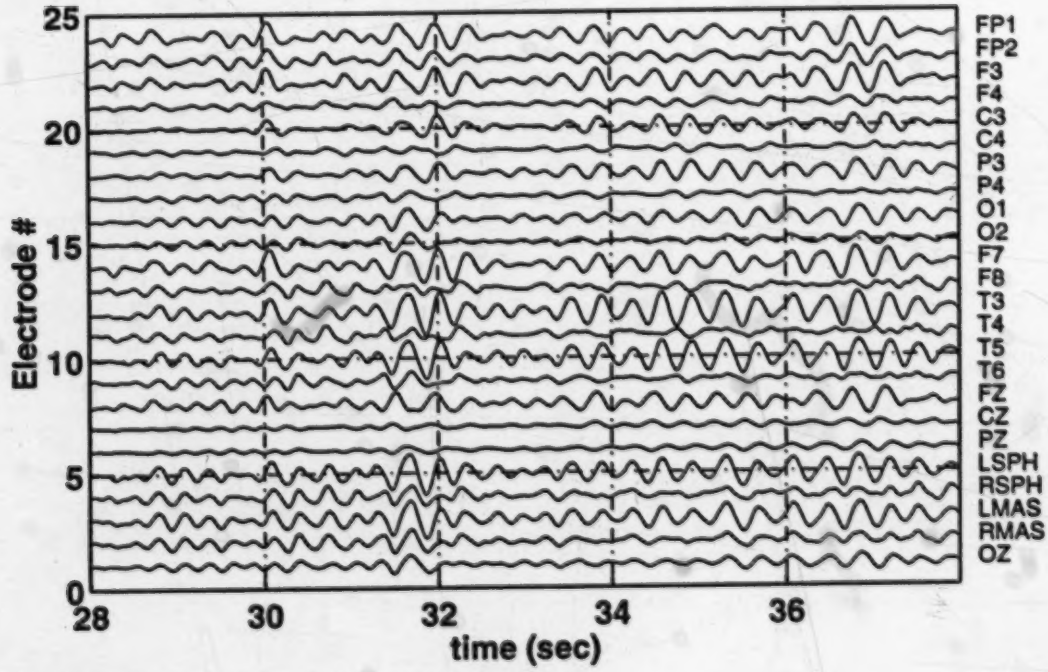

Figure 5.32b Temporally Filtered EEG; Patient 2

Spatial Filtering

To capture the complete epileptiform activity in one spatial pattern the abnormal onset for the spatial pattern filter design for this EEG was set for 31.5 seconds. Also a 5.5 second segment of the EEG was used to derive the spatial pattern filter. The seizure onset can be more clearly and accurately identified in the review of the SPF temporal waveforms, as seen in Figures 5.33a and 5.33b. The first burst of seizure can be seen at 26.5 seconds with a second burst at 31.5 seconds evolving into persistent epileptiform activity. Guided by the high percentage of variance, accounted for in the abnormal segment, of 89% and 83%, the temporally and spatially filtered EEG was reconstructed from the two corresponding spatial patterns and SPF temporal waveforms.

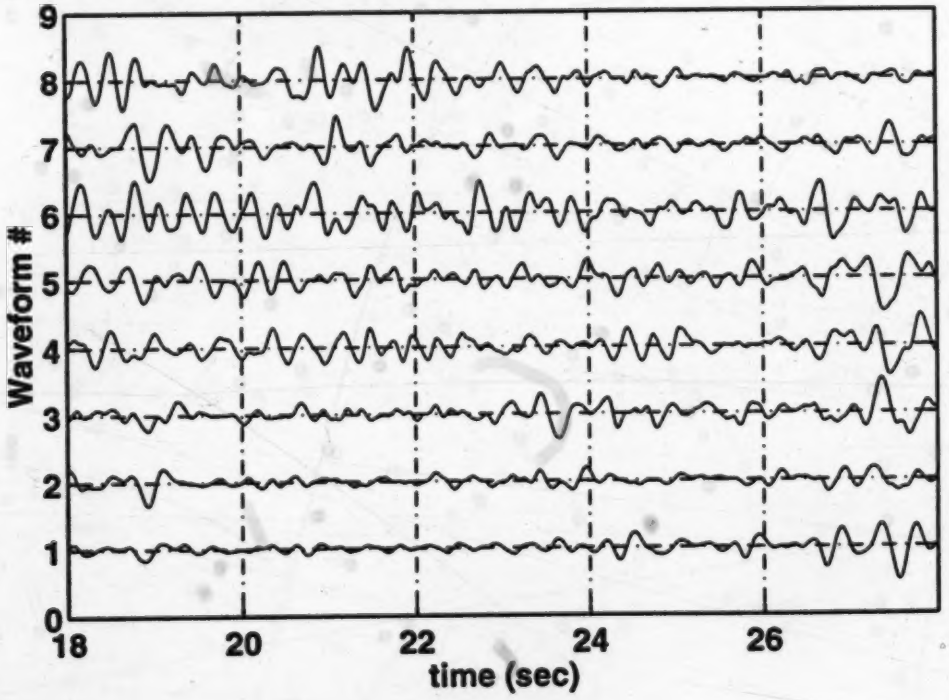

Figure 5.33a SPF Temporal Waveforms; Patient 2

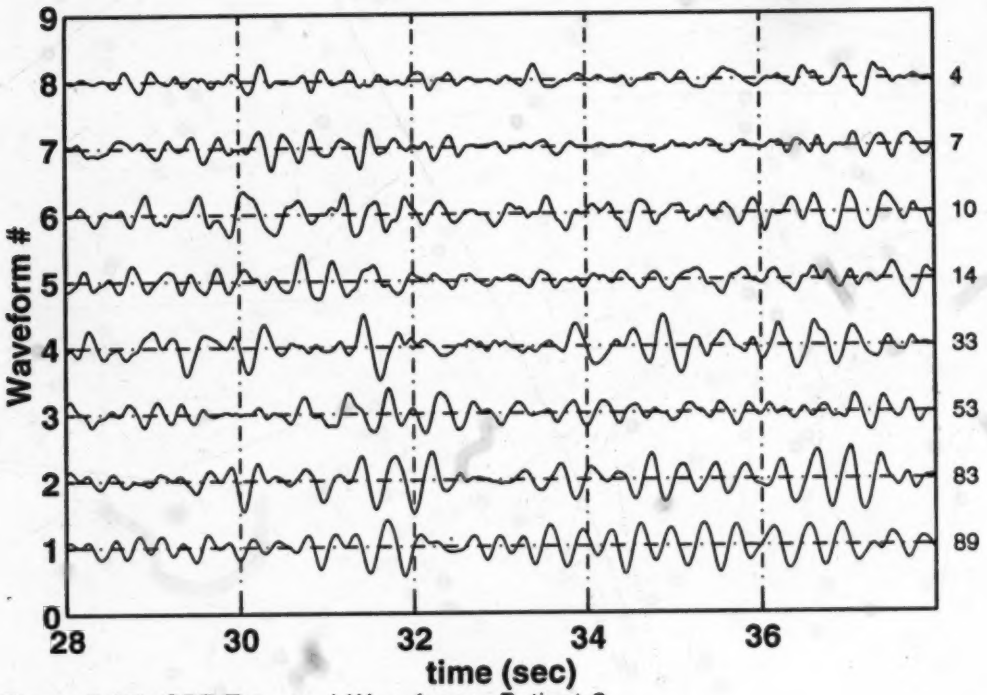

Figure 5.33b SPF Temporal Waveforms; Patient 2

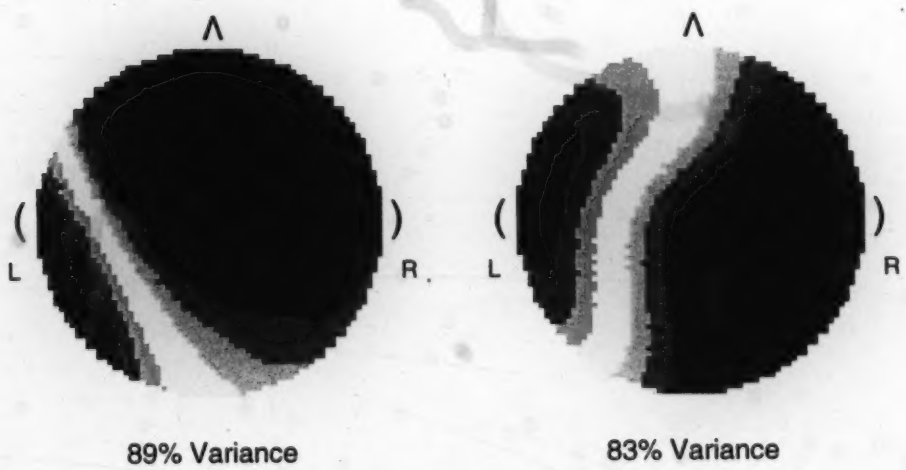

Figure 5.34 Mapping of the Spatial Patterns which Account for the 2 Largest Variances in the Abnormal EEG, Patient 2

Figure 5.34 presents the spatial maps of the spatial patterns which account for the 2 largest variances in the abnormal EEG segment. The two spatial maps corresponding to the distribution of abnormal activity suggest the seizure onset as well as the fully developed seizure activity is lateralized to the left temporal lobe.

Figures 5.35a and 5.35a present the temporally and spatially filtered EEG which was reconstructed from the two abnormal SPF temporal waveform and corresponding spatial patterns. The 6 Hz activity has now been eliminated and the seizure focus has been lateralized to left hemisphere electrode recordings with the largest amplitudes seen at the left temporal T3 and T5 electrode sites.

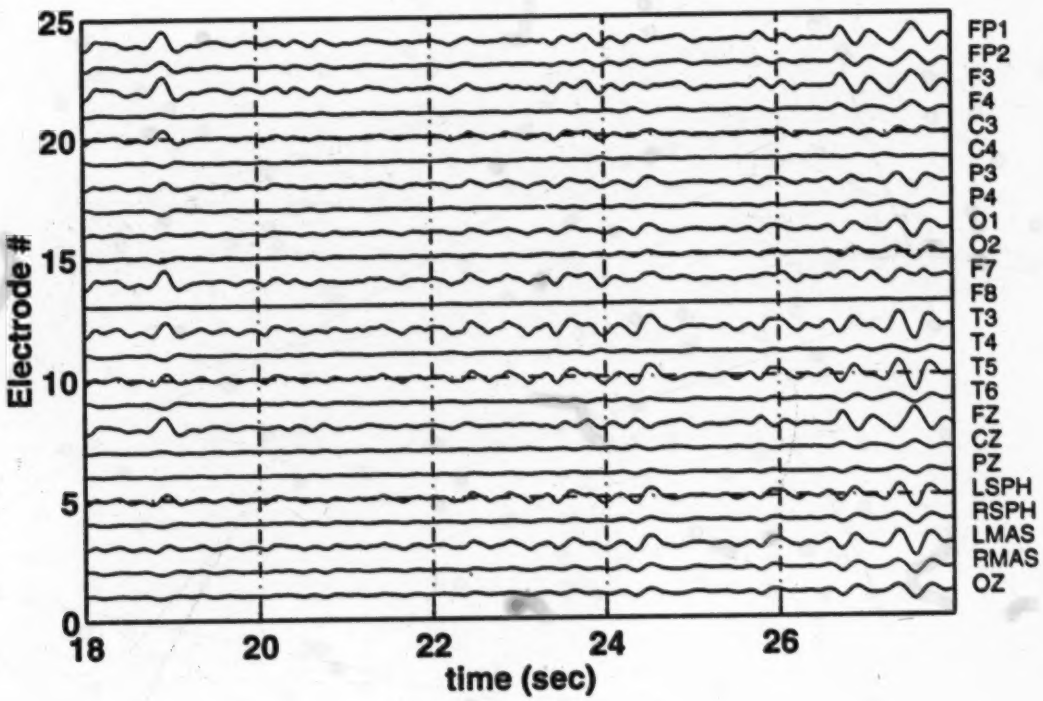

Figure 5.35a Temporally and Spatially Filtered EEG, Patient 2

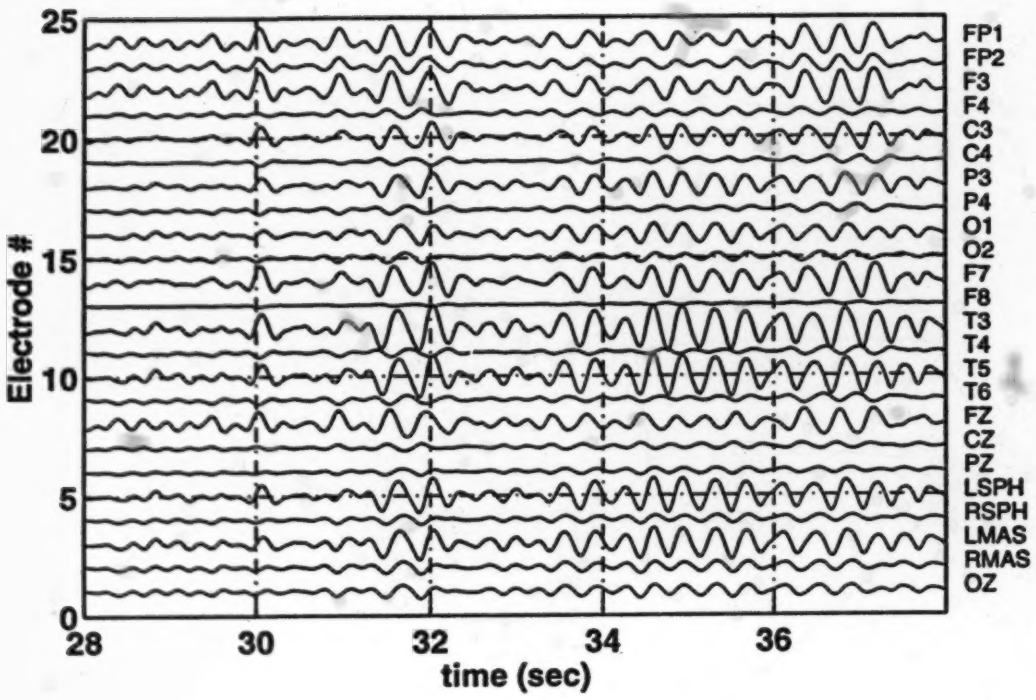

Figure 5.35b Temporally and Spatially Filtered EEG, Patient 2

This patient has undergone a left temporal lobectomy which included the mesial temporal structures and is now seizure free. Although this was a simple case, the utility of temporal and spatial filtering to isolate and separate the abnormal activity from normal, background, artifacts and noise has been illustrated. The value of this clinical tool is in the quantification and the confirmation of the visual and experiential analysis of the electrical information provided by the expert epileptologist.

6. CONCLUSION

The data dependent filter design procedure and the method of temporal and spatial filtering of an EEG are useful tools to enhance the seizure onset and to improve the accuracy of source localization. The method used is a variation of singular value decomposition and an extension of spatial filtering procedures [Koles 1991]. The analysis of autocovariance matrices of two segments from a single electrode recording results in a temporal pattern filter. This filter is a linear combination of selected temporal basis vectors, or temporal patterns, which are common to both abnormal and normal segments but account for maximum variance in the abnormal segment while accounting for minimum variance in the normal segment.

The improvement in presentation of the seizure onset from the raw EEG to the temporally filtered EEG is evident in all the cases presented in the previous chapter. The temporal pattern filter enhances the abnormal activity within each electrode recording of the EEG by suppressing the activity which does not pertain to the epileptiform activity. Prefiltering the simulated EEG with a temporal pattern filter prior to spatial filtering improved the source localization, shown by a reduction in the error between the assigned and derived spatial patterns. Temporal and spatial pattern filtering of surface recordings of simultaneously recorded depth, subdural and surface electrode recordings of clinical data, for Patient 1, showed that the surface designed temporal pattern filter is able to highlight the same seizure activity as a depth designed

temporal pattern filter and improved seizure onset identification and source localization. Whereas the seizure onset and lateralization of the seizure activity in the raw or bandpass filtered surface electrode recordings were inconclusive. The temporal and spatial filtering of the clinical EEG from Patient 2 showed that this analysis increases the utility of surface EEGs recorded from epileptic patients in a clinical setting. The filtering enables various temporal patterns within the activity during the seizure onset to be analyzed as to their contribution to the seizure activity. In general, each of the filtered EEGs, the bandpass filtered, the temporally filtered and the temporally and spatially filtered EEGs add a level of improvement over the raw EEG. Typically, the seizure onset can be confidently detected in the temporally filtered EEG while the temporally and spatially filtered EEG provides improved source lateralization.

The critical elements of temporal pattern filtering are the choices in the data dependent filter design. These choices make this approach dependent on an experienced human analyst for expert judgments. Specifically, the selection of a single electrode recording, the abnormal and the normal segments and the temporal patterns from which the filter is constructed.

Tests during this research suggested that temporal pattern filtering technique appears to be more sensitive to the normal segment selection than the abnormal segment selection. Filters based on ictal, interictal and even generalized abnormal segment selections provide results generally consistent with each other. This is helpful in situations when the seizure rapidly deteriorates into a

generalized seizure. When the normal segment contains similar frequency content as the abnormal segment, the choice of the normal segment is more critical. The indication of this is that the maximum variance accounted for in the abnormal segment or EEG is somewhat less than 100%, as in the analysis of Patient 2. It is then that the selection of the normal segment just prior to seizure onset may not be the best choice. Rather, a normal segment at some interval prior to the seizure onset may be a better choice.

The selection of the temporal patterns is another decision which will strongly determine the value of the final results. The results presented in this thesis follow the filter design criterion which is based on minimum spatial pattern error. The simulated EEG results indicated that the use of only the temporal pattern which accounts for the maximum variance in the filter will result in minimum error in source localization. The design criterion which provides the most cautious result is the based on the selection of temporal patterns which meet the following three limitations:

Each temporal pattern is evaluated and can be used in the temporal pattern filter design if;

i) the epileptiform activity is contained in the corresponding TPF temporal waveform,

ii) the percentage of variance accounted for by the temporal pattern in the abnormal segment is more than 70%, ideally near 100% and

iii) the difference between the percentage of variances accounted for in the abnormal segment by successive temporal patterns is less than 20%.

The data dependent filter design method for temporal and spatial pattern filters results in filters that are able to isolate the abnormal activity both temporally and spatially. The temporal pattern filter has been validated using both simulated and clinical data. The addition of temporal pattern filtering to spatial filtering of simulated and clinical EEGs results in improved source localization and seizure onset detection. An additional value of this filtering method as a clinical tool is the quantification and the analytical confirmation of the visual and experiential based EEG analysis provided by an expert epileptologist. In conclusion, the results suggest that in some cases both the ictal and preictal data information from scalp EEGs can be used in the filter design to effectivly reduce the number of active sources to a manageable few. These few sources can then be localized to provide insight into the behavior of complicated seizure activity.

Future Work

The development of a data dependent filter design procedure for temporal and spatial filters completes another step towards a real time automatic seizure detection and source localization tool. A next step would incorporate temporal patterns from more than one electrode in the temporal pattern filter design procedure.

An issue not addressed by this thesis is the impact of the length of segments to be used in the decomposition. This research used as a guideline, the definition that a seizure must have a sustained change in frequency and/or amplitude behaviour for a period of at least 3 seconds. Thus, the data segments were typically selected to be 3

seconds in length. Other lengths were tested, but a conclusive decision as to the most effective length for all cases was not determined. Experience suggests that lengths of segments chosen to match the length of the pattern (normal or abnormal) as seen in the EEG channel recording may provide better pattern isolation and result in identifiable temporal waveforms and higher variances. More exhaustive tests are required to evaluate this parameter with the aim of quantifying the best length for specific abnormalities. Also tied into the impact of the choice of length of segments is the particular choice of onset of normal and abnormal segments. The best choices are based on the knowledge of the seizure onset.

The development of a real time automated seizure onset detection algorithm based on the procedures presented in this thesis, would be a possible next step towards a comprehensive tool. The ultimate goal is to eliminate the need for decisions, completely. This goal requires further investigation into the quantification of each of these decisions and the introduction of real time processing.

References

Barlow, J. S. (1980) EEG transient detection by matched inverse digital filtering. Electroencephalography and Clinical Neurophysiology, 48: 246-248.

Barlow, J. S. (1984) Analysis of EEG changes with carotid clamping by selective analog filtering, matched inverse digital filtering and automatic adaptive segmentation: a comparative study, Electroencephalography and Clinical Neurophysiology, 58: 193-204.

Daly. D. D. and Pedley, T. A. (1990) Current Practice of Clinical Electroencephalography, Second Edition. Raven Press, New York.

Franaszczuk, P. J., Bergey, G. K. and Kaminski, M. J. (1994) Analysis of mesial temporal seizure onset and propagation using the directed transfer function method. Electroencephalography and Clinical Neurophysiology, 91: 413-427.

Fukunaga, K. (1972) Introduction to Statistical Pattern Recognition. Academic Press, New York.

Gevins, A., Le J., Brickett P., Reutter, B. and Desmond, J. (1991) Seeing through the skull: advanced EEGs use MRIs to accurately measure cortical activity from the scalp. Brain Topography, 4: 125-131.

Gotman, J. and Gloor, P. (1976) Automatic recognition and quantification of interictal epileptic activity in the human

scalp EEG. Electroencephalography and Clinical Neurophysiology, 41: 512-529.

Gotman, J., Ives, J. R. and Gloor, P. (1981) Frequency content of EEG and EMG at seizure onset: possibility of removal of EMG artifact by digital filtering. Electroencephalography and Clinical Neurophysiology, 52: 626-639.

Gotman, J. (1982) Automatic recognition of epileptic seizures in the EEG. Electroencephalography and Clinical Neurophysiology, 54: 530-540.

Harner, R. N. (1988) Brain mapping or spatial analysis? Brain Topography, 1: 73-75.

Harner, R. N. (1990) Singular value decomposition - a general linear model for analysis of multivariate structure in the electroencephalogram. Brain Topography, 3: 43-47

Hjorth, B. (1989) Eigenvectors and eigenfunctions in spatiotemporal EEG analysis. Brain Topography, 2: 57-61.

Hjorth, B. and Rodin, E. (1988) Extraction of "deep" components from scalp EEG. Brain Topography, 1: 65-69.

Hjorth, B. and Rodin, E. (1988) An eigenfunction approach to the inverse problem of EEG. Brain Topography, 1: 79-86.

Jobert, M., Poiseau, E., Jahnig, P., Schulz H. and Kubicki, S. (1992) Pattern recognition by matched filtering: an analysis of sleep spindle and K-complex density under the influence of Lormetazepam and Zopiclone, Neuropsychobiology, 26:100-107.

Kobayashi, K., Nakahori. T., Ohmori, I. Yoshinaga, H., Otsuka, Y., Oka, E. and Ohtahara, S. (1996) Estimation of obscure ictal epileptic activity in scalp EEG. Brain Topography, 9: 125-134.

Koles, Z. J. (1991) The quantitative extraction and topographic mapping of the abnormal components in the clinical EEG. Electroencephalography and Clinical Neurophysiology, 79: 440-447.

Koles, Z. J., Lind, J. C. and Soong, A. C. K. (1995) Spatio-temporal decomposition of the EEG: a general approach to the isolation and localization of sources. Electroencephalography and Clinical Neurophysiology, 4: 219-230.

Lopes Da Silva, F. H., Hulten, V., Lommen, J. G., Storm Van Leeuwen, W., Van Veelen, C. W. M. and Vliegenthart, W. (1977) Automatic detection and localization of epileptic foci. Electroencephalography and Clinical Neurophysiology, 43: 1-3.

Murro, A. M., King, D. W., Smith, J. R., Gallagher, B. B., Flanigin, H. F. and Meador, K. (1991) Computerized seizure detection of complex partial seizures. Electroencephalography and Clinical Neurophysiology, 79: 330-333.

Nunez, P. L. (1981) Electric Fields of the Brain: the Neurophysics of EEG. Oxford University Press, New York.

Nunez, P. L., Pilgreen, K. L., Westdorp, A. F., Law, S. K. and Nelson, A. V. (1991) A visual study of surface potentials and laplacians due to distributed neocortical sources: computer simulations and evoked potentials. Brain Topography, 4: 151-168.

O'Neill, N. S., Javidan, M. and Koles, Z. J. (1998) Localization of seizure onset in the EEG. Proceedings of The Canadian Medical and Engineering Society, Edmonton, 14-15.

Park, Y. D., Murro. A. M., King, D. W., Gallagher, B. B., Smith, J. R. and Yaghmai, F. (1996) The significance of ictal depth EEG patterns in patients with temporal lobe epilepsy. Electroencephalography and Clinical Neurophysiology, 99: 412-415.

Pfurtscheller, G. and Fischer, G. (1978) A new approach to spike detection using a combination of inverse and matched filter techniques. Electroencephalography and Clinical Neurophysiology, 44: 243-247.

Soong, A. C. K., Lind, J. C., Shaw, G. R. and Koles, Z. J. (1993) Systematic comparisons of interpolation techniques in topographic brain mapping. Electroencephalography and Clinical Neurophysiology, 87: 185-195.

Soong, A. C. K. and Koles, Z. J. (1995) Principal-component localization of the sources of the Background EEG. IEEE Transactions on Biomedical Engineering, 42: 59-67.

Strang, G. (1976) Linear Algebra and Its Applications. Academic Press, New York.

Tyner, F. S., Knott, J. R. and Mayer, W. B. (Jr.) (1983) Fundamentals of EEG Technology: Volume 1, Basic Concepts and Methods. Raven Press, New York.

Webster, J. G. (Editor) (1992) Medical Instrumentation: Application and Design. Houghton Mifflin Company, Boston.